Dissertation

submitted to the

Combined Faculties of the Natural Sciences and Mathematics
of the Ruperto-Carola-University of Heidelberg, Germany

for the degree of

Doctor of Natural Sciences

Put forward by

Sergey Bragin

born in Khabarovsk, Russia

Oral examination: 28.05.2019

Front-form approach to quantum electrodynamics in an intense plane-wave field with an application to the vacuum polarization

Referees:

PD Dr. Antonino Di Piazza

Prof. Dr. Joerg Jaeckel

Zusammenfassung

In dieser Arbeit wird Quantenelektrodynamik in einem intensiven ebene Wellen-Feld im Rahmen der Lichtkegel-Quantisierung untersucht. In diesem Kontext werden Vakuumdoppelbrechung und -dichroismus in intensiven Laserfeldern betrachtet. Insbesondere wird ein Aufbau analysiert, in dem Probe-gamma-Photonen mithilfe von Compton-Rückstreuung erzeugt werden, durch einen intensiven Laserpuls propagieren, und anschließend durch Paarerzeugung in materie detektiert werden. Die Polarisierung des Photonenstrahls wird durch Stokes-Parameter charakterisiert und deren Änderung aufgrund der Vakuumdoppelbrechung und des Vakuumdichroismus wird ermittelt. Die Größe der Polarisationseffekte wird für zukünftige Hochleistungs-Laseranlagen beurteilt. Optimale Parameter und Regimes werden identifiziert und sowohl die erforderliche Statistik als auch die Dauer des Experimentes, die nötig sind, um die Vorhersagen der Quantenelektrodynamik zu bestätigen, werden abgeschätzt. Des Weiteren wird ein Ansatz zur Behandlung des Bispinor-Teils der Streuamplituden in einem ebene Wellen-Feld eingeführt. Für die Vertex-Funktionen, die aus den Wechselwirkungstermen des Lichtfront-Hamiltonoperators entstehen, werden vereinfachte Ausdrücke gefunden. Es wird demonstriert, dass mit der entwickelten Technik die Berechnung der Gamma-Matrix Spuren für Streuung in externen ebene Wellen-Feldern in relativ einfacher Weise durchgeführt werden kann und dass das finale Ergebnis in kompakter Form geschrieben werden kann.

Abstract

Quantum electrodynamics in an intense plane-wave field is considered within the framework of light-cone quantization. In this context, high-energy vacuum birefringence and dichroism in an intense laser field are investigated. In particular, a setup is analyzed, in which probe gamma photons are generated via Compton backscattering, propagate through an intense laser pulse, and are subsequently detected via pair production in matter. The polarization of the photon beam is characterized by the Stokes parameters, and their change due to vacuum birefringence and dichroism is determined. The magnitude of the polarization effects is assessed for upcoming high-power laser facilities. Optimal parameters and regimes are identified, and the required statistics and the duration of the experiment in order to confirm the prediction of quantum electrodynamics are estimated. Furthermore, an approach for the treatment of the bispinor part of scattering amplitudes in a plane-wave field is introduced. Simplified expressions for the vertex functions, arising from the interaction terms of the lightfront Hamiltonian, are obtained. It is demonstrated that with the developed technique the evaluation of the gamma-matrix traces for scattering in an external plane-wave field can be performed in a relatively straightforward way and the final results can be written in a compact form.

List of Publications

Publications covered by this thesis:

- **Chapter 3:**
  High-Energy Vacuum Birefringence and Dichroism in an Ultrastrong Laser Field.
  S. Bragin, S. Meuren, C. H. Keitel, and A. Di Piazza.
  Phys. Rev. Lett. **119**, 250403 (2017).
  doi: 10.1103/PhysRevLett.119.250403

Acknowledgments

It would not have been possible to accomplish all those things, that I present in my thesis, without contributions, scientific and not only, from many people.

I am grateful to my supervisor, Antonino Di Piazza, for his knowledge, vision, dedication, readiness to help and to let me freely develop my ideas.

I thank Alexander Milstein for encouraging me to pursue a PhD in Heidelberg, and Christoph Keitel for giving me an opportunity to actually do so.

I am greatly indebted to Sebastian Meuren for many things that I have learned from him and for the inspiration that he had been constantly providing. Those hours of standing in front of a blackboard or sitting at a desk in trials to solve a problem, with a usual continuation on the way back home, are among the most valuable experiences for me.

I feel owing a lot to Oleg Skoromnik, who has always been willing to discuss and clarify all the difficulties that I have encountered while traveling across the wide and deep sea of theoretical physics. It is hard to overestimate the importance of his advice and help during the whole track of my PhD.

I am thankful to former and current members of my division, and other scientific and administrative staff at Max Planck Institute for Nuclear Physics, for creating a pleasant working atmosphere, for the encouragement, assistance, and fair critique. I also thank those colleagues of mine, who have found time to read some parts of this thesis and give comments on them, and Dominik Lentrodt for the help with the German translation.

I thank my friends, in Heidelberg and other parts of the world, for their positivity that has always given me a boost in confidence, and for pushing me to grow over myself.

I thank my family, who have been doing their best to support me despite thousands of kilometers separating us.

Sergey Bragin
Heidelberg, March 2019

Contents

Units and notation

Throughout the thesis, Heaviside and natural units are employed, i.e., $\epsilon_0 = \hbar = c = 1$.

Greek letters (μ, ν, ...) denote four-dimensional vector components. In the instant form, they take values 0, 1, 2, 3. In the front form, they take values +, −, 1, 2.

Latin letters starting with i (i, j, k, ...) denote two-dimensional transverse vector components in the front form. They take values 1, 2. Occassionally, those letters are used for other quantities that have two different components.

Three dimensional space vectors in the instant form are denoted by bold symbols, i.e., $\boldsymbol{a} = (a^1, a^2, a^3)$. Two dimensional transverse vectors in the front form are denoted by bold symbols with an upper index $\perp$, i.e., $\boldsymbol{a}^\perp = (a^1, a^2)$.

Metric tensor is given by $g^{\mu\nu} = (1, -1, -1, -1)$ in the instant form. For the front form, it is defined in Section 1.1.

If a sum over indices is not written explicitly, the Einstein summation rule is assumed for both greek and latin indices, only if one of the letters is an upper index and the other one is a lower index.

The scalar product of two four-vectors a^μ and b^μ is denoted as ab.

The Levi-Civita symbol $\epsilon^{\varkappa\lambda\mu\nu}$ is defined with $\epsilon^{0123} = 1$ in the instant form, and $\epsilon^{+-12} = -1$ in the front form. The Levi-Civita symbol ϵ^{ij} is defined with $\epsilon^{12} = 1$.

The dual tensor is defined as $(*F)^{\mu\nu} = \epsilon^{\mu\nu\sigma\tau} F_{\sigma\tau}/2$.

Gamma-matrix indices are treated as four-vector indices, i.e., $\gamma a = \gamma^\mu a_\mu$.

A star superscript denotes a complex conjugate quantity, e.g., $f^*(x)$ is complex conjugate to $f(x)$. Analogously, a dagger (†) denotes a Hermitian conjugate quantity.

A bar denotes a Dirac conjugate quantity, e.g., $\overline{\psi} = \psi^\dagger\gamma^0$ for a vector and $\overline{\Gamma} = \gamma^0\Gamma^\dagger\gamma^0$ for a matrix.

Physical constants:

Speed of light: $c = 2.998 \times 10^{10}$ cm/s.

Elementary charge: $e = 4.803 \times 10^{-10}$ CGS electrostatic units.

Electron mass: $m = 511.0$ keV/c^2.

Reduced Planck constant: $\hbar = 6.582 \times 10^{-16}$ eV $\cdot$ s.

Fine structure constant: $\alpha = 1/137.0$.

Reduced Compton wavelength: $\lambda_C = 3.862 \times 10^{-11}$ cm.

Classical electron radius: $r_e = 2.818 \times 10^{-13}$ cm.

Introduction

The Standard Model of particle physics, with its framework of quantum field theory, has been incredibly successful over the years, particularly at the perturbative level. In fact, the idea of pointlike particles, being fermions, interacting via the exchange of gauge bosons, and the representation of this interaction as a sequence of graphs, is what shapes our basic intuition about how the world is organized at the subatomic scale.

The Standard Model, however, does not embrace and explain all the knowledge, that we have about particle physics. Some facts simply do not fit into the formulation of the Standard Model, some others are parts of the model, but do not find a rationalization within it. One of the canonical examples is an experimental evidence, that neutrinos oscillate and therefore have nonzero masses [Super-Kamiokande, 1998; SNO, 2001, 2002], the fact that does not combine naturally with the coherent picture of the Standard Model. A related phenomenon is the quark flavor mixing. It is indeed incorporated into the Standard Model via the Cabibbo-Kobayashi-Maskawa (CKM) matrix [Cabibbo, 1963; Kobayashi and Maskawa, 1973], however, the components of the matrix are external parameters, not derived from the theory.

One of the ways to understand our theory deeper and, hopefully, to get some insight into the current problems within it, is to go beyond the perturbative approach. Nonlinear phenomena, which, from the theoretical point of view, require a resummation of the perturbation series, allow one to test the theory at the so-called intensity frontier. Quantum electrodynamics (QED) in an intense laser field is an example of a nonlinear quantum field theory, which, on the one hand, can be studied in a relatively tractable way, and on the other hand, is testable with current or near-future experimental capabilities.

Since 1950's, when the first amplifiers of electromagnetic radiation via stimulated emission for microwaves (masers) were devised and built, and later, for visible light, analogous devices (lasers) were constructed, the laser technology has made a huge leap forward. Due to the invention of the chirped pulse amplification [Strickland and Mourou, 1985] and optical parametric chirped pulse amplification [Piskarskas et al., 1986], nowadays, laser pulses of power up to several petawatt (PW) are produced in the labs [Vulkan; Sung et al., 2017] and 10-PW facilities are starting their operation [ELI-NP]. The upcoming 10-PW laser facilities are expected to deliver focused intensities up to $I \sim 10^{23}$ W/cm^2 [Di Piazza et al., 2012; Jeong and Lee, 2014; Danson et al., 2015].

Such great intensities indeed require taking nonlinear effects into account. This can be seen as follows. The strength of the interaction of an electron with a laser field can be characterized by the classical intensity parameter (for simplicity, we consider the case of a linearly polarized laser pulse) [Ritus, 1985; Di Piazza et al., 2012]

$$\xi = \frac{|e|E_0}{m\omega_0} \approx 0.7495\,\frac{1}{\omega_0[\mathrm{eV}]}\sqrt{\frac{I[\mathrm{W/cm^2}]}{10^{18}}}, \tag{1}$$

where E_0 is the peak electric field strength and ω_0 is the typical angular frequency of the field ($e < 0$ and m are the electron charge and mass, respectively; here and below we use units with $\hbar = c = \epsilon_0 = 1$).

If $\xi \ll 1$, the probability for an electron to interact with n laser photons scales as ξ^{2n} [Ritus, 1985; Di Piazza et al., 2012]. The scaling ξ^{2n} means that, when considering a process for QED in a laser field, the corrections to the leading-order diagrams are supressed, and the interaction with the laser field can be treated perturbatively.

On the other hand, if $\xi \gtrsim 1$, higher-order corrections become sizable and must be taken into account. For optical frequencies ($\omega_0 \sim 1$ eV), the regime $\xi \gtrsim 1$ implies intensities $I \gtrsim 10^{18}$ W/cm^2 [see Eq. (1)], which are already accessible. In essense, the parameter ξ is a typical number of laser photons that interact with a quantum system on a typical scale — (reduced) Compton wavelength $\lambda\!\!\!^{-}_C = 1/m$. If $\xi \gtrsim 1$, the interaction happens with several laser photons involved, and we need to consider the nonlinear regime.

An exciting prediction of QED, which has not been confirmed yet in a laboratory experiment, but which could potentially be confirmed with an experimental access to the nonlinear regime, is vacuum birefringence.

In the realm of classical electrodynamics the electromagnetic field experiences no self-interaction in vacuum, as a result, the superposition principle holds [Landau and Lifshitz, 1987]. In QED, however, a finite photon-photon coupling is induced by the presence of virtual charged particles in the vacuum [Berestetskii et al., 1982]. Due to the finite photon-photon coupling, the vacuum, subjected to an external field, behaves like a birefringent medium. This idea was initially proposed by Toll (1952), and then developed by other groups [Klein and Nigam, 1964; Baier and Breitenlohner, 1967; Bialynicka-Birula and Bialynicki-Birula, 1970].

An experimental observation of vacuum birefringence has been a great challenge, due to the relative smallness of the light-by-light scattering cross section in the low-energy regime. Laboratory experiments like BFRT [Cameron et al., 1993], BMV [Cadène et al., 2014], PVLAS [Della Valle et al., 2016], and Q&A [Chen et al., 2007] have so far employed magnetic fields to polarize the vacuum and optical photons to probe it, and they have not reached the required sensitivity. Recent astronomical observation results seem to confirm the existence of vacuum birefringence [Mignani et al., 2017] (see also the remarks in [Capparelli et al., 2017; Turolla et al., 2017]). However, a direct laboratory-based verification of this fundamental property of the vacuum is still missing.

As the light-by-light scattering cross section attains its maximum at the pair-production threshold [Berestetskii et al., 1982], it is natural to consider this regime to probe vacuum birefringence [Dinu et al., 2014; Ilderton and Marklund, 2016; Nakamiya and Homma, 2017; King and Elkina, 2016]. For a photon of energy $k^0 = \omega$, colliding head-on with a linearly-polarized laser pulse of intesity I, a typical center-of-momentum energy of the collision (in the units of the electron mass m) can be characterized by the quantum nonlinearity parameter

$$\chi = \frac{2\omega\omega_0}{m^2}\xi \approx 0.5741\,\omega\,[\text{GeV}]\sqrt{\frac{I\,[\text{W/cm}^2]}{10^{22}}}. \tag{2}$$

Gamma photons with energies $\omega \gtrsim 1$ GeV are obtainable with the use of Compton backscattering [Berestetskii et al., 1982; Ginzburg et al., 1984]; such energies have been reached, e.g., at SPring-8 [Muramatsu et al., 2014] and HIγS [Weller et al., 2009] facilities. Therefore, the regime $\chi \sim 1$ is attainable in future laser-based vacuum birefringence experiments.

From the theoretical point of view, the regime $\chi \gtrsim 1$ is interesting and somewhat intricate. If $\chi \gtrsim 1$, electron-positron photoproduction becomes sizable, and thus, the vacuum acquires dichroic properties, and moreover, in this regime, the vacuum exhibits anomalous dispersion [Becker and Mitter, 1975; Baier et al., 1976; Ritus, 1985; Heinzl and Ilderton, 2009; Dinu et al., 2014].

A study of vacuum birefringence and dichroism in an intense laser field with high-energy photons and the evaluation of the experimental prospectives to observe these effects at upcoming laser facilities is one of the major topics of my thesis.

Another challenge for theoretical QED in an intense laser field is tree-level second-order processes. Already at this level calculations are rather nontrivial with respect to the evaluation of the traces of the gamma-matrix products [Hartin, 2006], and also complicated with respect to the numerical calculation of the integrals. For the traces, the direct use of software packages like Feyn Calc [Mertig et al., 1991] would normally produce results, which are difficult to deal with. A full numerical evaluation is also possible, however, computationally more demanding, and provides less insight.

It turns out, that the evaluation of the bispinor part for the scattering diagrams in an intense laser field can be significantly simplified, if treated with the symmetry of the problem in mind. A simple but powerful idea is that the way, how we parametrize the spin dynamics of the system under consideration, should account for the presence of the laser field.

As was pointed out in his seminal paper by Dirac (1949), there are three forms of relativistic Hamiltonian dynamics (in fact, for theories, invariant under full Poincaré group transformations, there are two more possibilities, they are usually not taken in account though, due to the smallness of their stability group; for a review and details, see the lectures by Heinzl in [Latal et al., 2001]). One of them is the instant form, in which the parametrization of space-time is done in the same manner as in nonrelativistic physics, with time x^0 and space vector $\boldsymbol{x} = (x^1, x^2, x^3)$. This is the form, which is commonly used in relativistic physics.

Another form is the one which we will be interested in, it is the front form. In the front form, the surface of a constant "time" τ is defined as a light-like surface, e.g., $\tau = x^0 + x^3 = \text{const}$.

Upon defining the front-form time, as well as the corresponding space coordinates, which together form the light-cone coordinate system, one can construct a Hamiltonian, quantize it and consider quantum field theory in the front form. This approach, known as light-cone or lightfront quantization, has been applied to QED in vacuum [Kogut and Soper, 1970; Bjorken et al., 1971; Mustaki et al., 1991], other gauge theories [Brodsky et al., 1998; Srivastava and Brodsky, 2002], superstring theory [Metsaev et al., 2001], and has become one of the tools for studing nonperturbative quantum chromodynamics [Wilson et al., 1994; Brodsky, 2002; Brodsky et al., 2015].

With respect to QED in an intense laser field, the laser field itself is customary treated as a plane wave, i.e., the field tensor $F^{\mu\nu}$ is assumed to be dependent on the coordinates x^μ via the scalar product $k_0 x$, with k_0^μ being the characteristic laser photon four-momentum

($k_0^2 = 0$). The quantity $k_0 x$ provides a natural choice for the light-cone time [e.g., if we take a plane-wave propagating in the negative z-direction, then $k_0 x = \omega_0(x^0 + x^3)$].

Indeed, the front-form parametrization of space-time is convenient for describing physics in an external plane-wave field and has been employed in calculations [Neville and Rohrlich, 1971; Mitter, 1975; Meuren et al., 2013]. Recently, also light-cone quantization was applied for studing some processes in a plane-wave field [Ilderton and Torgrimsson, 2013; Dinu et al., 2014; Dinu and Torgrimsson, 2018a,b].

What I have found out during my work is that the bispinor part of scattering amplitudes can be conveniently parametrized in the same lightfront fashion. However, in order for this technique to be successful, one needs to split the interaction Hamiltonian of QED into the terms, which are exactly the terms which one encounters when employing quantization in the front form. This fact establishes one more relation and seemingly natural connection between QED in an external plane-wave field and the light-cone quantization approach.

In the view of what has been said above, I have organized my thesis in the following way. In Chapter 1 we review light-cone quantization and develop some new ideas in context of QED in a plane-wave field. The techniques, that we will draw from Chapter 1, could be obtained in the instant form as well, and we will keep the connection. However, with the front-form approach, those techniques appear in a natural way and together add up to a coherent picture.

Chapter 2 is devoted to first-order processes. In particular, we consider electron-positron annihilation into one photon. This process is a cross channel to nonlinear Compton scattering and nonlinear Breit-Wheeler process, which are well studied. The evaluation of electron-positron annihilation into one photon is useful for testing the method that we possess, and also for understanding how to describe two-particle scattering processes in an external plane-wave field.

In Chapter 3 we study the vacuum polarization. We review the derivation of the polarization operator in a plane-wave field and see, how it can be simplified, if the front-form approach is applied to the bispinor part. We go on with considering a setup for investigating vacuum birefringence and dichroism. The setup is based on Compton backscattering to produce polarized gamma photons and exploits pair production in matter to determine the polarization state of the probe photon after it has interacted with a linearly polarized intense laser pulse. As we will see, a significant improvement in the experimental sensitivity can be achieved by employing circularly polarized probe gamma photons. Assuming conservative experimental parameters, we find out that, with upcoming technologies, the quantitative verification of the intense-field QED prediction for vacuum birefringence and dichroism is feasible with an average statistical significance of 5σ on the time scale of a few days.

Finally, in Chapter 4 we consider electron-positron annihilation into two photons. This process may be sizable and important, e.g., for laser-plasma interactions. Up to now, it has not been thorougly studied. First, we update our understanding of scattering in an external plane-wave field, that we have gained in Chapter 2. Then, we proceed with calculating the cross section (the interference terms are not taken into account) and demonstrate a way to obtain compact results for this process.

1

Quantum electrodynamics in an intense plane-wave field

In this chapter, we introduce important concepts of the front-form approach. Upon defining light-cone coordinates and light-cone bispinor basis, we review light-cone quantization in the presence of an external plane-wave field. We proceed with considering the vertex functions and obtain convenient expressions for them, which will be used in later chapters. We consider momentum relations in a plane-wave field, and also discuss gauge invariance of the theory. Finally, we introduce parameters, which will be employed later for the description of scattering processes.

1.1 Light-cone coordinates

We start by introducing a parametrization of space-time. The front form is usually parametrized by new time x^+ and space coordinate x^- in place of x^0 and x^3, with x^1 and x^2 left unchanged [Brodsky et al., 1998]:

$$x^+ = (x^0 + x^3)/\sqrt{2}, \quad x^- = (x^0 - x^3)/\sqrt{2}, \quad x^i|_{\text{front}} = x^i|_{\text{instant}}. \tag{1.1}$$

Here and below $i, j, k, l, \ldots \in \{1, 2\}$. In Eq. (1.1), we use the convention as in [Kogut and Soper, 1970], other definitions are also used in the literature [Lepage and Brodsky, 1980].

We strive to maintain manifest Lorentz-covariance, therefore we generalize the coordinate system (1.1) by introducing light-cone four-vector basis $\{\eta^\mu, \bar{\eta}^\mu, e_1^\mu, e_2^\mu\}$ with the four-vectors of this basis having the following properties [Meuren et al., 2013]:

$$\eta^2 = \bar{\eta}^2 = 0, \quad \eta\bar{\eta} = 1, \quad \eta e_i = \bar{\eta} e_i = 0, \quad e_i e_j = -\delta_{ij}. \tag{1.2}$$

The propeties (1.2) ensure that the four-vectors in the basis $\{\eta^\mu, \bar{\eta}^\mu, e_1^\mu, e_2^\mu\}$ are linearly independent, therefore, the basis is complete and an arbitrary four-vector a^μ can be written as

$$a^\mu = a^+ \bar{\eta}^\mu + a^- \eta^\mu + a^1 e_1^\mu + a^2 e_2^\mu, \tag{1.3}$$

where

$$a^+ = a\eta, \quad a^- = a\bar{\eta}, \quad a^1 = -ae_1, \quad a^2 = -ae_2. \tag{1.4}$$

The metric tensor is given by

$$g^{\mu\nu} = \eta^\mu \bar{\eta}^\nu + \bar{\eta}^\mu \eta^\nu - e_1^\mu e_1^\nu - e_2^\mu e_2^\nu, \tag{1.5}$$

or in the matrix form (we choose the order of the components as +, −, 1, 2):

$$g^{\mu\nu} = \begin{pmatrix} 0 & 1 & 0 & 0 \\ 1 & 0 & 0 & 0 \\ 0 & 0 & -1 & 0 \\ 0 & 0 & 0 & -1 \end{pmatrix}, \tag{1.6}$$

Then the scalar product of two four-vectors a^μ and b^μ reads

$$ab = a^+b^- + a^-b^+ + a^ib_i = a^+b^- + a^-b^+ - \boldsymbol{a}^\perp\boldsymbol{b}^\perp, \tag{1.7}$$

where $\boldsymbol{a}^\perp = (a^1, a^2)$ and $\boldsymbol{b}^\perp = (b^1, b^2)$.

1.2 Light-cone bispinor basis

One of systematic ways of treating the bispinor part is by expanding it in a complete basis set. The bispinor basis, which is customary used in calculations, is [Halzen and Martin, 1984]

$$\{1, \gamma^5, \gamma^\mu, \gamma^\mu\gamma^5, \sigma^{\mu\nu}\}, \tag{1.8}$$

where 1 denotes the identity matrix, γ^μ are Dirac gamma matrices, $\sigma^{\mu\nu} = (\gamma^\mu\gamma^\nu - \gamma^\nu\gamma^\mu)/2$, and $\gamma^5 = (i/4!)\epsilon_{\varkappa\lambda\mu\nu}\gamma^\varkappa\gamma^\lambda\gamma^\mu\gamma^\nu$. Any product Γ of gamma matrices can be decomposed as

$$\Gamma = C_1 + C_5\gamma^5 + C_\mu\gamma^\mu + C_{5\mu}\gamma^\mu\gamma^5 + C_{\mu\nu}\sigma^{\mu\nu}, \tag{1.9}$$

where

$$\begin{aligned} C_1 =& \frac{1}{4}\mathrm{Tr}\{\Gamma\}, \quad C_5 = \frac{1}{4}\mathrm{Tr}\{\gamma^5\Gamma\}, \quad C_\mu = \frac{1}{4}\mathrm{Tr}\{\gamma_\mu\Gamma\}, \\ C_{5\mu} &= -\frac{1}{4}\mathrm{Tr}\{\gamma_\mu\gamma^5\Gamma\}, \quad C_{\mu\nu} = -\frac{1}{8}\mathrm{Tr}\{\sigma_{\mu\nu}\Gamma\}. \end{aligned} \tag{1.10}$$

An example of the use of the basis (1.8) is the evaluation of polarization tensor in a plane-wave field by Meuren et al. (2013). The basis (1.8) is also employed, e.g., to describe polarization states of quarks in hadrons [Barone et al., 2002].

Another approach is to use the basis (1.8) in order to perform the Fierz transformation [Okun, 1984] and write the total trace as a combination of traces with smaller amount of gamma matrices each. This approach was investigated by Hartin (2016).

With either of the approaches, the trace evaluation for scattering in a plane-wave field still remains a very tedious task. As we will see, there is a way to greatly simplify the challenging evaluation of the bispinor part. For this purpose, in this subsection we construct a light-cone bispinor basis, which is tailored to our needs. Later, it is shown how this basis can be used for obtaining compact expressions in a relatively easy way, in comparison with the previously developed methods.

We start by considering Dirac gamma-matrix algebra on the light cone. Light-cone gamma matrices are defined as in Eq. (1.4):

$$\gamma^+ = \gamma\eta, \quad \gamma^- = \gamma\bar{\eta}, \quad \gamma^i = -\gamma e_i, \quad i = 1, 2. \tag{1.11}$$

All possible linear combinations and products of γ^+ and γ^- will be customary refered to as longitudinal space, and all possible linear combinations and products of γ^1 and γ^2 will be called transverse space.

The usual relations for gamma matrices in the instant form, which are written in the Lorentz-covariant way (see, e.g.,[Berestetskii et al., 1982]), are of course also valid in the front form, since the light-cone gamma matrices are defined in the Lorentz-covariant way too. Apart from those, we have the following relations for γ^+ and γ^-:

$$\gamma^+\gamma^+ = \gamma^-\gamma^- = 0, \quad \gamma^+\gamma^-\gamma^+ = 2\gamma^+, \quad \gamma^-\gamma^+\gamma^- = 2\gamma^-. \tag{1.12}$$

The relations (1.12) are easily proved with the use of the general properties (1.2) and the relation $\gamma^\mu\gamma^\nu + \gamma^\nu\gamma^\mu = 2g^{\mu\nu}$. For example, for $\gamma^+\gamma^+$ we have:

$$\gamma^+\gamma^+ = \gamma^\mu\gamma^\nu\eta_\mu\eta_\nu = \frac{1}{2}g^{\mu\nu}\eta_\mu\eta_\nu = 0. \tag{1.13}$$

The other properties in Eq. (1.12) are verified in an analogous way.

Going further, we notice that due to $g^{\pm i} = 0$, gamma matrices in the transverse space anticommute with $\gamma^\pm$:

$$\{\gamma^\pm, \gamma^i\} = 0. \tag{1.14}$$

The anticommutativity allows us to prove the following relation:

$$\mathrm{Tr}\{\gamma^{i_1}\gamma^{i_2}\ldots\gamma^{i_n}\gamma^+\gamma^-\} = \mathrm{Tr}\{\gamma^{i_1}\gamma^{i_2}\ldots\gamma^{i_n}\gamma^-\gamma^+\} = \mathrm{Tr}\{\gamma^{i_1}\gamma^{i_2}\ldots\gamma^{i_n}\}. \tag{1.15}$$

For odd n, all the three traces are zero. For even n, in order to obtain Eq. (1.15), we exchange one of the matrices γ^+ or γ^- n times with the transverse gamma matrices and use the identity $\gamma^+\gamma^- + \gamma^-\gamma^+ = 2$.

With the obtained relations, we see that a trace of arbitrary number of gamma matrices, if treated on the light cone, is reduced to a trace over gamma matrices in the transverse space only, so, we can always reduce a problem to essentially a two-dimensional one.

Note also the following identities:

$$\gamma^i\gamma^j\gamma_i = 0; \tag{1.16}$$

$$\mathrm{Tr}\{\gamma^\lambda\gamma^\mu\gamma^\nu\gamma^1\gamma^2\gamma^+\} = 4\epsilon^{\varkappa\lambda\mu\nu}\eta_\varkappa, \quad \mathrm{Tr}\{\gamma^\lambda\gamma^\mu\gamma^\nu\gamma^1\gamma^2\gamma^-\} = -4\epsilon^{\varkappa\lambda\mu\nu}\bar{\eta}_\varkappa, \tag{1.17}$$

where for the Levi-Civita symbol $\epsilon^{\varkappa\lambda\mu\nu}$, we choose $\epsilon^{+-12} = -1$, which is consistent with the choice $\epsilon^{0123} = 1$ in the instant form, if we assume the coordinate system, defined by Eq. (1.1).

As one more step, we define the projectors $\Lambda_+ = \gamma^-\gamma^+/2$ and $\Lambda_- = \gamma^+\gamma^-/2$ [Mitter, 1975; Mustaki et al., 1991; Brodsky et al., 1998]. The projectors have the following properties:

$$\Lambda_+ + \Lambda_- = 1, \quad \Lambda_+\Lambda_+ = \Lambda_+, \quad \Lambda_-\Lambda_- = \Lambda_-, \quad \Lambda_+\Lambda_- = \Lambda_-\Lambda_+ = 0. \tag{1.18}$$

The first relation is just the statement $\gamma^+\gamma^- + \gamma^-\gamma^+ = 2$, and the rest follow directly from the identities (1.12).

Now, we are ready to construct the light-cone bispinor basis. Since any product of gamma matrices can be represented as a product with all the transverse matrices on one side from the longitudinal ones, we seek for the basis having the form of the product $\{\text{transverse}\} \times \{\text{longitudinal}\}$. In the transverse space there are four linearly independent combinations: 1, γ^1, γ^2, $\gamma^1\gamma^2$. In the longitudinal space there are four linearly independent combinations as well: $\gamma^{\pm}$, $\Lambda_{\pm}$ (the identity matrix is excluded due to $\Lambda_+ + \Lambda_- = 1$). Therefore, the 16 matrices

$$\left\{1, \gamma^1, \gamma^2, \gamma^1\gamma^2\right\} \times \left\{\gamma^+, \gamma^-, \Lambda_+, \Lambda_-\right\} \tag{1.19}$$

exhaust all possible combinations of linearly independent gamma-matrix products and any product Γ can be represented as

$$\Gamma = \sum_{a=\pm}(C_a + C_a^i\gamma_i + C_a^{12}\gamma^1\gamma^2)\gamma^a + \sum_{a=\pm}(D_a + D_a^i\gamma_i + D_a^{12}\gamma^1\gamma^2)\Lambda_a. \tag{1.20}$$

The coefficients are given by

$$\begin{aligned} C_\pm &= \frac{1}{4}\mathrm{Tr}\{\Gamma\gamma^\mp\}, \quad C_\pm^i = -\frac{1}{4}\mathrm{Tr}\{\Gamma\gamma^i\gamma^\mp\}, \quad C_\pm^{12} = -\frac{1}{4}\mathrm{Tr}\{\Gamma\gamma^1\gamma^2\gamma^\mp\}, \\ D_\pm &= \frac{1}{2}\mathrm{Tr}\{\Gamma\Lambda_\pm\}, \quad D_\pm^i = \frac{1}{2}\mathrm{Tr}\{\Gamma\gamma^i\Lambda_\pm\}, \quad D_\pm^{12} = -\frac{1}{2}\mathrm{Tr}\{\Gamma\gamma^1\gamma^2\Lambda_\pm\}. \end{aligned} \tag{1.21}$$

Let us conclude this section by demonstrating how the matrices (1.8) can be expressed via the basis (1.19). Apart from γ^μ, which are in both bases, the expansion for the combinations of the matrices in the transverse space via the basis (1.19) immediately follows from $\Lambda_+ + \Lambda_- = 1$. We also note that $\sigma^{+-} = \Lambda_- - \Lambda_+$ and $\sigma^{\pm i} = -\gamma^i\gamma^\pm$. The rest of the elements in the basis (1.8) are with γ^5, and they are given by

$$\gamma^5 = -i\gamma^1\gamma^2(\Lambda_+ - \Lambda_-), \quad \gamma^i\gamma^5 = i\epsilon^{ij}\gamma^j(\Lambda_+ - \Lambda_-), \quad \gamma^\pm\gamma^5 = -i\gamma^1\gamma^2\gamma^\pm, \tag{1.22}$$

where the Levi-Civita symbol ϵ^{ij} is defined with $\epsilon^{12} = 1$.

1.3 Classical plane-wave field

When considering a process in an external laser field, in principle, the laser field itself needs to be treated at quantum level. We assume, however, that the laser field intensity is high enough and the depletion of the field during a scattering process is small enough, such that it can be approximated as a classical one [Berson, 1969; Bergou and Varró, 1981]. In the following, we describe the laser field as a plane wave (not necessarily monochromatic though), i.e., it is defined by the antisymmetric field tensor $F^{\mu\nu}(\phi) = -F^{\nu\mu}(\phi)$, where $\phi = k_0x$ with k_0^μ being the characteristic four-momentum of the field ($k_0^\mu k_{0\mu} = 0$). For a treatment of the laser field beyond the plane-wave approximation, see [Di Piazza, 2014, 2015, 2016]. For examples of studying electrodynamic processes in an external single-mode quantized field, see [Bergou and Varró, 1981; Skoromnik et al., 2013].

Let us find a general form for the plane-wave field tensor $F^{\mu\nu}(\phi)$. We know that it satisfies homogeneous Maxwell's equations [Landau and Lifshitz, 1987]

$$\partial_\mu F^{\mu\nu} = 0, \quad \partial_\mu({*F})^{\mu\nu} = 0, \tag{1.23}$$

where $({*F})^{\mu\nu} = \epsilon^{\mu\nu\sigma\tau}F_{\sigma\tau}/2$ is the dual tensor.

We expand the field tensor $F^{\mu\nu}(\phi)$ in the basis, which is the product of the light-cone basis $\{\eta^\mu, \bar{\eta}^\mu, e_1^\mu, e_2^\mu\}$ with itself. In this basis, η^μ is defined as

$$\eta^\mu = k_0^\mu/m, \tag{1.24}$$

which means that $\phi = mx^+$ (the electron mass m is introduced in order to have η^μ dimensionless). The rest of the four-vectors may be arbitrary, under the conditions (1.2). Due to $F^{\mu\nu}(\phi)$ being antisymmetric, there are at most 6 nonzero linearly independent coefficients in this expansion.

We impose the condition that $F^{\mu\nu}(\phi)$ does not have a constant component, but contains only a ϕ-dependent part. Then, from the first of Maxwell's equations (1.23), it follows that all the coefficients for the tensor combinations with $\bar{\eta}^\mu$ must vanish, and from the second of Maxwell's equations (1.23) it follows that also the coefficient for the combination $e_1^\mu e_2^\nu - e_2^\mu e_1^\nu$ must vanish. Therefore, only two nonzero coefficients are left and the general form of a plane-wave field tensor can be written as

$$F^{\mu\nu}(\phi) = \sum_{i=1,2} f_i^{\mu\nu} \psi_i'(\phi), \tag{1.25}$$

where $f_i^{\mu\nu} = k_0^\mu a_i^\nu - k_0^\nu a_i^\mu$, four-vectors a_i^μ define the amplitude of the field in two polarizarion directions ($k_0 a_i = 0$, $a_1 a_2 = 0$), and functions $\psi_i(\phi)$ characterize the shape ($|\psi_i'| \lesssim 1$, with the prime denoting the derivative with respect to the function argument). Normally, we assume that the field vanishes asymptotically: $\psi_i'(\pm\infty) = 0$.

A field tensor $F^{\mu\nu}(x)$ can be expressed via a vector potential $A^\mu(x)$ as $F^{\mu\nu}(x) = \partial^\mu A^\nu(x) - \partial^\nu A^\mu(x)$. We adopt the light-cone gauge [Brodsky et al., 1998], which restricts $A^\mu(x)$ by the condition

$$A^+(x) = 0. \tag{1.26}$$

Then the vector potential for the field tensor (1.25) can be written as

$$A^\mu(\phi) = \sum_{i=1,2} a_i^\mu \psi_i(\phi). \tag{1.27}$$

Note that $A^\mu(\phi)$ in Eq. (1.27) satisfies the Lorenz condition $\partial_\mu A^\mu(\phi) = 0$.

The choice (1.24) is kept in all the following calculations (with the only exception being the derivation of the lightfront Hamiltonian in the next section; there we keep a general light-cone basis). As for the other components, we could introduce the coordinate system with the plane wave propagating along the z-axis (in the negative direction), such that our light-cone coordinates are analogous to Eq. (1.1):

$$x^+ = \frac{\omega_0}{m}(x^0 + x^3), \quad x^- = \frac{m}{2\omega_0}(x^0 - x^3), \quad x^i|_{\text{front}} = x^i|_{\text{instant}}. \tag{1.28}$$

Again, we would like to keep manifest Lorentz-covariance. Moreover, if one considers a particle (or a system of particles), which is characterized by some four-momentum q^μ, it is convenient to use a frame, in which this particle (the system of particles) does not have a transverse momentum component. The transition to this frame can be performed by defining the light-cone basis $\{\eta^\mu, \bar{\eta}^\mu, e_1^\mu, e_2^\mu\}$ as [Meuren, 2015]:

$$\eta^\mu = \frac{k_0^\mu}{m}, \quad \bar{\eta}^\mu = \frac{q^\mu}{q^+} - \frac{q^2\eta^\mu}{2q^{+2}}, \quad e_1^\mu = \Lambda_1^\mu = \frac{q_\nu f_1^{\nu\mu}}{mq^+\sqrt{-a_1^2}}, \quad e_2^\mu = \Lambda_2^\mu = \frac{q_\nu f_2^{\nu\mu}}{mq^+\sqrt{-a_2^2}}. \tag{1.29}$$

[the definition of η^μ is the same as in Eq. (1.24), it is repeated here for convenience]. Following Meuren (2015), we call the basis (1.29) canonical light-cone basis. The four-vector q^μ is such that $q^+ \neq 0$. The choice of q^μ will depend on the considered process.

Note that if $q^2 = 0$, then $\boldsymbol{q}$ always counterpropagates the plane wave in the frame defined by Eq. (1.29).

It should be pointed out that if we simultaneously changed the sign of both η^μ and $\bar{\eta}^\mu$, the resulting basis would still satisfy the conditions (1.2). This would change the sign of all '+' and '−' components though. In the case of η^μ defined by Eq. (1.24), in any frame $\eta^0 > 0$, therefore, for any on-shell particle with four-momentum q^μ the components q^+ and q^- are always nonnegative.

Before exploring the field theory of electromagnetic interaction, we spend a few moments on looking into classical dynamics of a pointlike charge in a plane-wave field. The reason is that the solution for this problem will reappear at quantum level, and in fact, will play a central role in describing the quantum dynamics as well.

We consider the Lorentz equation for an electron in a plane-wave background [Landau and Lifshitz, 1987]:

$$\frac{\mathrm{d}p^\mu}{\mathrm{d}\tau} = \frac{e}{m} F^{\mu\nu}(\phi) p_\nu, \tag{1.30}$$

where τ is the proper time. The solution is known [Landau and Lifshitz, 1987] and can be written in the form

$$\pi_p^\mu(\phi) = p^\mu - e[A^\mu(\phi) - A^\mu(\phi_0)] + \eta^\mu \left(\frac{ep[A(\phi) - A(\phi_0)]}{p^+} - \frac{e^2[A^2(\phi) - A^2(\phi_0)]}{2p^+} \right), \tag{1.31}$$

where p^μ is the electron four-momentum at $\phi = \phi_0$. We call $\pi_p^\mu(\phi)$ dressed four-momentum. Note that $\pi_p^2(\phi) = \pi_p^\mu(\phi)\pi_{p\mu}(\phi) = p^2$.

The dressed four-momentum $\pi_p^\mu(\phi)$ is gauge-invariant, it is clear from Eq. (1.30). It can be also explicitly shown by rewriting Eq. (1.31) in a manifestly gauge-invariant form:

$$\pi_p^\mu(\phi) = p^\mu + \frac{e}{mp^+} \mathcal{F}^{\mu\nu}(\phi, \phi_0) p_\nu + \frac{e^2}{2p^+ m^2} \mathcal{F}^{2\mu\nu}(\phi,\phi_0) \bar{\eta}_\nu, \tag{1.32}$$

where we introduced the integrated field tensor [Meuren et al., 2013]:

$$\mathcal{F}^{\mu\nu}(\phi, \phi_0) = \int_{\phi_0}^{\phi} \mathrm{d}\beta\, F^{\mu\nu}(\beta), \quad \mathcal{F}^{2\mu\nu}(\phi, \phi_0) = \mathcal{F}^{\mu\rho}(\phi, \phi_0) \mathcal{F}_\rho{}^\nu(\phi, \phi_0). \tag{1.33}$$

In the following, we assume that $A^\mu(-\infty) = 0$, i.e., $\psi_i(-\infty) = 0$, therefore, Eq. (1.31) can be written as

$$\pi_p^\mu(\phi) = p^\mu - eA^\mu(\phi) + \eta^\mu \left(\frac{epA(\phi)}{p^+} - \frac{e^2 A^2(\phi)}{2p^+} \right), \tag{1.34}$$

with p^μ being the asymptotic four-momentum.

For the case $\phi_0 = -\infty$ we suppress the second argument for the integrated field tensor in Eq. (1.33) and write simply

$$\mathcal{F}^{\mu\nu}(\phi) = \int_{-\infty}^{\phi} \mathrm{d}\beta\, F^{\mu\nu}(\beta) = \sum_i f_i^{\mu\nu} \psi_i(\phi), \quad \mathcal{F}^{2\mu\nu}(\phi) = -k_0^\mu k_0^\nu \sum_i a_i^2 \psi_i^2(\phi) \tag{1.35}$$

[the relations via $\psi_i(\phi)$ are due to Eq. (1.25) and $\psi_i(-\infty) = 0$].

We also impose the condition that the integration over the whole time duration does not leave a constant component:

$$\int_{-\infty}^{\infty} \mathrm{d}\beta \, F^{\mu\nu}(\beta) = 0, \tag{1.36}$$

which, together with $\psi_i(-\infty) = 0$, implies that $\psi_i(\infty) = 0$.

1.4 Lightfront Hamiltonian

Our aim now is to obtain the Hamiltonian for interacting electron-positron and photon fields on the light cone. In general, we follow the ideas introduced by Mustaki et al. (1991) and later reiterated by Brodsky et al. (1998), therefore, we will discuss only major steps and important concepts (some details on the derivation of the lightfront Hamiltonian are provided in Appendix A). It should be noted, that, in comparison to the previous works, we do not tie ourselves to a particular frame, but use general properties in a light-cone basis $\{\eta^\mu, \bar{\eta}^\mu, e_1^\mu, e_2^\mu\}$. Most of the steps and the result, as might be expected, are the same, but some relations have to be derived in a different way. For one of those relations, an explicit derivation is shown [Eq. (1.48) below], other cases are treated similarly. Another subtlety is the presence of an external plane-wave field, which we want to take into account exactly. This will be also discussed below.

In vacuum, the QED Lagrangian density is given by [Halzen and Martin, 1984]

$$\mathcal{L} = \overline{\Psi}(\gamma i\partial - m)\Psi - \frac{1}{4}\hat{F}_{\mu\nu}\hat{F}^{\mu\nu} + e\overline{\Psi}\gamma^\mu\Psi\hat{A}_\mu, \tag{1.37}$$

where Ψ and $\hat{A}^\mu$ are the electron-positron and photon fields, respectively, $\hat{F}_{\mu\nu} = \partial_\mu\hat{A}_\nu - \partial_\nu\hat{A}_\mu$, and a bar denotes the Dirac conjugate: $\overline{\Psi} = \Psi^\dagger\gamma^0$.

In an external plane-wave field, the Lagrangian density is obtained by the shift of the photon field [Fradkin et al., 1991]

$$\hat{A}^\mu \to \hat{A}^\mu + A^\mu, \tag{1.38}$$

with A^μ being the potential of the classical field. Then one obtains that

$$\mathcal{L} = \overline{\Psi}(\gamma i\partial - m)\Psi - \frac{1}{4}\hat{F}_{\mu\nu}\hat{F}^{\mu\nu} + e\overline{\Psi}\gamma^\mu\Psi(A_\mu + \hat{A}_\mu). \tag{1.39}$$

In Eq. (1.39) we do not write the terms with the free part of the classical field. With the help of integrations by parts it can be shown that the contribution from those terms vanishes.

Let us look at the equations of motion first. For the photon field, from the least action principle, we obtain Maxwell's equation

$$\partial_\mu\hat{F}^{\mu\nu} = J^\nu, \tag{1.40}$$

with $J^\mu = e\overline{\Psi}\gamma^\mu\Psi$. Since we employ the light-cone gauge [see Eq. (1.26)], the '+' component of Maxwell's equation is given by

$$\partial_\mu\hat{F}^{\mu+} = -(\partial_-)^2\hat{A}^- - \partial_-\partial_i\hat{A}^i = J^+. \tag{1.41}$$

Note that Eq. (1.41) does not contain time derivatives, therefore, it is not an equation of motion, but a constraint, which leaves just two independent degrees of freedom for $\hat{A}^\mu$. We split $\hat{A}^\mu$ into two parts: $\hat{A}^\mu = \mathcal{A}^\mu + \alpha^\mu$, where α^μ has only a '$-$' component, which is defined via

$$\alpha^- = \frac{1}{(i\partial_-)^2} J^+. \tag{1.42}$$

The rest of $\hat{A}^\mu$ is labeled as $\mathcal{A}^\mu$, it contains two independent degrees of freedom, with the third defined via

$$-(\partial_-)^2 \mathcal{A}^- - \partial_- \partial_i \mathcal{A}^i = 0. \tag{1.43}$$

By construction, the field $\mathcal{A}^\mu$ satisfies the Lorenz condition $\partial_\mu \mathcal{A}^\mu = 0$.

We proceed by considering the equation of motion for the electron-positron field. From Eq. (1.39) we obtain Dirac equation

$$[\gamma(i\partial - eA - e\hat{A}) - m]\Psi = 0. \tag{1.44}$$

Multiply Eq. (1.44) by γ^+ from the left, then:

$$2i\partial_-\Psi_- - [\gamma^k(i\partial_k - eA_k - e\hat{A}_k) + m]\gamma^+\Psi_+ = 0, \tag{1.45}$$

where $\Psi_\pm = \Lambda_\pm \Psi$ ($\Psi = \Psi_+ + \Psi_-$ due to $\Lambda_+ + \Lambda_- = 1$). Eq. (1.45) is again a constraint, which allows us to express Ψ_- via Ψ_+. We define $\chi = \chi_+ + \chi_-$ with $\chi_+ = 0$ and

$$\chi_- = -\frac{1}{2i\partial_-} e\gamma^k \hat{A}_k \gamma^+ \Psi_+. \tag{1.46}$$

The rest of Ψ is labeled as ψ, so, $\psi_+ = \Psi_+$ and

$$\psi_- = \frac{1}{2i\partial_-}[\gamma^k(i\partial_k - eA_k) + m]\gamma^+\psi_+. \tag{1.47}$$

Note that the classical field $A^\mu(x)$ is included into ψ_-.

As an intermediate result, we have introduced fields $\mathcal{A}^\mu$ and ψ that contain all independent degrees of freedom and also some dependent parts, which are connected to the independent ones as in the noninteracting theory. Since the remaining quantities α^μ and χ have to be functionals of $\mathcal{A}^\mu$ and ψ, the fields $\hat{A}^\mu$ and Ψ can be ultimately expressed completely via $\mathcal{A}^\mu$ and ψ. Indeed, it is clear from Eq. (1.46), that χ_- is a functional of only $\mathcal{A}^\mu$ and ψ. The same is true for α^- in Eq. (1.42), in particular, we have for J^+:

$$\begin{aligned} J^+ = e\overline{\Psi}\gamma^+\Psi = e(\Lambda_+\Psi_+ + \Lambda_-\Psi_-)^\dagger\gamma^0\gamma^+\Psi_+ &= e(\overline{\Psi}_+\Lambda_- + \overline{\Psi}_-\Lambda_+)\gamma^+\Psi_+ \\ &= e\overline{\Psi}_+\gamma^+\Psi_+ = e\overline{\psi}\gamma^+\psi. \end{aligned} \tag{1.48}$$

Now, we proceed with obtaining an expression for the lightfront Hamiltonian, with the goal in mind to write it in terms of $\mathcal{A}^\mu$ and ψ.

The canonical stress-energy tensor is obtained from the Lagrangian (1.39) in the usual way:

$$\begin{aligned} T^{\mu\nu} &= \sum_A \frac{\partial\mathcal{L}}{\partial(\partial_\mu\phi_A)}\partial^\nu\phi_A - g^{\mu\nu}\mathcal{L} \\ &= \overline{\Psi}[\gamma^\mu i\partial^\nu - g^{\mu\nu}(\gamma i\partial - m)]\Psi - \hat{F}^{\mu\sigma}\partial^\nu\hat{A}_\sigma + g^{\mu\nu}\frac{1}{4}\hat{F}_{\mu\nu}\hat{F}^{\mu\nu} - g^{\mu\nu}J^\sigma(A_\sigma + \hat{A}_\sigma). \end{aligned} \tag{1.49}$$

The (light-cone) time component of the stress-energy tensor defines the four-momentum of our system:

$$P^\nu = \int \mathrm{d}^2x^\perp \mathrm{d}x^- T^{+\nu}. \tag{1.50}$$

Correspondingly, the Hamiltonian is the '$-$' component of P^ν:

$$H = P^- = \int \mathrm{d}^2x^\perp \mathrm{d}x^- T^{+-}, \tag{1.51}$$

where [see Eq. (1.49)]

$$T^{+-} = \overline{\Psi}[\gamma^+ i\partial_+ - (\gamma i\partial - m)]\Psi - \hat{F}^{+\sigma}\partial_+\hat{A}_\sigma + \frac{1}{4}\hat{F}_{\mu\nu}\hat{F}^{\mu\nu} - J^\sigma(A_\sigma + \hat{A}_\sigma). \tag{1.52}$$

Expressing the dependent fields α^μ and χ via $\mathcal{A}^\mu$ and ψ, with the help of several integrations by parts, we arrive at the result (details are given in Appendix A) [Mustaki et al., 1991; Brodsky et al., 1998]:

$$H = H_0 + V_1 + V_2 + V_3 \tag{1.53}$$

with

$$\begin{aligned}
H_0 &= \int \mathrm{d}^2x^\perp \mathrm{d}x^- \left[\overline{\psi}\gamma^- i\partial_-\psi + e\overline{\psi}\gamma^+\psi A^- + \frac{1}{2}(\partial_-\mathcal{A}^-)^2 + \frac{1}{2}(\partial_1\mathcal{A}_2 - \partial_2\mathcal{A}_1)^2\right],\\
V_1 &= e\int \mathrm{d}^2x^\perp \mathrm{d}x^- \,\overline{\psi}\gamma^\mu\psi\mathcal{A}_\mu,\\
V_2 &= \int \mathrm{d}^2x^\perp \mathrm{d}x^- \,\overline{\chi}\gamma^- i\partial_-\chi = \frac{e^2}{2}\int \mathrm{d}^2x^\perp \mathrm{d}x^- \,\mathcal{A}_\mu\overline{\psi}\gamma^\mu\frac{\gamma^+}{i\partial_-}\gamma^\nu\psi\mathcal{A}_\nu,\\
V_3 &= \frac{1}{2}\int \mathrm{d}^2x^\perp \mathrm{d}x^- \,J^+\frac{1}{(i\partial_-)^2}J^+ = \frac{e^2}{2}\int \mathrm{d}^2x^\perp \mathrm{d}x^- \,\overline{\psi}\gamma^+\psi\frac{1}{(i\partial_-)^2}\overline{\psi}\gamma^+\psi.
\end{aligned} \tag{1.54}$$

The part H_0 of the Hamiltonian is the one, that remains if we turn off the interaction between fermions and photons, therefore, it is regarded as the free Hamiltonian. The interaction with the external field is included into the free part. The resulting representation upon quantinzation is known as the Furry picture [Furry, 1951] (see also [Fradkin et al., 1991]). The other three terms are interaction terms, they will be treated perturbatively. The three terms give rise to three types of interaction vertices, namely, V_1 corresponds to the usual three-point interaction vertex of QED, V_2 corresponds to the instant-fermion exchange vertex (the seagull vertex), and V_3 corresponds to the instant-photon exchange vertex (the self-interaction vertex).

Due to the split of Ψ according to Eqs. (1.46) and (1.47), in the interaction terms the classical field A^μ appears only inside ψ. Upon solving the equation of motion for ψ, the interaction of fermions with the classical field is taken into account exactly.

After the quantization of the Hamiltonian (1.53), we transfer into the interaction picture. In that picture the fields $\mathcal{A}^\mu$ and ψ in Eq. (1.54) obey the free equations of motion. Therefore, before actually quantizing H we would like to understand how (still classical) free fields $\mathcal{A}^\mu_{\text{free}}$ and ψ_{free} can be expanded in terms of Fourier modes (for simplicity, in the following we omit 'free' in the subscript and write simply $\mathcal{A}^\mu$ and ψ). For $\mathcal{A}^\mu$ the equations of motion are homogeneous Maxwell's equations, so, the expansion goes in terms of (monochromatic) plane waves. For ψ the equation of motion is Dirac equation in a plane-wave field. The solution is known as the Volkov solution and is discussed in the next section.

1.5 Volkov wave function

We need to find a solution for the Dirac equation

$$[\gamma(i\partial - eA) - m]\psi = 0. \tag{1.55}$$

The solution was first obtained by Volkov (1935), and it is known correspondingly as the Volkov solution or Volkov wave function. In this section, we demonstrate a way of deriving the Volkov wave function on the light cone. In our approach a convenient form of the Volkov solution appears in a natural fashion. Note that the ideas, that we will use in our derivation, were originally developed by Mitter (1975).

Let us start with defining an initial condition. We require that in some point $x^+ = x_0^+$ the Volkov wave function (positive-frequency $\psi_{p\sigma}$ and negative-frequency $\psi_{p\sigma}^{(-)}$) transforms into the corresponding solution for Dirac equation in vacuum (x_0^+ is customary chosen as zero or $-\infty$):

$$\psi_{p\sigma}(x)\big|_{x_0^+} = \psi_{0,p\sigma}(x)\big|_{x_0^+}, \quad \psi_{p\sigma}^{(-)}(x)\big|_{x_0^+} = \psi_{0,p\sigma}^{(-)}(x)\big|_{x_0^+}, \tag{1.56}$$

with

$$\psi_{0,p\sigma}(x) = \frac{u_{p\sigma}}{\sqrt{2p^+\mathcal{V}}}\mathrm{e}^{-ipx}, \quad \psi_{0,p\sigma}^{(-)}(x) = \frac{v_{p\sigma}}{\sqrt{2p^+\mathcal{V}}}\mathrm{e}^{ipx}, \tag{1.57}$$

where p denotes the asymptotic four-momentum p^μ and σ denotes a polarization state.

The notation, that is introduced in Eq. (1.57), needs to be explained. We assume to work in a finite (light-cone) space volume $\mathcal{V}$. However, the volume $\mathcal{V}$ is supposed to be so large, that we can approximate Kronecker symbols and sums with their continuous analogs:

$$\delta_{pp'} \to \frac{(2\pi)^3}{\mathcal{V}}\delta^{(+,\perp)}(p-p'), \quad \sum_p \to \int \frac{\mathcal{V}\mathrm{d}^2p^\perp}{(2\pi)^2}\int_0^\infty \frac{\mathrm{d}p^+}{2\pi}, \tag{1.58}$$

where $\delta^{(+,\perp)}(p-p') = \delta(p^+ - p'^+)\delta(p^1 - p'^1)\delta(p^2 - p'^2)$. Note that we have only on-shell particles as of now, therefore, p^+ is always positive.

With the rules (1.58), one can use the continuous notation, and at the same time keep track of the volume factors, such that it is easy to ensure that in the final expressions they cancel each other and observables do not depend on them. For observables, it is assumed that the limit of the infinite volume is taken, such that the integration in space-time coordinates is formally extended to $\mathbb{R}^4$.

The bispinors $u_{p\sigma}$ and $v_{p\sigma}$ in Eq. (1.57) are normalized according to

$$\overline{u}_{p\sigma}u_{p\sigma'} = -\overline{v}_{p\sigma}v_{p\sigma'} = 2m\delta_{\sigma\sigma'}, \tag{1.59}$$

therefore

$$\overline{u}_{p\sigma}\gamma^\mu u_{p\sigma'} = \overline{v}_{p\sigma}\gamma^\mu v_{p\sigma'} = 2p^\mu\delta_{\sigma\sigma'}, \tag{1.60}$$

and

$$\sum_\sigma u_{p\sigma}\overline{u}_{p\sigma} = \gamma p + m, \quad \sum_\sigma v_{p\sigma}\overline{v}_{p\sigma} = \gamma p - m. \tag{1.61}$$

Let us proceed with solving Eq. (1.55). We know from Eq. (1.47) that ψ_- is not a dynamical component, therefore, if ψ_+ is found, the whole solution can be reconstructed. First, let us obtain an equation for ψ_+. We multiply Eq. (1.55) by γ^- and subsequently take a derivative of it with respect to x^-. With the use of Eq. (1.47), it is found that

$$2i\partial_-(i\partial_+ - eA^-)\psi_+ - [m^2 - (i\partial_k - eA_k)^2]\psi_+ = 0. \tag{1.62}$$

An interesting feature of Eq. (1.62) is that it is diagonal with respect to the components of ψ_+ (compare with the corresponding second-order differential equation in [Berestetskii et al., 1982]).

We seek a solution of the original Dirac equation (1.55) in the form (we concentrate on the positive-frequency solution, the negative-frequency one is derived in the same way)

$$\psi_{p\sigma}(x) = \mathrm{e}^{-ipx} F(x^+), \tag{1.63}$$

therefore

$$\psi_{p\sigma+}(x) = \mathrm{e}^{-ipx} F_+(x^+). \tag{1.64}$$

We obtain the following differential equation for $F_+(x^+)$:

$$iF_+'(x^+) = [\pi_p^-(\phi) - p^- + eA^-(\phi)]F_+(x^+), \tag{1.65}$$

where $\pi_p^-(\phi) = [\boldsymbol{\pi}_p^{\perp 2}(\phi)+m^2]/2p^+$ is the '–' component of the classical dressed momentum from Eq. (1.34). The integration of Eq. (1.65) leads to $F_+(x^+) = F_{0,+}\exp[-i\mathcal{S}_p(\phi,\phi_0)]$, where

$$\mathcal{S}_p(\phi,\phi_0) = \frac{1}{m}\int\limits_{\phi_0}^{\phi} \mathrm{d}\beta\,[\pi_p^-(\beta) - p^- + eA^-(\beta)] = \int\limits_{\phi_0}^{\phi} \mathrm{d}\beta\left(\frac{epA(\beta)}{mp^+} - \frac{e^2A^2(\beta)}{2mp^+}\right) \tag{1.66}$$

with $\phi_0 = mx_0^+$ [the right-hand expression is due to Eq. (1.34)]. The constant bispinor $F_{0,+}$ is found from the initial condition in Eqs. (1.56) and (1.57) and we obtain:

$$\psi_{p\sigma+}(x) = \frac{\Lambda_+ u_{p\sigma}}{\sqrt{2p^+\mathcal{V}}}\mathrm{e}^{-ipx-i\mathcal{S}_p(\phi,\phi_0)}. \tag{1.67}$$

Having the '+' projection of the Volkov wave function, we proceed with the '–' one. The inversion of $i\partial_-$ in Eq. (1.47) gives the factor $1/p^+$, we also need to replace $i\partial_k$ with p_k. Then, upon summing the two parts, one obtains:

$$\psi_{p\sigma}(x) = K_p(\phi)\frac{u_{p\sigma}}{\sqrt{2p^+\mathcal{V}}}\mathrm{e}^{-ipx-i\mathcal{S}_p(\phi,\phi_0)}, \quad K_p(\phi) = [\gamma\pi_p(\phi)+m]\frac{\gamma^+}{2p^+}. \tag{1.68}$$

With the use of the Dirac equation $(\gamma p - m)u_{p\sigma} = 0$ the solution (1.68) can be recast into a different form:

$$\psi_{p\sigma}(x) = \mathcal{K}_p(\phi)\frac{u_{p\sigma}}{\sqrt{2p^+\mathcal{V}}}\mathrm{e}^{-ipx-i\mathcal{S}_p(\phi,\phi_0)}, \quad \mathcal{K}_p(\phi) = 1 + \frac{e\gamma^+\gamma A(\phi)}{2p^+}. \tag{1.69}$$

The form in Eq. (1.69) is well-known [Brown and Kibble, 1964; Nikishov and Ritus, 1964b], the form in Eq. (1.68) was presented and applied by Hartin (2016). We will use the former expression (1.68), which turns out to be more convenient, than the latter one.

For the negative-energy Volkov wave function we obtain:

$$\psi_{p\sigma}^{(-)}(x) = K_{-p}(\phi)\frac{v_{p\sigma}}{\sqrt{2p^+\mathcal{V}}}\mathrm{e}^{ipx-i\mathcal{S}_{-p}(\phi,\phi_0)} = \mathcal{K}_{-p}(\phi)\frac{v_{p\sigma}}{\sqrt{2p^+\mathcal{V}}}\mathrm{e}^{ipx-i\mathcal{S}_{-p}(\phi,\phi_0)}. \tag{1.70}$$

In the following, we choose $\phi_0 \to -\infty$ and write $\mathcal{S}_p(\phi,-\infty) = \mathcal{S}_p(\phi)$.

As we want to eventually expand our fermion field in Fourier modes, with each mode represented by the Volkov wave function, we consider orthogonality and particularly completeness of the Volkov solutions.

It is known, that the Volkov wave functions are orthogonal and complete in a fixed instant-form time point, though the prove is not straightforward, and in fact, this question has been tackled by several people [Ritus, 1985; Zakowicz, 2005; Boca and Florescu, 2010; Yakaboylu, 2015; Di Piazza, 2018]. The problem of orthogonality and completeness can be resolved in a somewhat elegant way on the light cone.

As for the orthogonality condition, written on the light cone as (again, we consider only the positive-energy solutions, for the negative-energy ones, the relation is the same)

$$\int \mathrm{d}^2x^\perp \mathrm{d}x^- \overline{\psi}_{p\sigma}(x)\gamma^+\psi_{p'\sigma'}(x) = \frac{(2\pi)^3}{\mathcal{V}}\delta^{(+,\perp)}(p-p')\delta_{\sigma\sigma'}, \tag{1.71}$$

it does not pose any problem and can be easily verified [Bergou and Varró, 1980].

The question of completeness is more subtle. It was shown by Bergou and Varró (1980), that in a fixed light-cone time point the Volkov wave functions do not satisfy the usual completeness relation, though the relation, that they satisfy, still allows an expansion of an arbitrary function.

From the perspective of quantizing the lightfront Hamiltonian [Eqs. (1.53) and (1.54)], in fact, we need to approach the problem in a different way. As we remember, only the '+' projection ψ_+ is a dynamical field. Therefore, what is actually required, is the completeness of the Volkov solutions in the subspace of the '+' projections. This can be proved in a straightforward fashion:

$$\begin{aligned}
&\sum_\sigma \int \frac{\mathcal{V}\mathrm{d}^2p^\perp}{(2\pi)^2}\int\limits_0^\infty \frac{\mathrm{d}p^+}{2\pi}\left[\psi_{p\sigma+}(x)\overline{\psi}_{p\sigma+}(x')\gamma^+ + \psi^{(-)}_{p\sigma+}(x)\overline{\psi}^{(-)}_{p\sigma+}(x')\gamma^+\right] \\
&= \left[\int\limits_0^\infty \frac{\mathrm{d}p^+}{2\pi}\mathrm{e}^{-ip^+(x-x')} + \int\limits_0^\infty \frac{\mathrm{d}p^+}{2\pi}\mathrm{e}^{ip^+(x-x')}\right]\Lambda_+\delta^{(\perp)}(x-x') = \Lambda_+\delta^{(-,\perp)}(x-x')
\end{aligned} \tag{1.72}$$

(for simplicity, we write x and x', but we keep in mind that the expression is evaluated at a common light-cone time point). Then any $\psi_+(x) = \Lambda_+\psi(x)$ can be expanded in terms of the Volkov solutions. Since the '−' projection $\psi_-(x)$ is defined via the Dirac equation of the noninteracting theory, upon summing $\psi_+(x)$ and $\psi_-(x)$ we recover the full Volkov wave functions, so, we obtain for our field in Eq. (1.54):

$$\psi(x) = \sum_\sigma \int \frac{\mathcal{V}\mathrm{d}^2p^\perp}{(2\pi)^2}\int\limits_0^\infty \frac{\mathrm{d}p^+}{2\pi}\left[a_{p\sigma}\psi_{p\sigma}(x) + b^*_{p\sigma}\psi^{(-)}_{p\sigma}(x)\right], \tag{1.73}$$

where the coefficients $a_{p\sigma}$ and $b^*_{p\sigma}$ are defined as:

$$a_{p\sigma} = \int \mathrm{d}^2x^\perp \mathrm{d}x^- \overline{\psi}_{p\sigma}(x)\gamma^+\psi(x), \quad b^*_{p\sigma} = \int \mathrm{d}^2x^\perp \mathrm{d}x^- \overline{\psi}^{(-)}_{p\sigma}(x)\gamma^+\psi(x). \tag{1.74}$$

The relations (1.73) and (1.74) look as they would for a usual complete set. However, $\psi(x)$ is not a general function in the Hilbert space, but restricted by the condition (1.47). In essense, the additional term, that was obtained by Bergou and Varró (1980) and that violates the usual completeness relation for the Volkov wave functions on the light cone, corresponds to the contribution to the interaction part, that we have separated out explicitly.

1.6 Quantized fields

We proceed by quantizing the fields $\mathcal{A}^\mu$ and ψ in the Hamiltonian H [Eqs. (1.53) and (1.54)]. The transition to the interaction representation is done basically in the same way, as in the vacuum case (see, e.g., [Itzykson and Zuber, 1980] or [Goldberger and Watson, 1964]). The difference is that our free Hamiltonian H_0 depends on time, this does not pose a problem though, since the dependence is through the classical field, which commutes in different time points. We obtain the following expression for the S-matrix:

$$S = \mathcal{T} \exp\left[-i \int \mathrm{d}x^+ (V_1 + V_2 + V_3)\right], \tag{1.75}$$

where $\mathcal{T}$ is the (light-cone) time-ordering operator.

For the quantized fields in the interaction representation one obtains respectively [Bjorken et al., 1971; Mustaki et al., 1991]:

$$\begin{aligned} \psi(x) &= \sum_\sigma \int \frac{\mathcal{V} \mathrm{d}^2 p^\perp}{(2\pi)^2} \int_0^\infty \frac{\mathrm{d}p^+}{2\pi} \left[a_{p\sigma} \psi_{p\sigma}(x) + b^\dagger_{p\sigma} \psi^{(-)}_{p\sigma}(x)\right], \\ \mathcal{A}^\mu(x) &= \sum_\lambda \int \frac{\mathcal{V} \mathrm{d}^2 k^\perp}{(2\pi)^2} \int_0^\infty \frac{\mathrm{d}k^+}{2\pi} \left[c_{k\lambda} \phi^\mu_{k\lambda}(x) + c^\dagger_{k\lambda} \phi^{*\mu}_{k\lambda}(x)\right], \end{aligned} \tag{1.76}$$

with the creation and annihilation operators satisfying the relations

$$\begin{aligned} \{a_{p\sigma}, a^\dagger_{p'\sigma'}\} &= \{b_{p\sigma}, b^\dagger_{p'\sigma'}\} = \frac{(2\pi)^3}{\mathcal{V}} \delta^{(+,\perp)}(p - p') \delta_{\sigma\sigma'}, \\ [c_{k\lambda}, c^\dagger_{k'\lambda'}] &= \frac{(2\pi)^3}{\mathcal{V}} \delta^{(+,\perp)}(k - k') \delta_{\lambda\lambda'}. \end{aligned} \tag{1.77}$$

In Eq. (1.76) $\phi^\mu_{k\lambda}(x)$ is a plane wave:

$$\phi^\mu_{k\lambda}(x) = \frac{\epsilon^\mu_{k\lambda}}{\sqrt{2k^+ \mathcal{V}}} \mathrm{e}^{-ikx}, \tag{1.78}$$

with the polarization four-vectors satisfying

$$\epsilon^\mu_{k\lambda} \epsilon^*_{k\lambda'\mu} = -\delta_{\lambda\lambda'}, \quad k_\mu \epsilon^\mu_{k\lambda} = 0. \tag{1.79}$$

There are two independent polarization states for the photon field, as well as for the electron-positron one, so, each λ and σ can have two different values. In the following, we will be always summing/averaging over the polarization states, therefore, we do not specify the choice of them, but note that several conventions exist [Brodsky et al., 1998]. Due to Eq. (1.5), one obtains

$$\sum_\lambda \epsilon^\mu_{k\lambda} \epsilon^{*\nu}_{k\lambda} = -g^{\mu\nu} + \frac{\eta^\mu k^\nu + \eta^\nu k^\mu}{k^+}. \tag{1.80}$$

Note that in vacuum the vector η^μ is chosen as a fixed light-like vector, which breaks the manifest Lorentz-covariance of the theory. Since in our case η^μ is a true four-vector, the theory in a plane-wave field formally remains manifestly Lorentz-covariant.

With Eq. (1.75) at hand, the whole machinery of the perturbative approach can be developed. In position space, one needs to insert the corresponding Volkov solutions for electrons and positrons in place of plane waves, which are employed in vacuum. In momentum space, the additional factors due to the presence of the classical field can be collected together in a vertex, and one obtains the usual QED in momentum space with, however, a modified or 'dressed' vertex (see [Meuren, 2015; Mitter, 1975]). In our case, there are three kinds of dressed vertices, which are discussed in the next section.

1.7 Dressed vertices

1.7.1 Three-point dressed vertex

We consider the interaction term V_1 in Eq. (1.54) and for definiteness assume to have an incoming electron with four-momentum p_1^μ, and two outgoing particles: an electron and a photon with four-momenta p_2^μ and k^μ, respectively. The particles are presumed to be also in some polarization states, we do not define them explicitly and suppress the corresponding indices, expecting to average/sum them out later with the use of Eqs. (1.61) and (1.80). For clarity, we also suppress the normalization factors for now and in the next two subsections. The complete expressions can be recovered if each bispinor u_p is divided by $\sqrt{2p^+\mathcal{V}}$ and each polarization four-vector ϵ_k^μ by $\sqrt{2k^+\mathcal{V}}$. One obtains:

$$-i\int \mathrm{d}x^+\langle kp_2|V_1|p_1\rangle \propto (2\pi)^3\delta^{(+,\perp)}(p_2+k-p_1)\overline{u}_2\left[-ie\Gamma^\mu_{21}(k)\right]u_1\epsilon^*_{k\mu}, \tag{1.81}$$

where

$$\Gamma^\mu_{21}(k) = \int \mathrm{d}x^+ K^\mu_{21}(\phi)\exp\left[i(p_2^- + k^- - p_1^-)x^+ + i\mathcal{S}_2(\phi) - i\mathcal{S}_1(\phi)\right] \tag{1.82}$$

and

$$K^\mu_{21}(\phi) = \overline{K}_2(\phi)\gamma^\mu K_1(\phi) = \frac{\gamma^+}{2p_2^+}\left[\gamma\pi_2(\phi)+m\right]\gamma^\mu\left[\gamma\pi_1(\phi)+m\right]\frac{\gamma^+}{2p_1^+}. \tag{1.83}$$

For simplicity, we replaced the subscripts $p_1 \to 1$, $p_2 \to 2$ (we will do the same below too, also for photons).

For later use, let us rewrite $K^\mu_{21}(\phi)$ in Eq. (1.83) in a convenient form. In particular, let us expand it in the light-cone bispinor basis (1.19). As can be noticed from Eq. (1.83), all the traces which involve γ^+, Λ_+, and Λ_- vanish, therefore, one needs to evaluate just three traces, which involve γ^- [see Eqs. (1.20) and (1.21)]. We obtain that

$$K^\mu_{21}(\phi) = \left[S^\mu_{21}(\phi) + V^{i\mu}_{21}\gamma_i + T^\mu_{21}(\phi)\gamma^1\gamma^2\right]\gamma^+, \tag{1.84}$$

where

$$\begin{aligned}
S^\mu_{21}(\phi) &= \frac{1}{2p_2^+p_1^+}\left\{p_2^+\pi_1^\mu(\phi) + p_1^+\pi_2^\mu(\phi) - \left[\pi_2(\phi)\pi_1(\phi) - m^2\right]g^{\mu+}\right\},\\
V^{i\mu}_{21} &= \frac{m}{2p_2^+p_1^+}\left[(p_2^+ - p_1^+)g^{\mu i} - (p_2^i - p_1^i)g^{\mu+}\right],\\
T^\mu_{21}(\phi) &= -\frac{1}{2p_2^+p_1^+}\epsilon_{\nu\rho\varkappa\lambda}g^{\mu\nu}\eta^\rho\pi_2^\varkappa(\phi)\pi_1^\lambda(\phi).
\end{aligned} \tag{1.85}$$

1.7.2 Seagull dressed vertex

Let us consider the interaction term V_2 in Eq. (1.54). Now we assume to have incoming fermion and photon with four-momenta p_1^μ and k_1^μ, respectively, and two outgoing particles: a fermion and a photon with four-momenta p_2^μ and k_2^μ, respectively. We obtain:

$$-i\int \mathrm{d}x^+ \langle k_2 p_2|V_2|k_1 p_1\rangle \propto (2\pi)^3\delta^{(+,\perp)}(p_2+k_2-p_1-k_1)$$
$$\times\,\overline{u}_2\Big[-\frac{ie^2}{2(p_1^+ + k_1^+)}\Gamma_{21}^{\mu\nu}(k_2,k_1)\Big]u_1\epsilon_{2\mu}^*\epsilon_{1\nu} + \{k_1\leftrightarrow -k_2, \epsilon_1\leftrightarrow\epsilon_2^*\}, \tag{1.86}$$

where

$$\Gamma_{21}^{\mu\nu}(k_2,k_1) = \int \mathrm{d}x^+ K_{21}^{\mu\nu}(\phi)\exp\Big[i(p_2^- + k_2^- - p_1^- - k_1^-)x^+ + i\mathcal{S}_2(\phi) - i\mathcal{S}_1(\phi)\Big], \tag{1.87}$$

$$K_{21}^{\mu\nu}(\phi) = \overline{K}_2(\phi)\gamma^\mu\gamma^+\gamma^\nu K_1(\phi) = \frac{\gamma^+}{2p_2^+}\left[\gamma\pi_2(\phi)+m\right]\gamma^\mu\gamma^+\gamma^\nu\left[\gamma\pi_1(\phi)+m\right]\frac{\gamma^+}{2p_1^+}, \tag{1.88}$$

and the term in the braces is the same as the first term, but with the photon momentum and polarization four-vectors exchanged, as designated.

For $K_{21}^{\mu\nu}(\phi)$, the expansion in the basis (1.19) goes in the same way, as in the case of the three-point interaction, and we obtain the following form, which again will be particularly useful for the evaluation of traces:

$$K_{21}^{\mu\nu}(\phi) = \Big[S_2^\mu + V_2^{i\mu}(\phi)\gamma_i\Big]\gamma^+\Big[S_1^\nu + V_1^{j\nu}(\phi)\gamma_j\Big], \tag{1.89}$$

where

$$S_p^\mu = \frac{m}{p^+}g^{\mu+}, \quad V_p^{i\mu}(\phi) = \frac{1}{p^+}\Big[p^+g^{\mu i} - \pi_p^i(\phi)g^{\mu+}\Big]. \tag{1.90}$$

1.7.3 Self-interaction dressed vertex

The last term out of the three interaction terms is V_3. Now there are two incoming electrons with four momenta p_1^μ and p_2^μ and two outgoing ones, with four-momenta p_3^μ and p_4^μ. We obtain:

$$-i\int \mathrm{d}x^+\langle p_4 p_3|V_3|p_2 p_1\rangle \propto (2\pi)^3\delta^{(+,\perp)}(p_4+p_3-p_2-p_1)$$
$$\times\int \mathrm{d}x^+\overline{u}_4\Gamma_{42}(\phi)u_2\frac{-ie^2}{(p_1^+ - p_3^+)^2}\overline{u}_3\Gamma_{31}(\phi)u_1 - \{e_3\leftrightarrow e_4\}, \tag{1.91}$$

where

$$\Gamma_{21}(\phi) = \gamma^+\exp\Big[i(p_2^- - p_1^-)x^+ + i\mathcal{S}_2(\phi) - i\mathcal{S}_1(\phi)\Big], \tag{1.92}$$

and the term in the braces is the same as the first one, but with the quantum numbers of the outgoing electrons exchanged.

The bispinor structure of $\Gamma_{21}(\phi)$ in Eq. (1.92) is the same as in the vacuum case, the only contribution from the classical field is the change of the phase.

1.8 Fermion and photon propagators

For the electron two-point correlation function one obtains the following expression:

$$G^{(\mathrm{ni})}(x_2,x_1) = -i\langle 0|\mathcal{T}\psi(x_2)\overline{\psi}(x_1)|0\rangle = -i\int \frac{\mathrm{d}^2p^\perp}{(2\pi)^2}\int\limits_0^\infty \frac{\mathrm{d}p^+}{2\pi 2p^+}$$
$$\times\Big[\theta(x_2^+ - x_1^+)K_p(\phi_2)(\gamma p + m)\overline{K}_p(\phi_1)\mathrm{e}^{-ip(x_2-x_1)-i\mathcal{S}_p(\phi_2,\phi_1)}$$
$$-\,\theta(x_1^+ - x_2^+)K_{-p}(\phi_2)(\gamma p - m)\overline{K}_{-p}(\phi_1)\mathrm{e}^{ip(x_2-x_1)-i\mathcal{S}_{-p}(\phi_2,\phi_1)}\Big], \quad (1.93)$$

which can be written as (we use the prescription $m^2 \to m^2 - i\epsilon$, $\epsilon \to +0$)

$$G^{(\mathrm{ni})}(x_2,x_1) = \int \frac{\mathrm{d}^4p}{(2\pi)^4}\mathrm{e}^{-ip(x_2-x_1)-i\mathcal{S}_p(\phi_2,\phi_1)}K_p(\phi_2)\frac{\gamma\tilde{p}+m}{p^2-m^2+i\epsilon}\overline{K}_p(\phi_1). \quad (1.94)$$

In Eq. (1.94) the four-momentum p^μ is off-shell with comparison to the one in Eq. (1.93), the part of the numerator is still the on-shell momentum though, which we denote by a tilde:

$$\tilde{p}^\mu = \left(p^+, \boldsymbol{p}^\perp, \frac{\boldsymbol{p}^{\perp 2}+m^2}{2p^+}\right), \quad \tilde{p}^2 = m^2. \quad (1.95)$$

We call $G^{(\mathrm{ni})}(x_2,x_1)$ noninstantaneous fermion propagator.

Though we will not use it in our calculations, in order to check the consistency, let us demonstrate that the noninstantaneous propagator can be combined with the contribution from the seagull dressed vertex such that we obtain the covariant Feynman propagator of the instant-form approach. It can be seen as follows. From Eqs. (1.86), (1.87), and (1.88) we notice, that the seagull dressed vertex interaction can be written as the second-order three-point one, but with the propagator

$$G^{(\mathrm{in})}(x_2,x_1) = \int \frac{\mathrm{d}^2p^\perp \mathrm{d}p^+}{(2\pi)^3}\mathrm{e}^{-ip^+(x_2^- - x_1^-)-ip_k(x_2^k - x_1^k)}\delta(x_2^+ - x_1^+)\frac{\gamma^+}{2p^+}$$
$$= \int \frac{\mathrm{d}^4p}{(2\pi)^4}\mathrm{e}^{-ip(x_2-x_1)-i\mathcal{S}_p(\phi_2,\phi_1)}\frac{\gamma^+}{2p^+}. \quad (1.96)$$

Replacing $K_p(\phi_2)$ and $\overline{K}_{-p}(\phi_1)$ with $\mathcal{K}_p(\phi_2)$ and $\overline{\mathcal{K}}_{-p}(\phi_1)$, respectively, for $G^{(\mathrm{ni})}(x_2,x_1)$ [see Eqs. (1.61), (1.68), and (1.69)], and noting that an arbitrary four-momentum p^μ can be decomposed as [Mantovani et al., 2016] (see also [Seipt and Kämpfer, 2012])

$$p^\mu = \tilde{p}^\mu + \hat{p}^\mu, \quad \hat{p}^\mu = \left(0, \mathbf{0}^\perp, p^- - \frac{\boldsymbol{p}^{\perp 2}+m^2}{2p^+}\right) = \frac{p^2-m^2}{2p^+}\eta^\mu, \quad (1.97)$$

we sum the two contributions and obtain the known form of the fermion propagator in a plane-wave field [Ritus, 1985]

$$G(x_2,x_1) = G^{(\mathrm{ni})}(x_2,x_1) + G^{(\mathrm{in})}(x_2,x_1)$$
$$= \int \frac{\mathrm{d}^4p}{(2\pi)^4}\mathrm{e}^{-ip(x_2-x_1)-i\mathcal{S}_p(\phi_2,\phi_1)}\mathcal{K}_p(\phi_2)\frac{\gamma p+m}{p^2-m^2+i\epsilon}\overline{\mathcal{K}}_p(\phi_1). \quad (1.98)$$

For the photon two-point correlation function, we proceed in an analogous way. We obtain:

$$D_{\mu\nu}^{(\mathrm{ni})}(x_2,x_1) = i\langle 0|\mathcal{T}\mathcal{A}_\mu(x_2)\mathcal{A}_\nu^*(x_1)|0\rangle = -i\int\frac{\mathrm{d}^2k^\perp}{(2\pi)^2}\int\limits_0^\infty\frac{\mathrm{d}k^+}{2\pi 2k^+}$$
$$\times\left(g_{\mu\nu}-\frac{k_\mu\eta_\nu+k_\nu\eta_\mu}{k^+}\right)\left[\theta(x_2^+-x_1^+)\mathrm{e}^{-ik(x_2-x_1)}+\theta(x_1^+-x_2^+)\mathrm{e}^{ik(x_2-x_1)}\right], \quad (1.99)$$

which, again, can be written as

$$D_{\mu\nu}^{(\mathrm{ni})}(x_2,x_1) = \int\frac{\mathrm{d}^4k}{(2\pi)^4}\mathrm{e}^{-ik(x_2-x_1)}\frac{1}{k^2+i\epsilon}\left(g_{\mu\nu}-\frac{\tilde{k}_\mu\eta_\nu+\tilde{k}_\nu\eta_\mu}{k^+}\right), \quad (1.100)$$

where

$$\tilde{k}^\mu = \left(k^+,\boldsymbol{k}^\perp,\frac{\boldsymbol{k}^{\perp 2}}{2k^+}\right), \quad \tilde{k}^2=0. \quad (1.101)$$

The noninstantaneous photon propagator $D_{\mu\nu}^{(\mathrm{ni})}(x_2,x_1)$, like the electron one, can be completed up to the Feynman propagator of the instant form. From Eqs. (1.91) and (1.92) we conclude that the instantaneous photon propagator is given by

$$D_{\mu\nu}^{(\mathrm{in})}(x_2,x_1) = -\int\frac{\mathrm{d}^4k}{(2\pi)^4}\mathrm{e}^{-ik(x_2-x_1)}\frac{\eta_\mu\eta_\nu}{k^{+2}}. \quad (1.102)$$

Then we obtain that

$$\begin{aligned} D_{\mu\nu}(x_2,x_1) &= D_{\mu\nu}^{(\mathrm{ni})}(x_2,x_1)+D_{\mu\nu}^{(\mathrm{in})}(x_2,x_1) \\ &= \int\frac{\mathrm{d}^4k}{(2\pi)^4}\mathrm{e}^{-ik(x_2-x_1)}\frac{1}{k^2+i\epsilon}\left(g_{\mu\nu}-\frac{k_\mu\eta_\nu+k_\nu\eta_\mu}{k^+}\right), \end{aligned} \quad (1.103)$$

which is the Feynman propagator in the light-cone gauge [Mantovani et al., 2016].

Note that if one starts with the instant-form formulation and then uses the light-cone decomposition of the Feynman propagators, some additional vertex interactions are generated besides the considered three ones. In particular, diagrams with two or more instant particles meeting at one vertex appear in calculations. It can be shown, however, that such diagrams vanish in the light-cone gauge [Kogut and Soper, 1970]. In the front-form formulation, these diagrams are absent from the beginning.

Also note that due to Eq. (1.98), the three-point and the seagull vertices can be represented as vertices of one type [Mitter, 1975; Meuren et al., 2013]:

$$\mathcal{G}_{21}^\mu(k) = \int\mathrm{d}x^+\overline{\mathcal{K}}_2(\phi)\gamma^\mu\mathcal{K}_1(\phi)\exp\left[i(p_2^-+k^--p_1^-)x^++i\mathcal{S}_2(\phi)-i\mathcal{S}_1(\phi)\right]. \quad (1.104)$$

With respect to the self-interaction vertex, as we see from Eq. (1.103), it arises due to the choice of the light-cone gauge.

Customary, in the diagrams the instantaneous propagators are depicted by lines with a hash [Bjorken et al., 1971; Mustaki et al., 1991; Brodsky et al., 1998; Mantovani et al., 2016]). Here, we will consider processes only up to the second order, and it is more convenient to draw diagrams similar to the covariant instant-form approach, i.e., with the propagators given by Eqs. (1.98) and (1.103). The rule is that each propagator consists of the instantaneous and noninstantaneous part, or, what is the same, each propagator gives rise to the corresponding four-point vertex, in addition to the combination of the two three-point ones. Another rule is that diagrams with two instantaneous propagators, meeting at one vertex, are to be excluded.

Also note, that we use the S-matrix perturbation theory, in comparison with the old-fashioned perturbation theory [Heitler, 1954], usually employed together with light-cone quantization. Both approaches are known to produce the same result [Thorn, 1979] (note that in the case of having an external plane-wave field, there are no stationary states, and one has to use a time-dependent approach).

One more important thing is that the instantaneous propagators are infrared divergent in the '+' momentum component. In fact, light-cone quantization approach is infamous for having infrared divergences [Brodsky et al., 1998]. In principle, they need to be regularized [Mustaki et al., 1991; Brodsky et al., 1998] (see also [Mandelstam, 1983; Leibbrandt, 1984]). In Chapter 4 we encounter this type of divergencies, instead of introducing a regulator, however, we rearrange the result such that the divergent terms cancel each other.

1.9 Four-momentum relations at the dressed vertices

Due to the presence of an external plane-wave field, only three asymptotic momentum components are conserved at the dressed vertices [Mitter, 1975] [in particular, the components + and $\perp = (1, 2)$ are conserved, see Eqs. (1.81), (1.86), and (1.91)].

We can rewrite the momentum conservation relations in terms of the dressed momenta. From Eq. (1.81), for the three-point vertex [or for the full dressed vertex, given by the vertex function (1.104)] we have:

$$[\pi_2(\phi) + k - \pi_1(\phi)]^{(+,\perp)} = 0. \tag{1.105}$$

As for the '–' components, we notice that for the phase

$$\Phi(x^+) = (p_2^- + k^- - p_1^-)x^+ + \mathcal{S}_2(\phi) - \mathcal{S}_1(\phi) \tag{1.106}$$

a derivative with respect to the light-cone time is given by

$$\partial_+\Phi(x^+) = \pi_2^-(\phi) + k^- - \pi_1^-(\phi). \tag{1.107}$$

Therefore, for the sum of the '–' momentum components we have the following integral

$$\delta_1(p_2, p_1, k) = \int \mathrm{d}x^+[\pi_2^-(\phi) + k^- - \pi_1^-(\phi)]\mathrm{e}^{i\Phi(x^+)} = -i\int \mathrm{d}x^+\partial_+[\mathrm{e}^{i\Phi(x^+)}]. \tag{1.108}$$

Our expectation is that boundary terms do not affect observables, which implies

$$\pi_2^-(\phi) + k^- - \pi_1^-(\phi) \sim 0. \tag{1.109}$$

In Eq. (1.109), we write a tilde instead of an equal sign, since the relation may not hold locally, but, if inside the integral in x^+, gives a vanishing contribution as a result. We also point out that relations, equivalent to the one in Eq. (1.109) have been employed before, with different arguments, justifying its validity [Mitter, 1975; Mackenroth and Di Piazza, 2011; Ilderton, 2011; Seipt and Kämpfer, 2012; Hartin, 2016]; the form (1.109) was noted by Hartin (2016).

Eq. (1.109) completes Eq. (1.105) to the full four-momentum conservation law (for the dressed momenta)

$$\pi_2^\mu(\phi) + k^\mu - \pi_1^\mu(\phi) \sim 0. \tag{1.110}$$

As was suggested by Ilderton (2011), a conservation relation could be also inferred from the requirement of gauge invariance, which is encoded in the Ward identity [Ward, 1950] and the more general Ward-Takahashi identity [Takahashi, 1957]. Due to the connection between momentum conservation and gauge invariance, in principle, one could verify whether Eq. (1.109) enforces gauge invariance of QED in a plane-wave field.

As an example, let us consider nonlinear Compton scattering (see Fig. 1.1). The leading-order matrix element $\langle kp_2|S|p_1\rangle$ is given by Eq. (1.81). We are interested in the preexponential factor of the integrand in Eq. (1.82). Replacing e_μ^* with k_μ we find that

$$\overline{K}_2(\phi)\gamma^\mu K_1(\phi)k_\mu = S_{21}^\mu(\phi)k_\mu\gamma^+ = [\pi_2^-(\phi) + k^- - \pi_1^-(\phi)]\gamma^+ \sim 0, \tag{1.111}$$

which is exactly the relation (1.109) (up to the factor γ^+). We conclude, that Eq. (1.109) guarantees gauge invariance for this case.

As a more elaborate example, let us consider double nonlinear Compton scattering. The two diagrams are shown in Fig. 1.2.

We are going to check the Ward identity upon the replacement $\epsilon_1^\nu \to k_1^\nu$. Again, we write down only the preexponential factors of the integrands for the vertex functions. For the noninstantaneous part we obtain:

$$\begin{aligned}
\Sigma^{(\mathrm{ni})} &= \left[K_{23}^\mu(\phi_2)\frac{\gamma\tilde{p}_3 + m}{p_3^3 - m^2}K_{31}^\nu(\phi_1) + K_{24}^\mu(\phi_2)\frac{\gamma\tilde{p}_4 + m}{p_4^3 - m^2}K_{41}^\nu(\phi_1)\right]k_{1\nu} \\
&= \frac{\gamma^+}{2p_2^+}[\gamma\pi_2(\phi_2) + m]\left\{\gamma^\mu[\gamma\pi_3(\phi_2) + m]\frac{\gamma^+}{2p_3^+}\,\frac{\gamma\tilde{p}_3 + m}{p_3^2 - m^2}\,\frac{\gamma^+}{2p_3^+}[\gamma\pi_3(\phi_1) + m]\gamma k_1\right. \\
&\quad \left. + \gamma k_1[\gamma\pi_4(\phi_2) + m]\frac{\gamma^+}{2p_4^+}\,\frac{\gamma\tilde{p}_4 + m}{p_4^2 - m^2}\,\frac{\gamma^+}{2p_4^+}[\gamma\pi_4(\phi_1) + m]\gamma^\mu\right\}[\gamma\pi_1(\phi_1) + m]\frac{\gamma^+}{2p_1^+}.
\end{aligned} \tag{1.112}$$

We notice that $\gamma^+(\gamma\tilde{p}_3 + m)\gamma^+ = 2p_3^+\gamma^+$, and analogously for the other propagator. Going further, we write γk_1 for the first and the second term respectively as

$$\begin{aligned}
\gamma k_1 &= \gamma\pi_1(\phi_1) - \gamma\pi_3(\phi_1) + \gamma^+\delta(\phi_1), \quad \delta(\phi_1) = \pi_3^-(\phi_1) + k_1^- - \pi_1^-(\phi_1); \\
\gamma k_1 &= \gamma\pi_4(\phi_2) - \gamma\pi_2(\phi_2) + \gamma^+\delta(\phi_2), \quad \delta(\phi_2) = \pi_2^-(\phi_2) + k_1^- - \pi_4^-(\phi_2).
\end{aligned} \tag{1.113}$$

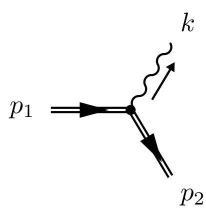

Fig. 1.1. The leading-order diagram for nonlinear Compton scattering.

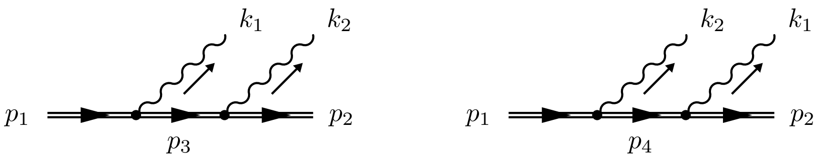

Fig. 1.2. The two leading-order diagrams for double nonlinear Compton scattering.

Employing the fact that $[\gamma\pi_p(\phi) \pm m][\gamma\pi_p(\phi) \mp m] = p^2 - m^2$, we obtain:

$$\Sigma^{(\mathrm{ni})} = \frac{\gamma^+}{2p_2^+}[\gamma\pi_2(\phi_2) + m]\Bigg\{\gamma^\mu[\gamma\pi_3(\phi_2) + m]\Bigg[-\frac{\gamma^+}{2p_3^+} + \frac{\gamma^+\delta(\phi_1)}{p_3^2 - m^2}\Bigg] \\ + \Bigg[\frac{\gamma^+}{2p_4^+} + \frac{\gamma^+\delta(\phi_2)}{p_4^2 - m^2}\Bigg][\gamma\pi_4(\phi_1) + m]\gamma^\mu\Bigg\}[\gamma\pi_1(\phi_1) + m]\frac{\gamma^+}{2p_1^+}. \tag{1.114}$$

For the sum of the two instantaneous terms we have:

$$\Sigma^{(\mathrm{in})} = \frac{\gamma^+}{2p_2^+}[\gamma\pi_2(\phi_2) + m]\Bigg\{\gamma^\mu\frac{\gamma^+}{2p_3^+}\gamma k_1 + \gamma k_1\frac{\gamma^+}{2p_4^+}\gamma^\mu\Bigg\}[\gamma\pi_1(\phi_1) + m]\frac{\gamma^+}{2p_1^+}. \tag{1.115}$$

Again, we use Eq. (1.113) (due to the adjacent γ^+ the third terms with δ's do not appear). After a permutation of gamma matrices for each term, one obtains:

$$\Sigma^{(\mathrm{in})} = \frac{\gamma^+}{2p_2^+}[\gamma\pi_2(\phi_2) + m]\Bigg\{\gamma^\mu[\gamma\pi_3(\phi_2) + m]\frac{\gamma^+}{2p_3^+} \\ - \frac{\gamma^+}{2p_4^+}[\gamma\pi_4(\phi_1) + m]\gamma^\mu\Bigg\}[\gamma\pi_1(\phi_1) + m]\frac{\gamma^+}{2p_1^+}. \tag{1.116}$$

We see that the two terms in Eq. (1.116) cancel the corresponding two terms in Eq. (1.114), and we are left with

$$\Sigma^{(\mathrm{ni})} + \Sigma^{(\mathrm{in})} = K_{23}^\mu(\phi_2)\frac{2p_3^+\delta(\phi_1)}{p_3^2 - m^2} + K_{41}^\mu(\phi_1)\frac{2p_4^+\delta(\phi_2)}{p_4^2 - m^2}. \tag{1.117}$$

Recovering the full expression of $\langle k_2k_1|S|p_2p_1\rangle$ (up to the delta function and the normalization factors), one obtains that

$$\langle k_2k_1|S|p_2p_1\rangle \propto \int\frac{\mathrm{d}p_3^-}{2\pi}\,\overline{u}_2\Gamma_{23}^\mu(k_2)u_1\frac{2p_3^+}{p_3^2 - m^2}\delta_1(p_3, p_1, k_1)\epsilon_{2\mu}^* \\ + \int\frac{\mathrm{d}p_4^-}{2\pi}\,\overline{u}_2\Gamma_{41}^\mu(k_2)u_1\frac{2p_4^+}{p_4^2 - m^2}\delta_1(p_2, p_4, k_1)\epsilon_{2\mu}^*, \tag{1.118}$$

where $\Gamma_{23}^\mu(k_2)$ and $\Gamma_{41}^\mu(k_2)$ are the three-point vertex functions [see Eq. (1.82)], and the δ_1-functions are from Eq. (1.108).

Eq. (1.109) guarantees that the expression in Eq. (1.118) vanishes upon the contraction with an arbitrary polarization four-vector $\epsilon_2^{*\mu}$, and for arbitrary initial and final momenta.

From what have been considered, we can make some general implications. Note that in vacuum the only change in the preexponential factor for any amplitude is the replacement of all $\pi_p^\mu(\phi)$ with p^μ. As we see from the check of the Ward identity for single and double nonlinear Compton scattering, the bispinors of the incoming and outgoing particles are not needed for obtaining the final expression. It implies that, if considered perturbatively, for any diagram the verification of the Ward (-Takahashi) identity goes in the same way for the vacuum case and for the external-field case. Therefore, we might expect that Eq. (1.109) allows us to preserve gauge invariance at any order.

With the four-momentum conservation relation (1.110) for the dressed momenta, we can derive useful relations for the scalar products of this momenta. We notice that the asymptotic momenta satisfy the condition

$$p_2^\mu + k^\mu = p_1^\mu + \varkappa\eta^\mu, \tag{1.119}$$

with some scalar $\varkappa$, which can be expressed as

$$\begin{aligned}\varkappa = \frac{1}{p_1^+}\left(kp_2 - \frac{p_1^2 - p_2^2 - k^2}{2}\right) &= \frac{1}{p_2^+}\left(kp_1 + \frac{p_2^2 - k^2 - p_1^2}{2}\right)\\ &= \frac{1}{k^+}\left(p_2p_1 + \frac{k^2 - p_2^2 - p_1^2}{2}\right).\end{aligned} \tag{1.120}$$

On the other hand,

$$\begin{aligned}\pi_2^-(\phi) + k^- - \pi_1^-(\phi) = \varkappa &+ \left(\frac{ep_2A(\phi)}{p_2^+} - \frac{e^2A^2(\phi)}{2p_2^+}\right)\\ &- \left(\frac{ep_1A(\phi)}{p_1^+} - \frac{e^2A^2(\phi)}{2p_1^+}\right).\end{aligned} \tag{1.121}$$

With the use of the above relations, we obtain:

$$\begin{aligned}k_2\pi_2(\phi) &= p_1^+\left[\pi_2^-(\phi) + k^- - \pi_1^-(\phi)\right] + \frac{1}{2}\left(p_1^2 - p_2^2 - k^2\right)\\ &\sim \frac{1}{2}\left(p_1^2 - p_2^2 - k^2\right),\\ k_2\pi_1(\phi) &= p_2^+\left[\pi_2^-(\phi) + k^- - \pi_1^-(\phi)\right] - \frac{1}{2}\left(p_2^2 - k^2 - p_1^2\right)\\ &\sim -\frac{1}{2}\left(p_2^2 - k^2 - p_1^2\right),\\ \pi_2(\phi)\pi_1(\phi) &= k^+\left[\pi_2^-(\phi) + k^- - \pi_1^-(\phi)\right] - \frac{1}{2}\left(k^2 - p_2^2 - p_1^2\right)\\ &\sim -\frac{1}{2}\left(k^2 - p_2^2 - p_1^2\right).\end{aligned} \tag{1.122}$$

Note that the relations (1.122) are in fact the same as in vacuum QED, however, they hold only for momenta evaluated in the same time point.

As a final remark on the four-momentum relations, we notice that for the seagull and self-interaction vertices the conservation relations are combinations of the relations from two three-point vertices. For the seagull vertex we have [see Eq. (1.87)]

$$\pi_2^\mu(\phi) + k_2^\mu - \pi_1^\mu(\phi) - k_1^\mu \sim 0, \tag{1.123}$$

and for the self-interaction vertex we obtain [see Eqs. (1.91) and (1.92)]

$$\pi_4^\mu(\phi) + \pi_3^\mu(\phi) - \pi_2^\mu(\phi) - \pi_1^\mu(\phi) \sim 0. \tag{1.124}$$

1.10 Parameters for the description of scattering

In the following, we consider QED processes, in which one or two particles collide with a laser pulse. In order to characterize them, it is convenient to employ gauge- and Lorentz-invariant parameters. One of them is the classical intensity parameter [Ritus, 1985; Di Piazza et al., 2012], which has been discussed in the introduction:

$$\xi_i = \frac{|e|\sqrt{-a_i^2}}{m}. \tag{1.125}$$

We will be mostly interested in the case of a linear polarization ($\xi_1 = \xi, \xi_2 = 0$) and the regime $\xi \gg 1$.

The second parameter is the quantum nonlinearity parameter [Ritus, 1985; Di Piazza et al., 2012], which has been also mentioned in the introduction:

$$\chi_b^{(i)} = \frac{p_b^+}{m}\xi_i, \tag{1.126}$$

where p_b^+ is the '+' component of the momentum of particle b, colliding with the laser pulse.

If we consider one particle colliding with a laser field, then we can always choose a frame, in which the collision is head-on [see Eq. (1.29)], therefore the parameters ξ_i and $\chi^{(i)}$ completely characterize the process [Ritus, 1985].

If we consider two particles and a laser field, then in general we can not make all the transverse momentum components equal zero by choosing a frame. For such cases, we introduce parameters t_i and $\zeta_i(\phi)$, which are defined via

$$t_i\xi_i = \frac{|e|p_{1\mu}f_i^{\mu\nu}p_{2\nu}}{m^3(p_1^+ + p_2^+)}, \quad \zeta_i(\phi)\xi_i = \frac{|e|\pi_{1\mu}(\phi)f_i^{\mu\nu}\pi_{2\nu}(\phi)}{m^3(p_1^+ + p_2^+)}. \tag{1.127}$$

If we change the order of the particles, then t_i and $\zeta_i(\phi)$ change their signs. Below, we consider electron-positron annihilation either in one photon, or in two photons. We will use the definitions (1.127) with p_1^μ being the electron four-momentum, and p_2^μ being the positron four-momentum.

Note that if we choose the canonical light-cone basis (1.29) with $q^\mu = p_1^\mu + p_2^\mu$, then $\boldsymbol{p}_1^\perp + \boldsymbol{p}_2^\perp = 0$ and $t_i = p_1^i/m = -p_2^i/m$, which shows that t_i is in fact the transverse momentum components of each of the colliding particles in their transverse center-of-momentum frame. The quantity $\zeta_i(\phi)$ is an analogous quantity for the dressed momenta.

2

Electron-positron annihilation into one photon

In comparison with vacuum QED, in QED with an external field first-order processes are possible. Among them, emission of a photon by an electron (nonlinear Compton scattering) and electron-positron photoproduction (nonlinear Breit-Wheeler process) are the most studied for QED in a plane-wave field. Little to no attention is usually paid to one more cross channel — electron-positron annihilation into one photon (see Fig. 2.1). This process has been studied by Nikishov and Ritus (1964a,b), Ritus (1985), and also Ilderton et al. (2011). The phase space for the latter process is completely different from the one for the two former processes: two incoming particles and only one outgoing. Due to this, electron-positron annihilation into one photon is regarded as generally less important for, e.g., laser-plasma interactions, than the first two processes [Gonoskov et al., 2015].

With respect to the evaluation of the reduced matrix element squared, all three processes are of course the same. We pick electron-positron annihilation into one photon nevertheless, since considering this process allows to understand, what limitations an external field imposes on the description of two-particle scattering. This will be useful later, in Chapter 4, when we consider electron-positron annihilation into two photons.

We start with reviewing scattering in vacuum from the front-form prospective. In this review we follow the ideas presented by Itzykson and Zuber (1980), Goldberger and Watson (1964), and Berestetskii et al. (1982). Then we construct cross section for the electron-positron annihilation into one photon in a plane-wave field, evaluate the reduced matrix element squared, obtain a final result, and analyze it.

2.1 Scattering in vacuum

We start with the fermionic states $|p\rangle$ with definite momenta, which, according to Eq. (1.77), satisfy

$$\langle p'|p\rangle = \frac{(2\pi)^3}{\mathcal{V}}\delta^{(+,\perp)}(p'-p) \tag{2.1}$$

(for brevity, we suppress the indices for the spin degree of freedom). In position space, $|p\rangle$ is a plane wave [see Eq. (1.57)]:

$$\langle x|p\rangle = \frac{\mathrm{e}^{-ipx}}{\sqrt{\mathcal{V}}}\cdot\frac{u_p}{\sqrt{2p^+}}, \tag{2.2}$$

A wave packet $|\psi_p\rangle$ with the central momentum p^μ is constructed according to

$$|\psi_p\rangle = \int \frac{\mathcal{V}\tilde{\mathrm{d}}^3 q}{(2\pi)^3} f_p(q)|q\rangle, \tag{2.3}$$

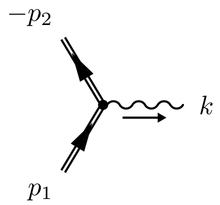

Fig. 2.1. The leading-order diagram for electron-positron annihilation into one photon.

where

$$\tilde{\mathrm{d}}^3 q = \frac{\mathrm{d}^2 q^\perp}{(2\pi)^2} \frac{\mathrm{d}q^+}{2\pi} \theta(q^+), \tag{2.4}$$

and $f_p(q)$ is the momentum distribution density [note that $f_p(q)$ depends on $\boldsymbol{q}^\perp$ and q^+, but not on q^-; for clarity we write simply q].

The density $f_p(q)$ is defined such that

$$\langle \psi_p | \psi_p \rangle = \int \frac{\mathcal{V} \tilde{\mathrm{d}}^3 q}{(2\pi)^3} |f_p(q)|^2 = 1. \tag{2.5}$$

We define

$$f_p(x) = \int \frac{\mathcal{V} \tilde{\mathrm{d}}^3 q}{(2\pi)^3} f_p(q) \frac{\mathrm{e}^{-iqx}}{\sqrt{\mathcal{V}}} = F_p(x) \mathrm{e}^{-ipx}, \tag{2.6}$$

where

$$F_p(x) = \int \frac{\mathcal{V} \tilde{\mathrm{d}}^3 q}{(2\pi)^3} f_p(q) \frac{\mathrm{e}^{-i(q-p)x}}{\sqrt{\mathcal{V}}} \tag{2.7}$$

is a relatively slowly varying function of x. The modulus squared $|F_p(x)|^2 = |f_p(x)|^2$ is the particle density.

The current density is defined as $j^\mu(x) = \overline{\psi}_p(x) \gamma^\mu \psi_p(x)$. Assuming that the wave packet is sharply peaked around p^μ and taking into account that the bispinor u_q is slowly varying with q^μ, we obtain that

$$j^\mu(x) \approx |f_p(x)|^2 \frac{p^\mu}{p^+}. \tag{2.8}$$

Now, let us consider scattering in vacuum. We take two wave packets of two fermions as the initial state (for simplicity, we assume that the fermions are distinguishable):

$$|i, \mathrm{in}\rangle = \int \frac{\mathcal{V} \tilde{\mathrm{d}}^3 q_2}{(2\pi)^3} \frac{\mathcal{V} \tilde{\mathrm{d}}^3 q_1}{(2\pi)^3} f_2(q_2) f_1(q_1) |q_2 q_1, \mathrm{in}\rangle. \tag{2.9}$$

Then the matrix element to scatter into a final state $|f, \mathrm{out}\rangle$ is given by

$$S_{fi} = \langle f, \mathrm{in} | S | i, \mathrm{in}\rangle = i \int \frac{\mathcal{V} \tilde{\mathrm{d}}^3 q_2}{(2\pi)^3} \frac{\mathcal{V} \tilde{\mathrm{d}}^3 q_1}{(2\pi)^3} f_2(q_2) f_1(q_1) (2\pi)^4 \delta^{(4)}(P_f - q_2 - q_1) \mathcal{T}(q_2, q_1), \tag{2.10}$$

where

$$\mathcal{T}(q_2, q_1) = \frac{M(q_2, q_1)}{2\mathcal{V}\sqrt{q_2^+ q_1^+}} \prod_a \frac{1}{\sqrt{2 p_a'^+ \mathcal{V}}}, \tag{2.11}$$

the reduced matrix element $M(q_2, q_1)$ is a slowly varying function of q_2^μ and q_1^μ, and the product in a is taken over all particles in the final state.

The modulus squared of S_{fi} is given by

$$|S_{fi}|^2 = \int \frac{\mathcal{V}\tilde{\mathrm{d}}^3 q_4}{(2\pi)^3}\frac{\mathcal{V}\tilde{\mathrm{d}}^3 q_3}{(2\pi)^3}\frac{\mathcal{V}\tilde{\mathrm{d}}^3 q_2}{(2\pi)^3}\frac{\mathcal{V}\tilde{\mathrm{d}}^3 q_1}{(2\pi)^3} f_2(q_4) f_2^*(q_2) f_1(q_3) f_1^*(q_1) \\ \times (2\pi)^4\delta^{(4)}(P_f - q_4 - q_3)(2\pi)^4\delta^{(4)}(P_f - q_2 - q_1)\mathcal{T}(q_4, q_3)\mathcal{T}^*(q_2, q_1). \tag{2.12}$$

We rewrite the delta functions as

$$(2\pi)^4\delta^{(4)}(P_f - q_4 - q_3)(2\pi)^4\delta^{(4)}(P_f - q_2 - q_1) \\ = (2\pi)^4\delta^{(4)}(q_4 + q_3 - q_2 - q_1)(2\pi)^4\delta^{(4)}(P_f - q_2 - q_1). \tag{2.13}$$

Assuming that the summation over the final states extends beyond the size of the wave packets, we replace q's with corresponding p's in the second delta function and in $\mathcal{T}$'s. Going further, we represent the first delta function as

$$(2\pi)^4\delta^{(4)}(q_4 + q_3 - q_2 - q_1) = \int \mathrm{d}^4 x\, \mathrm{e}^{-i(q_4+q_3-q_2-q_1)x}. \tag{2.14}$$

Then we obtain the following expression for $|S_{fi}|^2$:

$$|S_{fi}|^2 = \int \mathrm{d}^4 x |f_2(x)|^2 |f_1(x)|^2 (2\pi)^4\delta^{(4)}(P_f - p_2 - p_1)\frac{|M(p_2, p_1)|^2}{4p_2^+ p_1^+}\prod_a \frac{1}{2{p'_a}^+\mathcal{V}}. \tag{2.15}$$

Then the differential probability per unit time per unit volume is given by

$$\mathrm{d}\dot{w} = |f_2(x)|^2 |f_1(x)|^2 (2\pi)^4\delta^{(4)}(P_f - p_2 - p_1)\frac{|M(p_2, p_1)|^2}{4p_2^+ p_1^+}\prod_a \frac{\tilde{\mathrm{d}}^3 p'_a}{(2\pi)^3 2{p'_a}^+}. \tag{2.16}$$

An expression for the cross section is obtained from Eq. (2.16) by dividing it by the factor, accounting for the fluxes of the incoming particles. In order to understand, how to do it, let us recall the instant form approach [Itzykson and Zuber, 1980]. In the instant form, the current density for particle a is given by $j_a^\mu(x) = |g_a(x)|^2 p_a^\mu/p_a^0$ [compare with Eq. (2.8)], with $|g_a(x)|^2$ being the particle density. If we consider a reference frame, where particle 1 is at rest, then the cross section is equal to the probability per unit time per unit volume divided by the target density $j_1^0(x) = |g_1(x)|^2$ and by the incident flux density $|\boldsymbol{j}_2(x)| = |g_2(x)|^2 |\boldsymbol{p}_2|/p_2^0$. We can introduce the following invariant:

$$I = \sqrt{(p_2 p_1)^2 - m_2^2 m_1^2}, \tag{2.17}$$

with m_2 and m_1 being the masses of the colliding particles. Then

$$j_1^0(x)|\boldsymbol{j}_2(x)| = |g_1(x)|^2 |g_2(x)|^2 \frac{I}{p_2^0 p_1^0}. \tag{2.18}$$

Eq. (2.18) allows one to obtain a Lorentz-invariant expression for the cross section in the instant form [Itzykson and Zuber, 1980] (see also [Berestetskii et al., 1982]).

Let us proceed in a similar fashion in the front form. Taking into account the expression (2.8) for the current density, we conclude, that we need to divide the probability (2.16) by $|f_2(x)|^2 |f_1(x)|^2 I/(p_2^+ p_1^+)$. Then the differential cross section is given by

$$\mathrm{d}\sigma = (2\pi)^4\delta^{(4)}(P_f - p_2 - p_1)\frac{|M(p_2, p_1)|^2}{4I}\prod_a \frac{\tilde{\mathrm{d}}^3 p'_a}{(2\pi)^3 2{p'_a}^+}, \tag{2.19}$$

which is exactly the same cross section as in the instant form, since

$$\frac{\tilde{\mathrm{d}}^3 p}{(2\pi)^3 2p^+} = \frac{\mathrm{d}^2 p^\perp}{(2\pi)^2} \frac{\mathrm{d}p^+}{2\pi} \frac{\theta(p^+)}{2p^+} = \frac{\mathrm{d}^3 p}{(2\pi)^3 2p^0} = \mathrm{d}\Gamma_p. \tag{2.20}$$

The total cross section, summed over the final momentum and polarization states, and averaged over the initial polarization states, is respectively given by

$$\sigma = \prod_a \int \frac{\tilde{\mathrm{d}}^3 p'_a}{(2\pi)^3 2{p'_a}^+} (2\pi)^4 \delta^{(4)}(P_f - p_2 - p_1) \frac{1}{16I} \sum_{\text{polarization}} |M(p_2, p_1)|^2. \tag{2.21}$$

Note that, if some of the final particles are identical, the expression for the total cross section should be adjusted accordingly by multiplying it with a factor, which takes into account the symmetry of the final state.

Before we move to scatterring theory in a plane-wave field, let us to look at $|S_{fi}|^2$ in the position-space representation. For simplicity, let us consider a second-order tree-level process. An instructive case is electron-positron (Bhabha) scattering, with the two leading-order diagrams shown in Fig. 2.2.

For the diagram in Fig. 2.2a, the matrix element is given by

$$\begin{aligned} S^{(1)}_{fi} = \int \frac{\mathcal{V}\tilde{\mathrm{d}}^3 q_2}{(2\pi)^3} \frac{\mathcal{V}\tilde{\mathrm{d}}^3 q_1}{(2\pi)^3} f_2(q_2) f_1(q_1) \int \mathrm{d}^4 x_1 \mathrm{d}^4 x_2 \int \frac{\mathrm{d}^4 k_1}{(2\pi)^4} \\ \times\, \mathrm{e}^{i(k_1 - q_1 - q_2)x_1 + i(P_f - k_1)x_2} S^{(1)}(q_2, q_1, k_1), \end{aligned} \tag{2.22}$$

where $S^{(1)}(q_2, q_1)$ is a slowly varying function of the initial momenta q_1 and q_2, the intermediate momentum k_1, also of the final momenta (we do not denote this dependence for simplicity), and $P_f^\mu = {p'_2}^\mu + {p'_1}^\mu$.

Let us evaluate the integral in x_2^μ, then also the integral in k_1^μ. We obtain:

$$S^{(1)}_{fi} = \int \frac{\mathcal{V}\tilde{\mathrm{d}}^3 q_2}{(2\pi)^3} \frac{\mathcal{V}\tilde{\mathrm{d}}^3 q_1}{(2\pi)^3} f_2(q_2) f_1(q_1) \int \mathrm{d}^4 x_1\, \mathrm{e}^{i(P_f - q_1 - q_2)x_1} S^{(1)}(q_2, q_1, P_f). \tag{2.23}$$

Upon squaring, one obtains:

$$|S^{(1)}_{fi}|^2 = \int \frac{\mathcal{V}\tilde{\mathrm{d}}^3 q_4}{(2\pi)^3} \frac{\mathcal{V}\tilde{\mathrm{d}}^3 q_3}{(2\pi)^3} \frac{\mathcal{V}\tilde{\mathrm{d}}^3 q_2}{(2\pi)^3} \frac{\mathcal{V}\tilde{\mathrm{d}}^3 q_1}{(2\pi)^3} f_2(q_4) f_2^*(q_2) f_1(q_3) f_1^*(q_1) \tag{2.24}$$

$$\times \int \mathrm{d}^4 x_3 \mathrm{d}^4 x_1\, \mathrm{e}^{i(P_f - q_4 - q_3)x_3 - i(P_f - q_2 - q_1)x_1} S^{(1)}(q_4, q_3, P_f) S^{(1)*}(q_2, q_1, P_f). \tag{2.25}$$

One can notice that in order to obtain the integral as in Eq. (2.14) and transform the result into Eq. (2.15), obtained in the momentum representation, we need to introduce x^μ

Fig. 2.2. The two leading-order diagrams for Bhabha scattering in vacuum.

as the average $x^\mu = (x_3^\mu + x_1^\mu)/2$. Note, that we could have not evaluated the integral in x_2^μ in the first place [see Eq. (2.22)]. Then the variable x^μ could have been defined as the average over all four space-time coordinates, appearing upon the squaring of $S_{fi}^{(1)}$.

For the second diagram (see Fig. 2.2b) we obtain for the matrix element modulus squared:

$$\begin{aligned}|S_{fi}^{(2)}|^2 = &\int \frac{\mathcal{V}\tilde{\mathrm{d}}^3q_4}{(2\pi)^3}\frac{\mathcal{V}\tilde{\mathrm{d}}^3q_3}{(2\pi)^3}\frac{\mathcal{V}\tilde{\mathrm{d}}^3q_2}{(2\pi)^3}\frac{\mathcal{V}\tilde{\mathrm{d}}^3q_1}{(2\pi)^3} f_2(q_4)f_2^*(q_2)f_1(q_3)f_1^*(q_1) \\ &\times \int \mathrm{d}^4x_4\mathrm{d}^4x_3\mathrm{d}^4x_2\mathrm{d}^4x_1 \frac{\mathrm{d}^4k_4}{(2\pi)^4}\frac{\mathrm{d}^4k_2}{(2\pi)^4}\mathrm{e}^{i\Phi}S_{fi}^{(2)}(q_4,q_3,k_4)S_{fi}^{(2)*}(q_2,q_1,k_2),\end{aligned} \tag{2.26}$$

where

$$\Phi = (p_2' - k_4 - q_4)x_4 + (p_1' + k_4 - q_3)x_3 - (p_2' - k_2 - q_2)x_2 - (p_1' + k_2 - q_1)x_1. \tag{2.27}$$

In order to obtain Eq. (2.15), we introduce x^μ as $x^\mu = (x_4^\mu + x_3^\mu + x_2^\mu + x_1^\mu)/4$.

The interference terms can be elaborated in a similar way. The result is that the differential probability (2.16) for Bhabha scattering can be viewed as the one, evaluated at the space-time point, which is the average of the space-time points, occuring in the corresponding modulus squared of the matrix element in the position representation. This conclusion can be extended to other processes as well.

2.2 Cross section for electron-positron annihilation into one photon

Now we turn to the case of electron-positron annihilation into one photon in a plane-wave field. The definite-momentum states are normalized according to Eq. (2.1). In the position space those states are the Volkov states:

$$\langle x|p\rangle = \psi_p(x) = \frac{\mathrm{e}^{-ipx-\mathcal{S}_p(\phi)}}{\sqrt{\mathcal{V}}}\cdot\frac{K_p(\phi)u_p}{\sqrt{2p^+}}. \tag{2.28}$$

A wave-packet is formed in the same way, as in the vacuum case [see Eqs (2.3) and (2.5)], and the distribution density in position space defined as:

$$f_p(x) = \int \frac{\mathcal{V}\tilde{\mathrm{d}}^3q}{(2\pi)^3} f_p(q)\frac{\mathrm{e}^{-iqx-i\mathcal{S}_q(\phi)}}{\sqrt{\mathcal{V}}} = F_p(x)\mathrm{e}^{-ipx-i\mathcal{S}_p(\phi)}, \tag{2.29}$$

where

$$F_p(x) = \int \frac{\mathcal{V}\tilde{\mathrm{d}}^3q}{(2\pi)^3} f_p(q)\frac{\exp[-i(q-p)x - i\mathcal{S}_q(\phi) + i\mathcal{S}_p(\phi)]}{\sqrt{\mathcal{V}}}. \tag{2.30}$$

The modulus squared $|F_p(x)|^2 = |f_p(x)|^2$ is again the particle density.

The current density is given by (in the case of a sharply peaked wave packet)

$$j^\mu(x) \approx |f_p(x)|^2\frac{\pi_p^\mu(\phi)}{p^+}. \tag{2.31}$$

The matrix element for annihilation of an electron and positron, defined by wave packets, peaked at p_1^μ and p_2^μ, respectively, into a photon with four-momentum k^μ and polarization defined by ϵ^μ, is given by

$$S_{fi} = \int \frac{\mathcal{V}\tilde{\mathrm{d}}^3 q_2}{(2\pi)^3} \frac{\mathcal{V}\tilde{\mathrm{d}}^3 q_1}{(2\pi)^3} f_2(q_2) f_1(q_1) (2\pi)^3 \delta^{(+,\perp)}(k - q_2 - q_1) \\ \times \int \mathrm{d}x^+ \exp\left[i\Phi_{q_2 q_1}(x^+)\right] \frac{iM(\phi, q_2, q_1)}{\sqrt{2\mathcal{V}q_2^+ 2\mathcal{V}q_1^+ 2\mathcal{V}k^+}}, \tag{2.32}$$

where

$$\Phi_{q_2 q_1}(x^+) = k^- x^+ - q_2^- x^+ + \mathcal{S}_{-q_2}(\phi) - q_1^- x^+ - \mathcal{S}_{q_1}(\phi), \tag{2.33}$$
$$M(\phi, q_2, q_1) = -e\bar{v}_{q_2} K^\mu_{-q_2 q_1}(\phi) u_{q_1} \epsilon^*_\mu, \tag{2.34}$$

with $K^\mu_{-q_2 q_1}(\phi)$ given by Eq. (1.83). We define the reduced matrix element as

$$M(q_2, q_1) = \int \mathrm{d}x^+ \exp\left[i\Phi_{q_2 q_1}(x^+)\right] M(\phi, q_2, q_1). \tag{2.35}$$

Note, that it is different by its structure in comparison with the one in vacuum, since only the three momentum components are conserved in a plane-wave background. Also note, that $M(\phi, q_2, q_1)$ is a slowly varying function of q_2^μ and q_1^μ.

We take the modulus squared of S_{fi}, transform the delta functions in the same way, as in Eq. (2.13), and replace the momenta of the incoming particles with the central ones for all slowly varying functions and the one of the delta functions. We obtain:

$$|S_{fi}|^2 = \int \mathrm{d}^2 x^\perp \mathrm{d}x^- \mathrm{d}x_2^+ \mathrm{d}x_1^+ (2\pi)^3 \delta^{(+,\perp)}(k - p_2 - p_1) \\ \times f_2(\boldsymbol{x}^\perp, x^-, x_2^+) f_2^*(\boldsymbol{x}^\perp, x^-, x_1^+) f_1(\boldsymbol{x}^\perp, x^-, x_2^+) f_1^*(\boldsymbol{x}^\perp, x^-, x_1^+) \\ \times M(\phi_2, p_2, p_1) M^*(\phi_1, p_2, p_1) \frac{\mathrm{e}^{ik^-(x_2^+ - x_1^+)}}{8\mathcal{V}k^+ p_2^+ p_1^+}. \tag{2.36}$$

Let us discuss the result (2.36). As we find out, in Eq. (2.36) the wave packet densities are evaluated at different time points, therefore, in general, we can not define cross section in a way, as one does for the vacuum case, but need to take the dynamics of the wave packets into account.

Recalling the discussion of scattering in vacuum, one can introduce the following variables:

$$x^+ = (x_2^+ + x_1^+)/2, \quad \delta^+ = x_2^+ - x_1^+. \tag{2.37}$$

Then the product of the distribution densities for the electron is given by (for the positron it is analogous)

$$f_1(\boldsymbol{x}^\perp, x^-, x_2^+) f_1^*(\boldsymbol{x}^\perp, x^-, x_1^+) = f_1(\boldsymbol{x}^\perp, x^-, x^+ + \delta^+/2) f_1^*(\boldsymbol{x}^\perp, x^-, x^+ - \delta^+/2) \\ = F_1(\boldsymbol{x}^\perp, x^-, x^+ + \delta^+/2) F_1^*(\boldsymbol{x}^\perp, x^-, x^+ - \delta^+/2) \\ \times \exp\left[-ip_1^- x_2^+ - i\mathcal{S}_{p_1}(\phi_2) + ip_1^- x_1^+ + i\mathcal{S}_{p_1}(\phi_1)\right]. \tag{2.38}$$

On the one hand, we see that if it is possible to neglect δ^+ in the arguments of F_1's (and also of F_2's), then the expression for the differential probability, analogous to the one in vacuum, is recovered.

On the other hand, we are mainly interested in the highly nonlinear regime, i.e., the regime $\xi \gg 1$, with ξ being the classical intensity parameter (1.125) (for a linearly-polarized laser pulse). In this regime, the integrals in the light-cone time are highly oscillating and form in the region when the phase < 1, which would correspond to the integration in δ^+ up to $m\delta^+ \sim 1/\xi$ [Ritus, 1985], unless a cancellation of oscillating terms happen in the phase. It should be pointed out, that in general also the magnitude of the quantum nonlinearity parameter defines the convergence of the integral and the validity of our approximation [Baier et al., 1989; Dinu et al., 2016]. We always assume that $\chi \lesssim 1$ for all involved particles, such that the above statements remain true.

Moreover, we assume that the wave packets are sufficiently narrow, i.e., $|\Delta \boldsymbol{p}_i^\perp| \ll |\boldsymbol{p}_i^\perp|$ and $|\Delta p_i^+| \ll |p_i^+|$, where $\Delta \boldsymbol{p}_i^\perp$ and Δp_i^+ are widths of the wave packets in momentum space. As a result, the contribution to the phases of F_1's in Eq. (2.38) (and also F_2's) from the terms with δ^+ is $\ll 1$, when $m\delta^+ \sim 1/\xi$.

Therefore, anticipating that in a highly nonlinear regime the integral in δ^+ forms in the region $|m\delta^+| \ll 1$ and neglecting δ^+ in the arguments of F_1's and F_2's, we obtain the probability per unit time unit volume:

$$\mathrm{d}\dot{w} = |f_2(x)|^2 |f_1(x)|^2 (2\pi)^3 \delta^{(+,\perp)}(k - p_2 - p_1) \frac{\mathcal{M}(x^+, p_2, p_1)}{4p_2^+ p_1^+} \frac{\tilde{\mathrm{d}}^3 k}{(2\pi)^3 2k^+}, \tag{2.39}$$

where

$$\mathcal{M}(x^+, p_2, p_1) = \int \mathrm{d}\delta^+ \exp\left[i\Phi_{p_2 p_1}(x_2^+) - i\Phi_{p_2 p_1}(x_1^+)\right] \\ \times M(\phi_2, p_2, p_1) M^*(\phi_1, p_2, p_1). \tag{2.40}$$

Then the total cross section, averaged (summed) over the initial (final) polarization states, is given by

$$\sigma(x^+) = \frac{1}{32k^+ I(\phi)} \sum_{\text{polarization}} \mathcal{M}(x^+, p_2, p_1), \tag{2.41}$$

where [compare Eqs (2.8) and (2.31)]

$$I(\phi) = \sqrt{[\pi_{p_2}(\phi)\pi_{p_1}(\phi)]^2 - m^4}. \tag{2.42}$$

The quantity (2.41) can be viewed classically as the probability to annihilate into a photon in the point x^μ with the electron and positron fluxes, entering this point, normalized to one particle. However, since we define the in- and out-states at infinitely distant past and future, respectively, this interpretation should be taken with care. In our formulation, a clear physical meaning has the total probability

$$W = \int \mathrm{d}^4 x |f_2(x)|^2 |f_1(x)|^2 J(\phi) \sigma(x^+), \tag{2.43}$$

where the flux factor $J(\phi) = I(\phi)/(p_2^+ p_1^+)$.

The problem with the cross section (2.41) is that it contains the invariant (2.42) in the denominator. Due to the dependence on the external field, $I(\phi)$ may become zero, even if the initial particles are not at rest in the center-of-momentum frame (note that the invariant I in vacuum is zero only in the case, when the initial particles are at rest in the center-of-momentum frame). It does not affect observables, however [see Eq. (2.43)].

It is more convenient to normalize the probability (2.39) to the flux at $x^+ \to -\infty$ and define the cross section as

$$\sigma_0(x^+) = \frac{1}{32k^+ I} \sum_{\text{polarization}} \mathcal{M}(x^+, p_2, p_1), \tag{2.44}$$

with the invariant I given by Eq. (2.17). In the following, we use the cross section (2.44).

It should be pointed out, that the definition (2.39) is different from the one in [Ritus, 1985] and the definition (2.44) is different from the one in [Ilderton et al., 2011]. In [Ritus, 1985; Ilderton et al., 2011], the differential probability is obtained as an average of the integration over a large time interval. In our case, the integration in time is naturally limited by the time interval of the overlap of the wave packets.

2.3 Evaluation of the trace

The preexponential factor in Eq. (2.40), averaged and summed over the polarization states, is given by:

$$\frac{1}{4} \sum_{\text{polarization}} M(\phi_2, p_2, p_1) M^*(\phi_1, p_2, p_1) = e^2 \mathcal{T}_{-21}(\phi_2, \phi_1) \tag{2.45}$$

(we denote momenta simply by numbers: $p_1 \to 1$, $-p_2 \to -2$), where

$$\mathcal{T}_{-21}(\phi_2, \phi_1) = -\mathrm{Tr}\{\rho_2^{(-)} K^{\mu}_{-21}(\phi_2) \rho_1 K^{\nu}_{1,-2}(\phi_1)\} g_{\mu\nu}. \tag{2.46}$$

The density matrices are given by (the incoming particles are assumed to be unpolarized)

$$\rho_1 = \frac{1}{2}(\gamma p_1 + m), \quad \rho_2^{(-)} = \frac{1}{2}(\gamma p_2 - m) = -\rho_{-2}. \tag{2.47}$$

During the evaluation of the trace, for clarity, we relabel the momentum of the positron as $p_2 \to -p_2$, such that

$$\mathcal{T}_{-21}(\phi_2, \phi_1) \to \mathcal{T}_{21}(\phi_2, \phi_1) = \mathrm{Tr}\{\rho_2 K^{\mu}_{21}(\phi_2) \rho_1 K^{\nu}_{12}(\phi_1)\} g_{\mu\nu}. \tag{2.48}$$

From the expansion (1.84) we conclude, that in the density matrices only the terms with γ^- give nonvanishing result, so, we obtain:

$$\begin{aligned}
\mathcal{T}_{21}(\phi_2, \phi_1) = \frac{1}{4}\mathrm{Tr}\Big\{&(\gamma p_2 + m)\left[S^{\mu}_{21}(\phi_2) + V^{i\mu}_{21}\gamma_i + T^{\mu}_{21}(\phi_2)\gamma^1\gamma^2\right]\gamma^+ \\
&\times (\gamma p_1 + m)\left[S^{\nu}_{12}(\phi_1) + V^{j\nu}_{12}\gamma_j + T^{\nu}_{12}(\phi_1)\gamma^1\gamma^2\right]\gamma^+\Big\} g_{\mu\nu} \\
= \frac{1}{2} p_2^+ p_1^+ \mathrm{Tr}\Big\{&\left[S^{\mu}_{21}(\phi_2) + V^{i\mu}_{21}\gamma_i + T^{\mu}_{21}(\phi_2)\gamma^1\gamma^2\right] \\
&\times \left[S^{\nu}_{12}(\phi_1) + V^{j\nu}_{12}\gamma_j + T^{\nu}_{12}(\phi_1)\gamma^1\gamma^2\right]\Big\} g_{\mu\nu}.
\end{aligned} \tag{2.49}$$

We obtain what has been noticed before: the initial trace is possible to reduce to a trace in the transverse space only. The evaluation is trivial:

$$\mathcal{T}_{21}(\phi_2, \phi_1) = 2p_2^+ p_1^+ \left[S^{\mu}_{21}(\phi_2) S^{\nu}_{12}(\phi_1) + V^{i\mu}_{21} V^{j\nu}_{12} g_{ij} - T^{\mu}_{21}(\phi_2) T^{\nu}_{12}(\phi_1)\right] g_{\mu\nu}. \tag{2.50}$$

Performing the contractions with $g_{\mu\nu}$, we find that

$$\begin{aligned}\mathcal{T}_{21}(\phi_2,\phi_1) = \frac{1}{p_2^+ p_1^+}[&p_1^{+2}\pi_2(\phi_2)\pi_2(\phi_1) + p_2^{+2}\pi_1(\phi_2)\pi_1(\phi_1)\\ &-p_2^+ p_1^+ \pi_2(\phi_2)\pi_1(\phi_2) - p_2^+ p_1^+ \pi_1(\phi_1)\pi_2(\phi_1)\\ &-p_2^{+2}m^2 - p_1^{+2}m^2 + 4p_2^+ p_1^+ m^2].\end{aligned} \tag{2.51}$$

With the use of the four-momentum relations [see Eq. (1.122)]

$$\begin{aligned}&\pi_2^\mu(\phi) + k^\mu - \pi_1^\mu(\phi) \sim 0,\\ &k\pi_2(\phi) \sim 0, \quad k\pi_1(\phi) \sim 0, \quad \pi_2(\phi)\pi_1(\phi) \sim m^2,\end{aligned} \tag{2.52}$$

(in the following, we will write simply an equal sign) the result can be rewritten as

$$\mathcal{T}_{21}(\phi_2,\phi_1) = 2m^2 - \frac{1}{2}\left(\frac{p_2^+}{p_1^+} + \frac{p_1^+}{p_2^+}\right)\Delta^2(\phi_2,\phi_1), \tag{2.53}$$

where

$$\begin{aligned}\Delta^2(\phi_2,\phi_1) = [\pi_p(\phi_2) - \pi_p(\phi_1)]^2 &= e^2[A(\phi_2) - A(\phi_1)]^2\\ &= -m^2 \sum_{i=1,2} \xi_i^2[\psi_i(\phi_2) - \psi_i(\phi_1)]^2\end{aligned} \tag{2.54}$$

does not depend on p^μ. Recovering the complete expression, we obtain:

$$\mathcal{T}_{-21}(\phi_2,\phi_1) = 2m^2 - \frac{m^2}{2}\left(\frac{p_2^+}{p_1^+} + \frac{p_1^+}{p_2^+}\right)\sum_{i=1,2} \xi_i^2[\psi_i(\phi_2) - \psi_i(\phi_1)]^2, \tag{2.55}$$

which is the same form, as obtained for nonlinear Compton scattering, with the change $p_2^\mu \to -p_2^\mu$ (see, e.g., [Hartin, 2016] or [Di Piazza et al., 2018]).

2.4 Phase

The phase in Eq. (2.40) is given by

$$\Phi = (k^- - p_2^- - p_1^-)\delta^+ + \mathcal{S}_{-2}(\phi_2,\phi_1) - \mathcal{S}_1(\phi_2,\phi_1). \tag{2.56}$$

The field-dependent part can be written as [Meuren et al., 2013]

$$\begin{aligned}&\mathcal{S}_{-2}(\phi_2,\phi_1) - \mathcal{S}_1(\phi_2,\phi_1) = \mathcal{S}_{-21}(\phi_2,\phi_1)\\ &\qquad = \int_{\phi_1}^{\phi_2} \mathrm{d}\beta \left[\frac{e p_{1\mu} p_{2\nu} \mathcal{F}^{\mu\nu}(\beta)}{m^2 p_1^+ p_2^+} - \frac{e^2(p_1^+ + p_2^+) p_{1\mu} p_{2\nu} \mathcal{F}^{2\mu\nu}(\beta)}{2m^3 p_1^{+2} p_2^{+2}}\right],\end{aligned} \tag{2.57}$$

where the integrated field-tensors are given by Eq. (1.35). With the use of the conservation laws for the asymptotic momenta

$$(p_2 + p_1)^{(+,\perp)} = k^{(+,\perp)}, \tag{2.58}$$

one obtains:

$$\Phi = -\frac{k^+ m^2 \delta^+}{2p_2^+ p_1^+}\left[1 + \sum_i (t_i + \xi_i I_i)^2 + \sum_i \xi_i^2 (J_i - I_i^2)\right]. \tag{2.59}$$

where

$$I_i = \int_{-1}^{1} \mathrm{d}\lambda\, \psi_i\left(\phi + \frac{1}{2} m\delta^+ \lambda\right), \quad J_i = \int_{-1}^{1} \mathrm{d}\lambda\, \psi_i^2\left(\phi + \frac{1}{2} m\delta^+ \lambda\right), \tag{2.60}$$

$\phi = mx^+$, and the parameter t_i is defined by Eq. (1.127). The result (2.59) can be conveniently derived in the canonical light-cone basis (1.29) with $q^\mu = p_2^\mu + p_1^\mu$ (note that in this basis $t_i = p_1^i/m = -p_2^i/m$).

2.5 Final result

The cross section (2.44) is given by

$$\sigma_0(x^+) = \frac{e^2}{8Ik^+} \int \mathrm{d}\delta^+\, \mathrm{e}^{i\Phi}\, \mathcal{T}_{-21}(\phi_2, \phi_1), \tag{2.61}$$

where $\mathcal{T}_{-21}(\phi_2, \phi_1)$ is given by Eq. (2.55) and Φ by Eq. (2.59).

Since the phase Φ is odd in δ^+ and the preexponential factor $\mathcal{T}_{-21}(\phi_2, \phi_1)$ is even in δ^+, the result can be written as

$$\sigma_0(x^+) = \frac{e^2}{8Ik^+} \mathrm{Re} \int_0^\infty \mathrm{d}\delta^+\, \mathrm{e}^{i\Phi}\, \mathcal{T}_{-21}(\phi_2, \phi_1), \tag{2.62}$$

with Re denoting the real part.

In general, the integral in δ^+ has to be evaluated numerically. It can be expressed via special functions, e.g., in the case of a constant-crossed field, which we consider below.

But first let us verify that in the high-intensity regime the integral in δ^+ indeed forms in the region $m\delta^+ \ll 1$. Consider a linearly-polarized pulse ($\xi_1 = \xi$, $\xi_2 = 0$). Then for the phase we have

$$\Phi = -\frac{k^+ m^2 \delta^+}{2p_2^+ p_1^+}\left[1 + t_2^2 + (t_1 + \xi I_1)^2 + \xi^2 (J_1 - I_1^2)\right]. \tag{2.63}$$

The phase is negative for all δ^+ (the relation $J_1 - I_1^2 \geq 0$ follows from the Cauchy-Bunyakovsky-Schwarz inequality; it can be also verified directly). For $\delta^+ \ll 1$ we have

$$J_1 - I_1^2 \approx [\psi'(\phi)]^2 \frac{m^2 \delta^{+2}}{12}, \tag{2.64}$$

which shows that for $\chi_1, \chi_2 \lesssim 1$ [see Eq. (1.126)] the last term becomes of order one at $m\delta^+ \sim 1/\xi \ll 1$.

2.6 Constant-crossed field case

We consider the case of a linear polarization, with $\psi_1(\phi) = \phi$. Then the integral in δ^+ is evaluated to produce the result

$$\sigma_0(x^+) = \frac{4\pi^2 r_e^2 m^2}{\varkappa I}\left(\frac{\chi_2 \chi_1}{\varkappa}\right)^{1/3}\left[1 + \rho\left(\frac{\chi_2}{\chi_1} + \frac{\chi_1}{\chi_2}\right)\left(\frac{\chi_2 \chi_1}{\varkappa}\right)^{2/3}\right] \mathrm{Ai}(\rho), \tag{2.65}$$

where $\mathrm{Ai}(\rho)$ is the Airy function [Olver et al., 2010], ρ is given by

$$\rho = \left(\frac{\varkappa}{\chi_2\chi_1}\right)^{2/3} [1 + t_2^2 + \zeta^2(\phi)], \tag{2.66}$$

the parameter $\zeta(\phi)$ is given by [see Eq. (1.127)]

$$\zeta(\phi) = (t_1 + \xi\phi)/\xi. \tag{2.67}$$

the quantities χ_1 and χ_2 are the quantum nonlinearity parameters for the electron and positron, respectively [see Eq. (1.126)], and in order to distinguish the photon we denoted its quantum nonlinearity parameter as $\varkappa$.

The obtained result is similar to the one for nonlinear Compton scattering [Ritus, 1985], however, due to the presence of the parameters $\zeta(\phi)$ and t_2 in the argument of the Airy function, the cross section is exponentially suppressed, if those parameters $\gtrsim 1$, as was also pointed out by Ritus (1985). Since the parameters $\zeta(\phi)$ and t_2 characterize the transverse momentum of the colliding system, a nonnegligible probability for the annihilation is obtained only if those momentum components are sufficiently small.

3

High-energy vacuum birefringence and dichroism

In this chapter, we study the vacuum polarization. For low-frequency (in comparison to the electron mass m) electromagnetic fields $F^{\mu\nu}$ vacuum polarization effects are described by the effective Euler-Heisenberg Lagrangian density, which was derived by Heisenberg and Euler (1936), independently by Weisskopf (1936), and later obtained by Schwinger (1951) with the use of the proper-time method (for more recent reviews of the Euler-Heisenberg Lagrangian, see, e.g., [Berestetskii et al., 1982; Dittrich and Gies, 2000; Dunne, 2012]). Below the QED critical field $E_{\text{cr}} = m^2/|e| \approx 1.3 \times 10^{18}$ V/m, low-frequency vacuum polarization effects are suppressed and the density is given by

$$\mathcal{L}_{\text{EH}} = -\mathcal{F} + \frac{\alpha}{90\pi E_{\text{cr}}^2}(4\mathcal{F}^2 + 7\mathcal{G}^2) + \cdots , \tag{3.1}$$

where $\mathcal{F} = F_{\mu\nu}F^{\mu\nu}/4$ and $\mathcal{G} = (*F)_{\mu\nu}F^{\mu\nu}/4$ are the electromagnetic field invariants, $(*F)^{\mu\nu} = \epsilon^{\mu\nu\sigma\tau}F_{\sigma\tau}/2$ is the dual tensor.

The critical intensity $I_{\text{cr}} = E_{\text{cr}}^2 \approx 4.6 \times 10^{29}$ W/cm^2 is well above even the envisaged $I \sim 10^{23}$ W/cm^2 for future 10 PW-class optical lasers. Therefore, the leading-order correction given in Eq. (3.1) is sufficient to describe low-frequency vacuum polarization effects. Recently, various schemes have been considered to measure them: vacuum birefringence with x-rays [Heinzl et al., 2006; Karbstein and Sundqvist, 2016; Schlenvoigt et al., 2016; Shakeri et al., 2017], diffraction [Di Piazza et al., 2006; King et al., 2010], four-wave mixing [Lundström et al., 2006; Tennant, 2016], Bragg scattering [Kryuchkyan and Hatsagortsyan, 2011], and other setups [Tommasini et al., 2008; Homma et al., 2011; King and Keitel, 2012; Monden and Kodama, 2012; Hu and Huang, 2014; Mohammadi et al., 2014; Fillion-Gourdeau et al., 2015; Gies et al., 2015; Karbstein and Shaisultanov, 2015; Zavattini et al., 2016], but all suggested experiments will remain challenging in the foreseeable future.

Searches for optical vacuum polarization effects have also been proposed as a way to discover low-energy physics beyond the Standard Model, e.g., axionlike or minicharged particles and paraphotons [Gies et al., 2006; Abel et al., 2008; Tommasini et al., 2009; Villalba-Chávez and Di Piazza, 2013; Villalba-Chávez et al., 2016] (see also [Jaeckel and Ringwald, 2010] for a review and [Jaeckel and Spannowsky, 2016] for some recently updated limits on low-energy new physics).

The combination of a high-intensity laser field and high-energy probe photon beam, however, allows to reach the critical intensity in the center-of-momentum frame and, therefore, to explore vacuum polarization effects at their maximal value [Berestetskii et al., 1982]. In this regime, i.e., in the regime $\chi \gtrsim 1$, the Euler-Heisenberg approximation is no longer applicable, as the probe photon field can not be treated as slowly varying anymore.

Instead, the polarization operator in the background field must be employed (see Fig. 3.1). In the regime $\chi \gtrsim 1$, the imaginary part of the polarization operator is not suppressed, with comparison to the regime $\chi \ll 1$, and as a manifestation of this, dichroic properties of the vacuum become sizable.

We start by reviewing the polarization operator in a plane-wave field with the use of the lightfront formalism. Employing the polarization operator in the locally constant field approximation, we derive how the polarization of a generic photon beam changes, while traversing through an intense laser pulse. Finally, we consider an experimental scheme to measure high-energy vacuum birefringence and dichroism in an intense laser field.

3.1 Polarization operator in a plane-wave field

The first calculation of the polarization operator in a monochromatic plane-wave field was published by Becker and Mitter (1975). The polarization operator in an arbitrary plane-wave field was obtained by Baier et al. (1976) with the use of the so-called operator technique, and later by Meuren et al. (2013) by the direct evaluation of the Feynman diagram.

Here, we employ the front-form approach and present a simplified derivation of the polarizaton operator in a plane-wave field of an arbitrary shape. Generally, we follow the ideas presented by Meuren et al. (2013), however, due to the split of the vertices into the three-point and seagull parts and the use of the light-cone expansion, the amount of the calculations is significantly reduced, especially at the step of the evaluation of the derivatives with respect to the "sources" (see [Meuren et al., 2013] for details), in fact, there is no need to explicitly introduce the sources.

3.1.1 General structure

The leading-order diagram for the polarization operator is shown in Fig. 3.1. To be precise, the diagram corresponds to $k_{2\mu} i\mathcal{P}^{\mu\nu}(k_2, k_1)k_{1\nu}$, with $\mathcal{P}^{\mu\nu}(k_2, k_1)$ being the polarization operator, which we are going to evaluate (this definition is consistent with [Berestetskii et al., 1982], up to 4π, due to the fact that we use Heaviside units). The radiative corrections to the polarization operator can be neglected for $\chi \lesssim 1$ [Ritus, 1985] (see [Fedotov, 2017] for a review).

In the diagram, there are two electron propagators, each consisting of the noninstantaneous and instantaneous parts. They give rise to the three terms, which we correspondingly denote as 'nn' for the term including the combination of the two noninstantaneous propagators, 'ni' for the term including the combination of the noninstantaneous and the instantaneous propagators, and 'in' for the term with the latter combination in the opposite order [we use the first letter for the propagator with p_2^μ, and the second letter for the

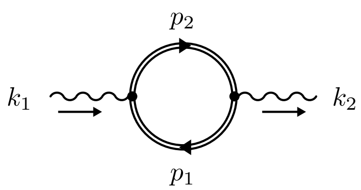

Fig. 3.1. The leading-order diagram for the polarization operator in a plane-wave field.

propagator with p_1^μ (see Fig. 3.1)]. So, we have:

$$\mathcal{P}^{\mu\nu}(k_2,k_1)=\mathcal{P}^{\mu\nu}_{\rm nn}(k_2,k_1)+\mathcal{P}^{\mu\nu}_{\rm ni}(k_2,k_1)+\mathcal{P}^{\mu\nu}_{\rm in}(k_2,k_1). \tag{3.2}$$

Note that, according to our definition, the left index μ of $\mathcal{P}^{\mu\nu}(k_2,k_1)$ is contracted with the polarization four-vector of the outgoing photon, and the right index ν is contracted with the polarization four-vector of the incoming photon (see Fig. 3.1). In [Meuren et al., 2013] and [Baier et al., 1976] the order is the opposite, therefore, the comparison of the results needs to be made after the swap of the tensor indices.

The 'nn' contribution is given by

$$\begin{aligned}\mathcal{P}^{\mu\nu}_{\rm nn}(k_2,k_1)=ie^2(2\pi)^3\delta^{(+,\perp)}(k_2-k_1)\int\frac{\mathrm{d}p_2^-}{2\pi}\int\frac{\mathrm{d}^4p_1}{(2\pi)^4}\int\mathrm{d}x_2^+\mathrm{d}x_1^+\\ \times\frac{\mathrm{e}^{i\Phi}\,\mathcal{T}^{\mu\nu}_{\rm nn}}{(p_2^2-m^2+i\epsilon)(p_1^2-m^2+i\epsilon)},\end{aligned} \tag{3.3}$$

where

$$\Phi=(p_2^-+k_2^--p_1^-)x_2^++(p_1^--k_1^--p_2^-)x_1^++\mathcal{S}_2(\phi_2,\phi_1)-\mathcal{S}_1(\phi_2,\phi_1), \tag{3.4}$$

and

$$\mathcal{T}^{\mu\nu}_{\rm nn}=\mathrm{Tr}\{(\gamma\tilde{p}_2+m)K^\mu_{21}(\phi_2)(\gamma\tilde{p}_1+m)K^\nu_{12}(\phi_1)\}. \tag{3.5}$$

The trace is evaluated analogously to the evaluation of the trace for first-order processes:

$$\mathcal{T}^{\mu\nu}_{\rm nn}=8p_2^+p_1^+\left[S^\mu_{21}(\phi_2)S^\nu_{12}(\phi_1)+V^{i\mu}_{21}V^{j\nu}_{12}g_{ij}-T^\mu_{21}(\phi_2)T^\nu_{12}(\phi_1)\right]. \tag{3.6}$$

The 'ni' contribution is given by

$$\mathcal{P}^{\mu\nu}_{\rm ni}(k_2,k_1)=ie^2(2\pi)^3\delta^{(+,\perp)}(k_2-k_1)\int\frac{\mathrm{d}^4p_2}{(2\pi)^4}\int\mathrm{d}x^+\frac{\mathrm{e}^{i(k_2^--k_1^-)x^+}\,\mathcal{T}^{\mu\nu}_{\rm ni}}{p_2^2-m^2+i\epsilon}, \tag{3.7}$$

where

$$\mathcal{T}^{\mu\nu}_{\rm ni}=\frac{1}{2p_1^+}\mathrm{Tr}\{(\gamma\tilde{p}_2+m)K^{\mu\nu}_{22}(\phi)\}=\frac{2p_2^+}{p_1^+}\left[S^\mu_2S^\nu_2-V^{i\mu}_2(\phi)V^{j\nu}_2(\phi)g_{ij}\right]. \tag{3.8}$$

Finally, the 'in' contribution is the same, as the 'ni' contribution, but with the exchange $p_2^\mu\leftrightarrow p_1^\mu$:

$$\mathcal{P}^{\mu\nu}_{\rm in}(k_2,k_1)=\mathcal{P}^{\mu\nu}_{\rm ni}(k_2,k_1)\Big|_{p_2^\mu\leftrightarrow p_1^\mu},\quad \mathcal{T}^{\mu\nu}_{\rm in}=\mathcal{T}^{\mu\nu}_{\rm ni}\Big|_{p_2^\mu\leftrightarrow p_1^\mu}. \tag{3.9}$$

Note, that formally we also need to swap the indices μ and ν for $K^{\mu\nu}_{11}(\phi)$ in $\mathcal{T}^{\mu\nu}_{\rm in}$, however, it is not necessary, since, as we see from Eq. (3.8), the tensor $\mathcal{T}^{\mu\nu}_{\rm ni}$ (and therefore $\mathcal{T}^{\mu\nu}_{\rm in}$) is symmetric.

For the "+" and "⊥" momentum components the following conservation relations are valid:

$$p_2^{(+,\perp)}=(p_1-k_2)^{(+,\perp)}=(p_1-k_1)^{(+,\perp)}. \tag{3.10}$$

We are interested in the evaluation of the field-dependent part of the polarization operator, therefore, we subtract the vacuum part $\mathcal{P}^{\mu\nu}_0(k_2,k_1)$ and calculate the quantity

$$\mathcal{P}^{\mu\nu}_F(k_2,k_1)=\mathcal{P}^{\mu\nu}(k_2,k_1)-\mathcal{P}^{\mu\nu}_0(k_2,k_1). \tag{3.11}$$

3.1.2 Ward-Takahashi identity

For the polarization operator $\mathcal{P}^{\mu\nu}(k_2, k_1)$, the Ward-Takahashi identity, applied to each of the two external photon legs, results in the following relations [Peskin and Schroeder, 1995]:

$$k_{2\mu}\mathcal{P}^{\mu\nu}(k_2, k_1) = 0, \quad \mathcal{P}^{\mu\nu}(k_2, k_1)k_{1\nu} = 0. \tag{3.12}$$

It is instructive to check explicitly, how the four-momentum conservation relations, discussed in Section 1.9, lead to Eq. (3.12). We prove the first identity in Eq. (3.12), the second one can be proved in an analogous way.

For $k_{2\mu}\mathcal{T}^{\mu\nu}_{\text{nn}}$ we need to find the contractions of k_2^μ with $S^\mu_{21}(\phi_2)$, $V^{i\mu}_{21}$, and $T^\mu_{21}(\phi_2)$ [see Eq. (3.6)]. We obtain:

$$\begin{gathered} k_2 S_{21}(\phi_2) = \frac{1}{2p_2^+ p_1^+}\left\{p_2^+ k_2\pi_1(\phi_2) + p_1^+ k_2\pi_2(\phi_2) - k_2^+\left[\pi_2(\phi_2)\pi_1(\phi_2) - m^2\right]\right\}, \\ k_2 V^i_{21} = k_2 T_{21}(\phi_2) = 0. \end{gathered} \tag{3.13}$$

Using the momentum relations (for simplicity, we write an equal sign instead of '$\sim$')

$$\begin{gathered} k_2\pi_2(\phi_2) = \frac{1}{2}(p_1^2 - p_2^2 - k_2^2), \quad k_2\pi_1(\phi_2) = -\frac{1}{2}(p_2^2 - p_1^2 - k_2^2), \\ \pi_2(\phi_2)\pi_1(\phi_2) = -\frac{1}{2}(k_2^2 - p_2^2 - p_1^2), \end{gathered} \tag{3.14}$$

we obtain that

$$k_{2\mu}\mathcal{T}^{\mu\nu}_{\text{nn}} = (p_1^2 - m^2)\Delta\mathcal{T}^\nu_{\text{ni}} + (p_2^2 - m^2)\Delta\mathcal{T}^\nu_{\text{in}}, \tag{3.15}$$

where

$$\Delta\mathcal{T}^\nu_{\text{ni}} = 4p_2^+ S^\nu_{12}(\phi_1), \quad \Delta\mathcal{T}^\nu_{\text{in}} = -4p_1^+ S^\nu_{12}(\phi_1). \tag{3.16}$$

The four-vectors $\Delta\mathcal{T}^\nu_{\text{ni}}$ and $\Delta\mathcal{T}^\nu_{\text{in}}$ in Eq. (3.16) are to be combined with the 'ni' and 'in' parts, respectively.

For $k_{2\mu}\mathcal{T}^{\mu\nu}_{\text{ni}}$ we need to find the contractions of k_2^μ with S_2^μ and $V_2^{i\mu}(\phi)$ [see Eq. (3.8)]. We have:

$$k_2 S_2 = \frac{mk_2^+}{p_2^+}, \quad k_2 V_2^i(\phi) = k_2^i - \frac{k_2^+}{p_2^+}\pi_2^i(\phi). \tag{3.17}$$

After combining $k_{2\mu}\mathcal{T}^{\mu\nu}_{\text{ni}}$ and $\Delta\mathcal{T}^\nu_{\text{ni}}$ we obtain, that

$$k_{2\mu}\mathcal{T}^{\mu\nu}_{\text{ni}} + \Delta\mathcal{T}^\nu_{\text{ni}} = 4\pi_2^\nu(\phi) + \frac{2}{p_2^+}\left(m^2 - p_2^2\right)g^{\nu+}. \tag{3.18}$$

Performing the same calculations for the 'in' term, we obtain, that

$$k_{2\mu}\mathcal{T}^{\mu\nu}_{\text{in}} + \Delta\mathcal{T}^\nu_{\text{in}} = -4\pi_1^\nu(\phi) - \frac{2}{p_1^+}\left(m^2 - p_1^2\right)g^{\nu+}. \tag{3.19}$$

The momenta p_1^μ and p_2^μ are the integration variables. After relabeling $p_2^\mu \to p_1^\mu$ in the integral of the 'ni' contribution, we see that this contribution transforms into the 'in' contribution, but with the opposite sign. Therefore, the sum of both contributions is zero, which concludes the proof.

3.1.3 Tensor expansion

Having the identities (3.12) in mind, we represent the tensor structure of the polarization operator by expanding it in the two complete and orthogonal basis sets [Meuren et al., 2013; Baier et al., 1976]

$$\{k_2^\mu, \Lambda_1^\mu, \Lambda_2^\mu, Q_2^\mu\}\,, \quad \{k_1^\nu, \Lambda_1^\nu, \Lambda_2^\nu, Q_1^\nu\}\,, \tag{3.20}$$

where the four-vectors Λ_i^μ are from Eq. (1.29) and $Q_i^\mu = (k_i^2\eta^\mu - q^+k_i^\mu)/q^+$ (note that $Q_i^2 = -k_i^2$). We are free to choose any q^μ (under the condition $q^+ \neq 0$). The four-vector q^μ will be specified in a moment, but for now, let us proceed with the general case. In the following, we utilize the canonical light-cone Lorentz basis (1.29).

Due to Eq. (3.12), essentially, we need to know the contractions of the polarization operator only with Λ_1^μ, Λ_2^μ, and η^μ. Let us start with the 'ni' contribution. One can find that

$$\Lambda_j S_2 = 0, \quad \Lambda_j V_2^i(\phi) = g^{ij}, \quad \eta S_2 = \eta V_2^i(\phi) = 0, \tag{3.21}$$

and analogously for the products from the left side. We see, that the 'ni' part contains only terms proportional to $\Lambda_1^\mu\Lambda_1^\nu$ and $\Lambda_2^\mu\Lambda_2^\nu$, with the coefficients not depending on the external field [see Eq. (3.7)], as a result, it does not contribute to $\mathcal{P}_F^{\mu\nu}(k_2, k_1)$ [see Eq. (3.11)]. Absolutely analogous considerations are true also for the 'in' part. Therefore, only the 'nn' part needs to be evaluated.

For the calculation of the 'nn' term, we choose $q^\mu = k_1^\mu$, which implies that $\boldsymbol{k}_1^\perp = \boldsymbol{k}_2^\perp = 0$ and $\boldsymbol{p}_1^\perp = \boldsymbol{p}_2^\perp$. With this choice, we obtain that

$$\begin{gathered}\Lambda_k S_{21}(\phi) = \frac{p_2^+ + p_1^+}{2p_2^+p_1^+}\pi_1^k(\phi), \quad \Lambda_k V_{21}^i = \frac{m(p_2^+ - p_1^+)}{2p_2^+p_1^+}g^{ik}, \\ \Lambda_k T_{21}(\phi) = -\frac{p_2^+ - p_1^+}{2p_2^+p_1^+}\epsilon^{kl}\pi_{1l}(\phi), \quad \eta S_{21}(\phi) = 1, \quad \eta V_{21}^i = \eta T_{21}(\phi) = 0.\end{gathered} \tag{3.22}$$

The results for the contractions from the left side are obtained with the use of the symmetry relations

$$S_{12}^\mu(\phi) = S_{21}^\mu(\phi), \quad V_{12}^{i\mu} = -V_{21}^{i\mu}, \quad T_{12}^\mu(\phi) = -T_{21}^\mu(\phi). \tag{3.23}$$

Combining all the terms together, we obtain:

$$\begin{aligned}\mathcal{T}_{\text{nn}}^{\mu\nu} = a^{12}\Lambda_1^\mu\Lambda_2^\nu + a^{21}\Lambda_2^\mu\Lambda_1^\nu + b^{12}\Lambda_1^\mu\Lambda_1^\nu + b^{21}\Lambda_2^\mu\Lambda_2^\nu + c_5 Q_2^\mu Q_1^\nu \\ + d^1(\phi_1)Q_2^\mu\Lambda_1^\nu + d^2(\phi_1)Q_2^\mu\Lambda_2^\nu + d^1(\phi_2)\Lambda_1^\mu Q_1^\nu + d^2(\phi_2)\Lambda_2^\mu Q_1^\nu,\end{aligned} \tag{3.24}$$

where

$$\begin{gathered}a^{ij} = \frac{2(p_2^+ + p_1^+)^2}{p_2^+p_1^+}\pi_1^i(\phi_2)\pi_1^j(\phi_1) - \frac{2(p_2^+ - p_1^+)^2}{p_2^+p_1^+}\pi_1^j(\phi_2)\pi_1^i(\phi_1), \\ b^{ij} = \frac{2(p_2^+ + p_1^+)^2}{p_2^+p_1^+}\pi_1^i(\phi_2)\pi_1^i(\phi_1) + \frac{2(p_2^+ - p_1^+)^2}{p_2^+p_1^+}\pi_1^j(\phi_2)\pi_1^j(\phi_1) + \frac{2m^2(p_2^+ - p_1^+)^2}{p_2^+p_1^+}, \\ c_5 = \frac{8p_2^+p_1^+}{k_1^{+2}}, \quad d^i(\phi) = \frac{4(p_2^+ + p_1^+)}{p_2^+ - p_1^+}\pi_1^i(\phi).\end{gathered} \tag{3.25}$$

3.1.4 Evaluation of the integrals

This part of the derivation is basically the same, as in [Meuren et al., 2013], up to the point of the evaluation of the integrals in the transverse momentum components. Let us go through major steps.

We make a change of variables:

$$x^+ = (x_2^+ + x_1^+)/2, \quad \delta^+ = x_2^+ - x_1^+. \tag{3.26}$$

Then we write the phase (3.4) as

$$\begin{aligned}\Phi = p_2^- \delta^+ - p_1^- \delta^+ + k_2^- \left(x^+ + \frac{\delta^+}{2}\right) - k_1^- \left(x^+ - \frac{\delta^+}{2}\right) \\ + \frac{k_1^+ \delta^+}{2p_2^+ p_1^+} \sum_i \left(2m\xi_i p_1^i I_i + m^2 \xi_i^2 J_i\right),\end{aligned} \tag{3.27}$$

where

$$I_i = \frac{1}{2}\int_{-1}^{1} \mathrm{d}\lambda \, \psi_i \left(\phi + \frac{1}{2} m\delta^+ \lambda\right), \quad J_i = \frac{1}{2}\int_{-1}^{1} \mathrm{d}\lambda \, \psi_i^2 \left(\phi + \frac{1}{2} m\delta^+ \lambda\right). \tag{3.28}$$

For the propagators [see Eq. (3.3)], the proper-time representation is employed:

$$\begin{aligned}\frac{1}{(p_2^2 - m^2 + i\epsilon)(p_1^2 - m^2 + i\epsilon)} = -\int_0^\infty \mathrm{d}s \, \mathrm{d}t \, \exp\left[i(2p_2^+ p_2^- - \boldsymbol{p}_2^{\perp 2} - m^2 + i\epsilon)s\right] \\ \times \exp\left[i(2p_1^+ p_1^- - \boldsymbol{p}_1^{\perp 2} - m^2 + i\epsilon)t\right].\end{aligned} \tag{3.29}$$

We will not write the terms with $i\epsilon$ in the following, but will keep them in mind.

With the use of the representation (3.29), one is able to evaluate the integrals in p_2^- and p_1^-. We obtain two delta functions, which are transformed as

$$\delta(\delta^+ + 2p_2^+ s)\delta(\delta^+ - 2p_1^+ t) = \frac{1}{2(s+t)}\delta\left(\delta^+ - \frac{2k_1^+ st}{s+t}\right)\delta\left(p_1^+ - \frac{k_1^+ s}{s+t}\right). \tag{3.30}$$

Subsequently, the obtained delta functions are used for the evaluation of the integrals in δ^+ and p_1^+.

As the next step, we introduce new variables τ and v:

$$\tau = s + t, \quad v = \frac{s-t}{s+t}, \qquad \int_0^\infty \mathrm{d}s \, \mathrm{d}t \to \int_{-1}^{1} \mathrm{d}v \int_0^\infty \mathrm{d}\tau \, \frac{\tau}{2}. \tag{3.31}$$

We obtain:

$$\delta^+ = 2k_1^+ \mu, \quad p_1^+ = \frac{k_1^+ \mu}{\tau}, \tag{3.32}$$

$$\Phi = (k_2^- - k_1^-)x^+ + \mu k_2 k_1 - (\boldsymbol{p}_1^{\perp 2} + m^2)\tau - \tau \sum_i \left(2m\xi_i p_1^i I_i + m^2 \xi_i^2 J_i\right), \tag{3.33}$$

where $\mu = (1 - v^2)\tau/4$. The 'nn' term (3.3) takes the form:

$$\mathcal{P}_{\mathrm{nn}}^{\mu\nu}(k_2, k_1) = -\frac{i\alpha}{2}(2\pi)^3 \delta^{(+,\perp)}(k_2 - k_1) \int \frac{\mathrm{d}^2 p_1^\perp}{(2\pi)^2} \int \mathrm{d}x^+ \int_{-1}^{1} \mathrm{d}v \int_0^\infty \mathrm{d}\tau \, \mathrm{e}^{i\Phi} \, \mathcal{T}_{\mathrm{nn}}^{\mu\nu}. \tag{3.34}$$

We notice that the the coefficients $d^i(\phi)$ in Eq. (3.24) are proportional to v [see Eq. (3.25)], therefore, the integration in v yields zero for those coefficients, and we need to consider the coefficients only in the first line of Eq. (3.24). For those coefficients we change the order of the integrations and integrate in $\boldsymbol{p}_1^{\perp}$. The integrals are the Fresnel integrals, or may be expressed as derivatives of the Fresnel integrals, in particular:

$$\begin{aligned}
I_0^{(\perp)} &= \int \frac{\mathrm{d}^2 p_1^{\perp}}{(2\pi)^2}\, \mathrm{e}^{-i\tau(\boldsymbol{p}_1^{\perp 2}+2\boldsymbol{p}_1^{\perp}\boldsymbol{R}^{\perp})} = -\frac{i}{4\pi\tau}\mathrm{e}^{i\tau\boldsymbol{R}^{\perp 2}},\\
I_{1i}^{(\perp)} &= \int \frac{\mathrm{d}^2 p_1^{\perp}}{(2\pi)^2}\, p_1^i\, \mathrm{e}^{-i\tau(\boldsymbol{p}_1^{\perp 2}+2\boldsymbol{p}_1^{\perp}\boldsymbol{R}^{\perp})} = -R^i I_0^{(\perp)},\\
I_2^{(\perp)} &= \int \frac{\mathrm{d}^2 p_1^{\perp}}{(2\pi)^2}\, (p_1^i)^2\, \mathrm{e}^{-i\tau(\boldsymbol{p}_1^{\perp 2}+2\boldsymbol{p}_1^{\perp}\boldsymbol{R}^{\perp})} = \left[-\frac{i}{2\tau} + (R^i)^2\right] I_0^{(\perp)},
\end{aligned} \tag{3.35}$$

where $R^i = m\xi_i I_i$ [see Eq. (3.33)].

After the integration and subtraction of the vacuum part, the final result is given by

$$\begin{aligned}
\mathcal{P}_F^{\mu\nu}(k_2,k_1) = -\frac{\alpha}{2\pi}(2\pi)^3\delta^{(+,\perp)}(k_2-k_1)\int \mathrm{d}x^+ \int_{-1}^{1}\mathrm{d}v \int_0^{\infty}\frac{\mathrm{d}\tau}{\tau}\,\mathrm{e}^{i\Phi_0}\\
\times\left(b_1\Lambda_1^\mu\Lambda_2^\nu + b_2\Lambda_2^\mu\Lambda_1^\nu + b_3\Lambda_1^\mu\Lambda_1^\nu + b_4\Lambda_2^\mu\Lambda_2^\nu + b_5 Q_2^\mu Q_1^\nu\right),
\end{aligned} \tag{3.36}$$

where

$$\Phi_0 = (k_2^- - k_1^-)x^+ + \mu k_2 k_1 - \tau m^2, \tag{3.37}$$

and

$$\begin{aligned}
b_1 &= 2m^2\xi_2\xi_1\frac{\tau}{4\mu}\left(X_{21} - v^2 X_{12}\right)\mathrm{e}^{i\tau\beta},\\
b_2 &= 2m^2\xi_2\xi_1\frac{\tau}{4\mu}\left(X_{12} - v^2 X_{21}\right)\mathrm{e}^{i\tau\beta},\\
b_3 &= \left[\frac{i(1+v^2)}{\tau(1-v^2)} - \frac{m^2\tau}{2\mu}\right]\left(\mathrm{e}^{i\tau\beta}-1\right) - 2m^2\frac{\tau}{4\mu}\left(\xi_2^2 X_{22} + \xi_1^2 v^2 X_{11}\right)\mathrm{e}^{i\tau\beta},\\
b_4 &= \left[\frac{i(1+v^2)}{\tau(1-v^2)} - \frac{m^2\tau}{2\mu}\right]\left(\mathrm{e}^{i\tau\beta}-1\right) - 2m^2\frac{\tau}{4\mu}\left(\xi_1^2 X_{11} + \xi_2^2 v^2 X_{22}\right)\mathrm{e}^{i\tau\beta},\\
b_5 &= -\frac{2\mu}{\tau}\left(\mathrm{e}^{i\tau\beta}-1\right).
\end{aligned} \tag{3.38}$$

The quantities X_{ij} and β in Eq. (3.38) are defined as

$$X_{ij} = \left[I_i - \psi_i(\phi + mk_1^+\mu)\right]\left[I_j - \psi_j(\phi - mk_1^+\mu)\right] \tag{3.39}$$

and

$$\beta = m^2\sum_i \xi_i^2(I_i^2 - J_i). \tag{3.40}$$

The obtained result is the same as known from the literature [Meuren et al., 2013; Baier et al., 1976], apart from the form of the coefficients b_3 and b_4 in Eq. (3.38). These coefficients can be cast into the known form by an integration by parts in τ. For the second term in the square brackets in b_3 and b_4 we use the relation

$$\int_0^\infty \frac{d\tau}{\tau}\, e^{i(\mu k_2 k_1 - \tau m^2)} \left(e^{i\tau\beta} - 1\right) = \int_0^\infty \frac{d\tau}{\tau}\, e^{i(\mu k_2 k_1 - \tau m^2)} \times \left[\left(\frac{i}{\tau m^2} + \frac{\mu k_2 k_1}{\tau m^2} \right) \left(e^{i\tau\beta} - 1\right) - e^{i\tau\beta} \sum_i \xi_i^2 (X_{ii} + Z_i) \right], \tag{3.41}$$

where

$$Z_i = \frac{1}{2}\left[\psi_i(\phi + m k_1^+ \mu) - \psi_i(\phi - m k_1^+ \mu)\right]^2. \tag{3.42}$$

Note that the boundary terms vanish: the one at $\tau \to \infty$ due to the factor $1/\tau$ and also due to the exponential damping, that we have been keeping in mind [see Eq. (3.29)]; the one at $\tau \to 0$ due to $\beta \propto \tau^2$ in this limit.

So, we obtain:

$$\begin{aligned} b_3 \to b_3 &= -\left(\frac{i}{\tau} + \frac{k_2 k_1}{2}\right)\left(e^{i\tau\beta} - 1\right) + 2m^2 \left[\frac{\tau}{4\mu}\left(\xi_1^2 Z_1 + \xi_2^2 Z_2\right) + \xi_1^2 X_{11}\right] e^{i\tau\beta}, \\ b_4 \to b_4 &= -\left(\frac{i}{\tau} + \frac{k_2 k_1}{2}\right)\left(e^{i\tau\beta} - 1\right) + 2m^2 \left[\frac{\tau}{4\mu}\left(\xi_1^2 Z_1 + \xi_2^2 Z_2\right) + \xi_2^2 X_{22}\right] e^{i\tau\beta}, \end{aligned} \tag{3.43}$$

which is the same form, as was derived by Meuren et al. (2013).

3.1.5 Locally constant field approximation

The locally constant field approximation [valid in the regime $\xi \gg 1$, $\chi = (k_1^+/m)\xi \lesssim 1$] for a linearly polarized plane-wave field [$\psi_1(\phi) = \psi(\phi)$, $\psi_2(\phi) = 0$] was obtained by Meuren et al. (2013). Later, the polarization operator in this approximation will be used for the derivation of the effective photon wave function. Despite having a different representation of the polarization operator [Eq. (3.38)], one can proceed in exactly the same way, as was done by Meuren et al. (2013), and obtain the same expression (up to the swap of the indices μ and ν, as has been pointed out before). Therefore, here we do not discuss the derivation. The final result is given by

$$\mathcal{P}_F^{\mu\nu}(k_2, k_1) = -(2\pi)^3 \delta^{(+,\perp)}(k_2 - k_1) \int dx^+ e^{i(k_2^- - k_1^-)x^+} \times \left[p_1(\phi,\chi)\Lambda_1^\mu \Lambda_1^\nu + p_2(\phi,\chi)\Lambda_2^\mu \Lambda_2^\nu + p_3(\phi,\chi) G^{\mu\nu}\right], \tag{3.44}$$

where

$$\begin{aligned} p_1(\phi,\chi) &= \frac{\alpha m^2}{3\pi} \int_{-1}^{1} dv \left[\frac{\chi(\phi)}{w}\right]^{2/3} (w-1) f'(u), \\ p_2(\phi,\chi) &= \frac{\alpha m^2}{3\pi} \int_{-1}^{1} dv \left[\frac{\chi(\phi)}{w}\right]^{2/3} (w+2) f'(u), \\ p_3(\phi,\chi) &= \frac{\alpha k_2 k_1}{\pi} \int_{-1}^{1} dv\, \frac{f_1(u)}{w}, \end{aligned} \tag{3.45}$$

with w and u defined as

$$w = \frac{4}{1 - v^2}, \quad u = \left[\frac{w}{\chi(\phi)}\right]^{2/3} \left(1 - \frac{k_2 k_1}{w m^2}\right), \tag{3.46}$$

and $\chi(\phi) = \chi|\psi'(\phi)|$ being the local value of the quantum nonlinearity parameter. In Eq. (3.44) the tensor $G^{\mu\nu} = g^{\mu\nu} - (k_1^\mu k_2^\nu)/k_1 k_2$ is introduced and in Eq. (3.45) the Ritus functions [Ritus, 1985; Meuren et al., 2013] are employed:

$$
\begin{aligned}
f(u) &= i\int_0^\infty \mathrm{d}t\, \mathrm{e}^{-i(ut+t^3/3)} = \pi\mathrm{Gi}(u) + i\pi\mathrm{Ai}(u),\\
f_1(u) &= \int_0^\infty \frac{\mathrm{d}t}{t}\, \mathrm{e}^{-iut}\left(\mathrm{e}^{-it^3/3} - 1\right),
\end{aligned}
\tag{3.47}
$$

where $\mathrm{Gi}(u)$ and $\mathrm{Ai}(u)$ are the Scorer and Airy functions, respectively [Olver et al., 2010].

3.2 Effective photon wave function in a plane-wave field

An external plane-wave field changes the photon dispersion relation via the radiative corrections, induced by virtual particles (see Fig. 3.2). In the regime $\xi \gg 1$, $\chi \lesssim 1$, the effective photon wave function can be obtained in a closed form [Meuren et al., 2015].

We start with the Dyson equation [Berestetskii et al., 1982] for the photon external line:

$$
\Phi_k^\mu(x) = \int \mathrm{d}^4x_2 \mathrm{d}^4x_1 D_{\sigma\mu}(x, x_2)\mathcal{P}^{\mu\nu}(x_2, x_1)\Phi_{k\nu}(x_1), \tag{3.48}
$$

where $\Phi_k^\mu(x)$ is the effective photon wave function (the index k denotes the four-momentum k^μ; we suppress the normalization factor $1/\sqrt{2k^+\mathcal{V}}$ in the following), $D_{\sigma\mu}(x, x_2)$ is the photon propagator, and $\mathcal{P}^{\mu\nu}(x_2, x_1)$ is the polarization operator in the position space representation, i.e.,

$$
\mathcal{P}^{\mu\nu}(x_2, x_1) = \int \frac{\mathrm{d}^4k_2}{(2\pi)^4}\frac{\mathrm{d}^4k_1}{(2\pi)^4}\mathrm{e}^{-ik_2x_2}\mathcal{P}^{\mu\nu}(k_2, k_1)\mathrm{e}^{ik_1x_1}. \tag{3.49}
$$

From Eq. (3.48) we obtain that

$$
-\partial^\sigma\partial_\sigma\Phi_k^\mu(x) = \int \mathrm{d}^4y\, \mathcal{P}^{\mu\nu}(x, y)\Phi_{k\nu}(x), \tag{3.50}
$$

In the regime $\xi \gg 1$, $\chi \lesssim 1$, we use the locally constant field approximation for the polarization operator [see Eq. (3.44)]. We seek the solution of Eq. (3.50) as

$$
\Phi_k^\mu(x) = \epsilon^\mu(\phi)\mathrm{e}^{-ikx}, \quad \epsilon^\mu(\phi) = \sum_{i=1,2} c_i(\phi)\Lambda_i^\mu, \tag{3.51}
$$

with initial condition $\Phi_k^\mu(x) \to \Phi_k^{(0)\mu}(x) = \epsilon^{(0)\mu}\mathrm{e}^{-ikx}$ as $x^+ \to -\infty$, where $\epsilon^{(0)\mu}$ is the initial polarization four-vector:

$$
\epsilon^{(0)}\epsilon^{(0)*} = -1, \quad k\epsilon^{(0)} = 0, \quad \epsilon^{(0)\mu} = \sum_{i=1,2} c_i^{(0)}\Lambda_i^\mu. \tag{3.52}
$$

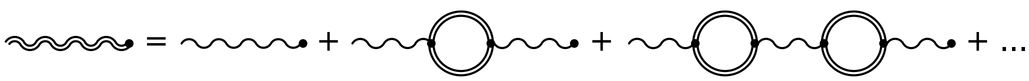

Fig. 3.2. Diagrammatic representation of the Dyson equation for the external photon line. We neglect the radiative corrections to the polarization operator for $\chi \lesssim 1$.

Solving Eq. (3.50), we obtain that [Meuren et al., 2015]

$$c_i(\phi) = c_i^{(0)} \exp\left[i\kappa_i(\phi) - \lambda_i(\phi)\right], \tag{3.53}$$

where

$$\kappa_i(\phi) = -\frac{1}{2k^+}\int_{-\infty}^{\phi} \mathrm{d}\tau\, \mathrm{Re}\{p_i(\tau,\chi)\}, \quad \lambda_i(\phi) = -\frac{1}{2k^+}\int_{-\infty}^{\phi} \mathrm{d}\tau\, \mathrm{Im}\{p_i(\tau,\chi)\}, \tag{3.54}$$

and the functions $p_i(\tau,\chi)$ are given by Eq. (3.45). We refer to $\kappa_i = \kappa_i(\phi \to \infty)$ as phase shifts and to $\lambda_i = \lambda_i(\phi \to \infty)$ as decay parameters:

$$\kappa_i = -\frac{1}{2k^+}\int_{-\infty}^{\infty} \mathrm{d}\tau\, \mathrm{Re}\{p_i(\tau,\chi)\}, \quad \lambda_i = -\frac{1}{2k^+}\int_{-\infty}^{\infty} \mathrm{d}\tau\, \mathrm{Im}\{p_i(\tau,\chi)\}. \tag{3.55}$$

In the matrix form, the relation between the initial $c_i^{(0)}$ and final $c_i = c_i(\phi \to \infty)$ coefficients can be written as

$$c_i = \sum_j T_{ij} c_j^{(0)}, \tag{3.56}$$

where

$$T = \begin{pmatrix} \mathrm{e}^{i\kappa_1 - \lambda_1} & 0 \\ 0 & \mathrm{e}^{i\kappa_2 - \lambda_2} \end{pmatrix}. \tag{3.57}$$

In order to extend the above result from a single photon to a photon beam (which is, in general, not in a pure polarization state), we introduce the following density tensors, which describe the initial ($\varrho^{(0)\mu\nu}$) and the final ($\varrho^{\mu\nu}$) polarization state of the beam [Berestetskii et al., 1982; Blum, 2012; Meuren et al., 2016]

$$\varrho^{(0)\mu\nu} = \sum_a w_a \epsilon_a^{(0)\mu} \epsilon_a^{(0)*\nu} = \sum_{i,j} \rho_{ij}^{(0)} \Lambda_i^\mu \Lambda_j^\nu, \quad \varrho^{\mu\nu} = \sum_a w_a \epsilon_a^\mu \epsilon_a^{*\nu} = \sum_{i,j} \rho_{ij} \Lambda_i^\mu \Lambda_j^\nu, \tag{3.58}$$

where w_a is the probability to find a photon with polarization four-vector $\epsilon_a^{(0)\mu}$ (ϵ_a^μ) in the initial (final) beam.

The initial $\rho^{(0)}$ and final ρ density matrices are related by

$$\rho = T\rho^{(0)}T^\dagger, \tag{3.59}$$

where the matrix T is given by Eq. (3.57).

Using the identity matrix and the Pauli matrices $\boldsymbol{\sigma} = (\sigma_1, \sigma_2, \sigma_3)$, which are given by [Berestetskii et al., 1982]

$$\sigma_1 = \begin{pmatrix} 0 & 1 \\ 1 & 0 \end{pmatrix}, \quad \sigma_2 = \begin{pmatrix} 0 & -i \\ i & 0 \end{pmatrix}, \quad \sigma_3 = \begin{pmatrix} 1 & 0 \\ 0 & -1 \end{pmatrix}, \tag{3.60}$$

we expand the initial ($\rho_{ij}^{(0)}$) and the final (ρ_{ij}) polarization density matrices as [Berestetskii et al., 1982; Blum, 2012; Meuren et al., 2016]

$$\rho^{(0)} = \frac{1}{2}\left(S_0^{(0)} + \boldsymbol{S}^{(0)}\boldsymbol{\sigma}\right), \quad \rho = \frac{1}{2}\left(S_0 + \boldsymbol{S}\boldsymbol{\sigma}\right). \tag{3.61}$$

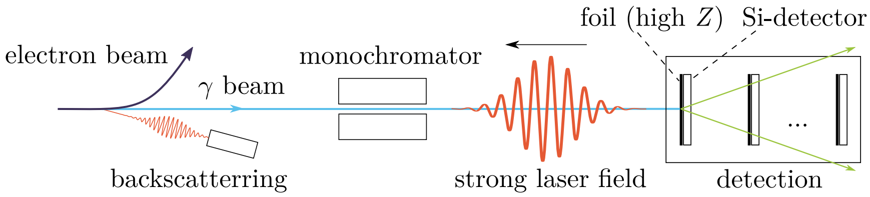

Fig. 3.3. Experimental setup. Polarized highly energetic gamma photons (produced via Compton backscattering) propagate through a strong laser field, which induces vacuum birefringence and dichroism. Afterward, the gamma photons are converted into electron-positron pairs. From their azimuthal distribution, the polarization state is deduced.

We note that $\mathrm{Tr}\{\rho^{(0)}\} = S_0^{(0)}$, $\mathrm{Tr}\{\rho\} = S_0$, with $S_0 \leq S_0^{(0)}$, in general, as the photons can decay in the strong background field.

The Stokes parameters $S^{(0)} = \{S_0^{(0)}, \boldsymbol{S}^{(0)}\}$ [$\boldsymbol{S}^{(0)} = (S_1^{(0)}, S_2^{(0)}, S_3^{(0)})$] and $S = \{S_0, \boldsymbol{S}\}$ [$\boldsymbol{S} = (S_1, S_2, S_3)$] are real numbers that completely characterize respectively the initial and final polarization state of the beam [Blum, 2012; Born and Wolf, 1999]. Therefore, the following relations describe any possible vacuum birefringence and/or dichroism experiment [see Eqs. (3.57), (3.59), and (3.61)]

$$\begin{aligned} \begin{pmatrix} S_0 \\ S_3 \end{pmatrix} &= \mathrm{e}^{-(\lambda_1+\lambda_2)} \begin{pmatrix} \cosh\delta\lambda & \sinh\delta\lambda \\ \sinh\delta\lambda & \cosh\delta\lambda \end{pmatrix} \begin{pmatrix} S_0^{(0)} \\ S_3^{(0)} \end{pmatrix}, \\ \begin{pmatrix} S_1 \\ S_2 \end{pmatrix} &= \mathrm{e}^{-(\lambda_1+\lambda_2)} \begin{pmatrix} \cos\delta\kappa & -\sin\delta\kappa \\ \sin\delta\kappa & \cos\delta\kappa \end{pmatrix} \begin{pmatrix} S_1^{(0)} \\ S_2^{(0)} \end{pmatrix}. \end{aligned} \tag{3.62}$$

Here, $\delta\kappa = \kappa_2 - \kappa_1$ is related to vacuum birefringence and $\delta\lambda = \lambda_2 - \lambda_1$ to vacuum dichroism.

Note that S_1 and S_3 correspond to linear polarization as $\varrho^{\mu\nu} = \epsilon^\mu \epsilon^{*\nu}$ with $\epsilon^\mu = \cos\varphi \Lambda_1^\mu + \sin\varphi \Lambda_2^\mu$ implies $S_0 = 1$, $S_1 = \sin(2\varphi)$, $S_2 = 0$, and $S_3 = \cos(2\varphi)$; whereas S_2 corresponds to circular polarization as $\epsilon^\mu = (\Lambda_1^\mu \pm i\Lambda_2^\mu)/\sqrt{2}$ implies $S_0 = 1$, $S_1 = 0$, $S_2 = \pm 1$, and $S_3 = 0$.

3.3 High-energy vacuum birefringence/dichroism experiment

Having deduced, how the polarization of a generic photon beam changes, while the photons traverse an intense laser pulse, we are ready to study the feasibility of a detection of that change in a near-future experiment.

For the discussion of the vacuum birefringence/dichroism experiment we do not employ the lightfront formalism, but formulate dynamics in the instant form, with space-time four-vector $x^\mu = (x^0, \boldsymbol{x})$, time x^0, and space vector $\boldsymbol{x} = (x^1, x^2, x^3)$. The four-momentum is $p^\mu = (p^0, \boldsymbol{p})$ with p^0 being the energy and $\boldsymbol{p}$ being the three-momentum. The metric tensor is $g^{\mu\nu} = \mathrm{diag}(1, -1, -1, -1)$.

We consider the setup, shown in Fig. 3.3. Polarized gamma photons are produced via Compton backscattering off a highly energetic electron beam. The photons propagate through an intense linearly polarized laser pulse, which induces vacuum birefringence and dichroism. Afterward, the gamma photons are converted into electron-positron pairs. From the azimuthal distribution of the pairs, the polarization state is deduced.

We assume that the collision between the gamma beam and the laser pulse is head-on, and direct the z-axis along the gamma beam propagation, i.e., $k^\mu = \omega(1,0,0,1)$ and $k_0^\mu = \omega_0(1,0,0,-1)$ for the gamma and laser photons, respectively. We direct the x-axis along the laser polarization direction, which implies that $\Lambda_1^\mu = (0,1,0,0)$. We choose $\Lambda_2^\mu = (0,0,1,0)$, such that the spatial components of Λ_1^μ and Λ_2^μ and z-axis form a right-handed coordinate system. Note that for a linear polarization the four-vector Λ_2^μ in Eq. (1.29) is not defined, since there is no $f_2^{\mu\nu}$. We can form Λ_2^μ via the dual tensor $(*F)^{\mu\nu}$:

$$\Lambda_2^\mu = \frac{k_\nu (*F)^{\nu\mu}}{mk^+\sqrt{-a_1^2}} \tag{3.63}$$

(in general, the sign in front of Λ_2^μ is arbitrary).

Five different sets of the parameters are evalauted. Three of them are based on the parameters of three laser facilities, which are currently under construction (each of those facilities is planned to have at least two high-power lasers with at least one of them being a 10-PW machine): the Apollon facility (F1, F2 lasers) [Papadopoulos et al., 2016], ELI-NP (two 10 PW lasers) [Negoita et al., 2016; Turcu et al., 2016], and ELI-Beamlines (denoted as ELI-BL; L3, L4 lasers) [Rus et al., 2013; Le Garrec et al., 2014; ELI-Beamlines]. For each facility, we assume that a 10 PW laser is employed to polarize the vacuum and the second laser is utilized to produce electron bunches via laser wakefield acceleration [Wang et al., 2013; Leemans et al., 2014; Kim et al., 2017].

The fourth considered case is the proposed FACET-II facility at SLAC, which is planned to deliver up to 10-GeV high-density electron beams [FACET-II]. In our setup, FACET-II is combined with a 100-TW laser, which has also been proposed as a future upgrade of the existing 10-TW laser [Fry, 2017].

Finally, we evaluate a possible experiment (denoted as LINAC-PW) at a conventional electron accelerator, e.g., the European XFEL (electron energies up to 17.5 GeV) [EuroXFEL], SACLA (electron energies up to 8.5 GeV) [Yabashi et al., 2015], or previously mentioned FACET-II, combined with a high-repetition (10 Hz) 1 PW laser.

The parameters of the high-power lasers, employed for polarizing vacuum in the experiment, are summarized in Table 3.1.

Let us assess the magnitude of the effects first. Take the rectangular pulse profile with N periods:

$$\psi'(\phi) = \begin{cases} \sin\phi & \text{if } \phi \in [-N\pi, N\pi], \\ 0 & \text{otherwise.} \end{cases} \tag{3.64}$$

In the case (3.64) the integrals (3.55) are simplified to

$$\kappa_i = -\frac{\xi N}{m^2\chi}\int_0^\pi \mathrm{d}\tau\,\mathrm{Re}\left[p_i(\tau,\chi)\right], \quad \lambda_i = -\frac{\xi N}{m^2\chi}\int_0^\pi \mathrm{d}\tau\,\mathrm{Im}\left[p_i(\tau,\chi)\right]. \tag{3.65}$$

As we see from Eq. (3.65), the shift and decay parameters depend only on two quantities: χ and ξN. The dependence of $\delta\kappa$ and $\delta\lambda$ on these quantities, as well as the estimations for the three 10-PW laser facilities, are shown in Fig. 3.4.

As we see from Fig. 3.4, vacuum dichroism is suppressed in the regime $0.1 \lesssim \chi < 1$. This can be also checked analytically, expanding the expressions in Eq. (3.65) with respect to $\chi \ll 1$:

$$\begin{pmatrix}\kappa_1\\ \kappa_2\end{pmatrix} \approx \frac{\alpha\xi N\chi}{90}\begin{pmatrix}4\\ 7\end{pmatrix}, \quad \begin{pmatrix}\lambda_1\\ \lambda_2\end{pmatrix} \approx \sqrt{\frac{\pi}{2}}\frac{\alpha\xi N\sqrt{\chi}}{16}\mathrm{e}^{-8/(3\chi)}\begin{pmatrix}3\\ 6\end{pmatrix}. \tag{3.66}$$

Table 3.1. Parameters of the ultrahigh-intensity lasers which are considered in the numerical calculations: pulse energy $\mathcal{E}$, pulse duration Δt, peak focused intensity I, and pulse repetition rate (PRR). From them we deduce ξ, χ, the number of cycles N for the rectangular enveloper and the pulse width $\Delta\phi$ used for the Gaussian envelope (the details are given in the main text). For ELI-NP the laser wavelength $\lambda_0 = 800$ nm (the angular frequency $\omega_0 = 1.55$ eV), for other facilities this value is not stated in the literature, we use the same value as for ELI-NP. For Apollon F1, the envisioned intensity $> 2 \times 10^{22}$ W/cm^2, we use 10^{23} W/cm^2. For FACET-II, focusing down to 4 μm (radius) is assumed. For LINAC-PW, we assume to use a laser, similar to the L3 laser of ELI-BL. Also note that ELI-NP hosts two lasers with the designated parameters.

	$\mathcal{E}$ [J]	Δt [fs]	I [W/cm^2]	PRR [Hz]	ξ	χ	ξN	$\Delta\phi$
Apollon F1	150	15	10^{23}	1/60	150	$1.8 \times \omega$ [GeV]	860	30
ELI-NP (x2)	250	25	10^{23}	1/60	150	$1.8 \times \omega$ [GeV]	1400	50
ELI-BL L4	1500	150	10^{22}	1/60	50	$0.57 \times \omega$ [GeV]	2700	300
FACET-II	4	35	2.3×10^{20}	5	7.3	$0.09 \times \omega$ [GeV]	95	70
LINAC-PW	30	30	10^{21}	10	15	$0.18 \times \omega$ [GeV]	170	60

So, λ_i and therefore pair production are exponentially suppressed for $\chi \ll 1$.

In the regime $0.1 \lesssim \chi < 1$ a clean vacuum birefringence measurement is possible. As can be seen in Fig. 3.4, for the three shown facilities this regime requires probe photons with energies of ~ 100 MeV and allows to reach $|\delta\kappa| \lesssim 0.1$.

In Fig. 3.4, we do not plot the results for FACET-II and LINAC-PW because of their much smaller values for ξN (see Table 3.1). Nevertheless, we include them into the consideration of the vacuum birefringence experiment, since those setups allow for faster accumulation of the statistics, due to higher repetition rate of their lasers (and also due to the high-density electron beam in the case of FACET-II). As we will see, this compensates for the relatively low intensity of the laser pulse.

As for the regime $\chi \gtrsim 1$, it can be accessible if probe photons with energies of ~ 1 GeV are employed. The most promising setup for exploring this regime is ELI-NP, and we will consider it for the vacuum birefringence/dichroism experiment. Notably, the quantity $\delta\kappa$ decreases with the increase of the probe photon energy for $\chi \gtrsim 2.5$, which characterizes the anomalous dispersion of the vacuum in this regime [Becker and Mitter, 1975; Baier

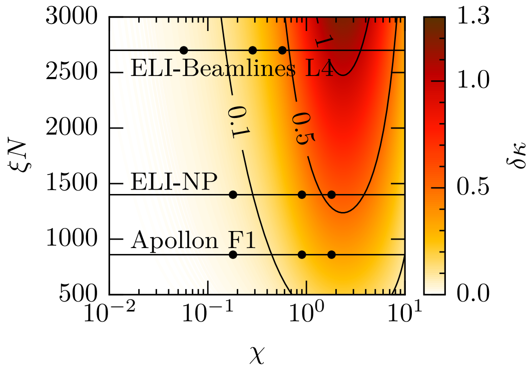

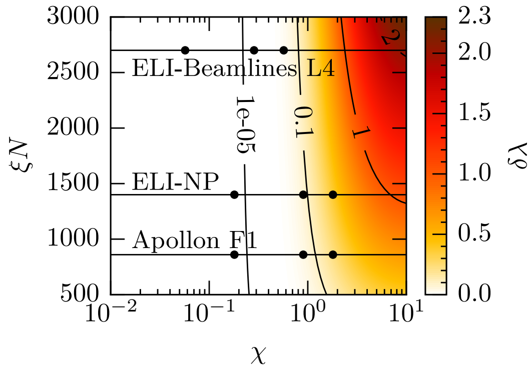

Fig. 3.4. Plots of $\delta\kappa$ and $\delta\lambda$ as functions of χ and ξN for a rectangular pulse profile [see Eq. (3.64)]. For each facility gamma photons with energy $\omega = 100$ MeV (left point), $\omega = 500$ MeV (central point) and $\omega = 1$ GeV (right point) are indicated.

et al., 1976; Ritus, 1985; Heinzl and Ilderton, 2009; Dinu et al., 2014].

Below, first, we discuss each of the stages of the experiment in detail. Then we combine everything together in order to obtain the results for the vacuum birefringence experiment (we consider $\chi = 0.25$) for the five mentioned facilities. After that, we make similar estimations for the experiment in the regime $\chi = 2.5$ for the case of ELI-NP.

For obtaining better estimates as those given in Fig. 3.4, in the following, we employ a Gaussian pulse envelope

$$\psi'(\phi) = \exp\big[-(\phi/\Delta\phi)^2\big]\sin\phi, \tag{3.67}$$

where $\Delta\phi$ is related to the duration of the pulse Δt (FWHM of the intensity) via $\Delta\phi = \omega_\mathrm{L}\Delta t/\sqrt{2\ln 2}$. The values of $\Delta\phi$ are given in Table 3.1.

The pulse collides with

$$N_\gamma = N_e\sigma_\mathrm{bs}\frac{I_\mathrm{bs}}{\omega_\mathrm{bs}}\Delta t_\mathrm{bs} \tag{3.68}$$

gamma photons, where σ_bs is the cross section of Compton scattering [Berestetskii et al., 1982] and the index "bs" indicates the parameters characterizing the backscattering process. To obtain a high degree of polarization, we consider only photons which are scattered in the region $\theta \in (0, \theta_\mathrm{max} \ll 1)$, where θ denotes the polar angle ($\theta = 0$ corresponds to perfect backscattering) [Berestetskii et al., 1982; Ginzburg et al., 1984; Fukuda et al., 2003; Weller et al., 2009; Muramatsu et al., 2014].

We employ $\Delta t_\mathrm{bs} = \Delta t$, $\omega_\mathrm{bs} = 1.55$ eV, and $I_\mathrm{bs} = 4.3\times 10^{16}$ W/cm^2 (considering linear Compton scattering is sufficient as $\xi_\mathrm{bs} = 0.1$ for this laser).

It turns out, that a significant improvement in the experimental sensitivity can be achieved by employing circularly polarized probe gamma photons (this point will be justified below), as was also considered for low-energy experimental schemes by Cantatore et al. (1991) and Wistisen and Uggerhøj (2013). Circularly polarized gamma photons from Compton backscattering have been generated, e.g., at KEK [Fukuda et al., 2003]. We assume the use of a right-handed circularly polarized laser for producing high-energy photons for the experiment.

3.3.1 Compton backscattering

The four-vectors $p^\mu = (\epsilon, \boldsymbol{p})$ and $k^\mu_\mathrm{bs} = (\omega_\mathrm{bs}, \boldsymbol{k}_\mathrm{bs})$ [$p'^\mu = (\epsilon', \boldsymbol{p}')$ and $k^\mu = (\omega, \boldsymbol{k})$] denote the four-momenta of the initial [final] electron and photon, respectively. We assume a head-on collision and direct the z-axis along the initial electron momentum $\boldsymbol{p}$ [$p^\mu = (\epsilon, 0, 0, p_z)$, $k^\mu_\mathrm{bs} = \omega_\mathrm{bs}(1, 0, 0, -1)$].

We consider an unpolarized incoming electron beam and sum over the polarization of the outgoing electrons. The polarization state of the initial photon beam and the state selected by the detector, which measures the final photon polarization, are described by the density tensors $\varrho^{\mu\nu}_\mathrm{bs}$ and $\varrho'^{\mu\nu}$, respectively [Berestetskii et al., 1982]:

$$\varrho^{\mu\nu}_\mathrm{bs} = \sum_{i,j=1,2}\rho^\mathrm{bs}_{ij}e^\mu_i e^\nu_j, \quad \varrho'^{\mu\nu} = \sum_{i,j=1,2}\rho'_{ij}e^\mu_i e^\nu_j, \tag{3.69}$$

where

$$e^\mu_1 = \frac{N^\mu}{\sqrt{-N^2}}, \quad e^\mu_2 = \frac{P^\mu}{\sqrt{-P^2}}, \tag{3.70}$$

$$P^\mu = (g^{\mu\nu} - \frac{K^\mu K^\nu}{K^2})(p+p')_\nu, \quad N^\mu = \epsilon^{\mu\nu\rho\sigma} P_\nu Q_\rho K_\sigma, \tag{3.71}$$

with $K^\mu = k^\mu_{\rm bs} + k^\mu$ and $Q^\mu = k^\mu - k^\mu_{\rm bs}$. We introduce the Stokes vectors $\boldsymbol{\xi}^{\rm bs} = (\xi_1^{\rm bs}, \xi_2^{\rm bs}, \xi_3^{\rm bs})$ and $\boldsymbol{\xi}' = (\xi_1', \xi_2', \xi_3')$ via [compare with Eq. (3.61)]

$$\rho^{\rm bs} = \frac{1}{2}(1 + \boldsymbol{\xi}^{\rm bs}\boldsymbol{\sigma}), \quad \rho' = \frac{1}{2}(1 + \boldsymbol{\xi}'\boldsymbol{\sigma}), \tag{3.72}$$

Using the above notation, the differential cross section for Compton scattering reads [Berestetskii et al., 1982] (see also [Akhiezer and Berestetskii, 1969] and [Ginzburg et al., 1984])

$$d\sigma_{\rm C} = \frac{1}{16\pi^2} |M_{fi}|^2 \frac{\omega^2 d\Omega}{m^4 x^2}, \tag{3.73}$$

where $d\Omega = \sin\theta d\theta d\varphi$ is the solid angle for the scattered photon, i.e., $k^\mu = \omega(1, \cos\varphi\sin\theta, \sin\varphi\sin\theta, \cos\theta)$. The modulus squared of the reduced matrix element is given by

$$|M_{fi}|^2 = 16\pi^2 r_e^2 m^2 \left[F_0 + F_3\left(\xi_3^{\rm bs} + \xi_3'\right) + F_{11}\xi_1^{\rm bs}\xi_1' + F_{22}\xi_2^{\rm bs}\xi_2' + F_{33}\xi_3^{\rm bs}\xi_3'\right], \tag{3.74}$$

with

$$\begin{gathered} F_0 = V - F_3, \quad F_3 = -(U^2 + 2U), \\ F_{11} = 2(1+U), \quad F_{22} = V(1+U), \quad F_{33} = 2 - F_3, \end{gathered} \tag{3.75}$$

$$U = 2/x - 2/y, \quad V = x/y + y/x, \tag{3.76}$$

and

$$x = \frac{2pk_{\rm bs}}{m^2} = \frac{2\epsilon\omega_{\rm bs}}{m^2}(1+\beta), \quad y = \frac{2pk}{m^2} = \frac{2\epsilon\omega}{m^2}(1+\beta\cos\theta). \tag{3.77}$$

The energy ω of the final photon is determined via four-momentum conservation $p^\mu + k^\mu_{\rm bs} = p'^\mu + k^\mu$ and is given by

$$\omega = \frac{(1+\beta)\epsilon\omega_{\rm bs}}{\epsilon + \omega_{\rm bs} - (\epsilon\beta - \omega_{\rm bs})\cos\theta}, \tag{3.78}$$

where $\beta = |\boldsymbol{p}|/\epsilon$. Correspondingly, the highest energy is obtained for perfect backscattering ($\theta = 0$):

$$\omega_{\max} = \frac{(1+\beta)^2\epsilon^2\omega_{\rm bs}}{m^2 + 2(1+\beta)\epsilon\omega_{\rm bs}} \approx \frac{4\epsilon^2\omega_{\rm bs}}{m^2 + 4\epsilon\omega_{\rm bs}} \tag{3.79}$$

(the last relation holds for ultrelativistic electrons). We assume that in the experiment the monochromator selects photons scattered by angles $\varphi \in (0, 2\pi)$ and $\theta \in (0, \theta_{\max})$, where $\theta_{\max} \ll 1$. The total cross section (averaged over the initial and summed over the final photon polarization) for those photons is

$$\sigma_{\rm bs} = \frac{4\pi r_e^2}{m^2 x^2} \int_0^{\theta_{\max}} d\theta\, \omega^2 F_0 \sin\theta. \tag{3.80}$$

In order to consider polarization effects we first note that [see Eq. (3.70)]

$$e_1^\mu = (0, \sin\varphi, -\cos\varphi, 0), \quad e_2^\mu = -[\tan(\theta/2), \cos\varphi, \sin\varphi, -\tan(\theta/2)]. \tag{3.81}$$

Therefore, the Stokes parameters $\xi_i^{\rm bs}$ and ξ_i' [see Eq. (3.72)] implicitly depend on φ. We eliminate this dependence (to leading order in $\theta \ll 1$) by introducing another basis $\tilde{e}_i^\mu$ $(i = 1, 2)$ which is given by

$$\tilde{e}_i^\mu = \sum_{j=1,2} R_{ij}(\varphi) e_j^\mu, \quad R(\varphi) = \begin{pmatrix} \cos\varphi & \sin\varphi \\ -\sin\varphi & \cos\varphi \end{pmatrix}, \tag{3.82}$$

such that

$$\tilde{e}_1^\mu(\theta = 0) = -\Lambda_2^\mu = (0, 0, -1, 0), \quad \tilde{e}_2^\mu(\theta = 0) = -\Lambda_1^\mu = (0, -1, 0, 0). \tag{3.83}$$

We denote the Stokes parameters for the initial beam and the state selected by the detector in the new basis by $S_i^{\rm bs}$ and S_i', respectively. They are related to $\xi_i^{\rm bs}$ and ξ_i' via

$$\begin{pmatrix} \xi_1^{\rm bs} \\ \xi_3^{\rm bs} \end{pmatrix} = R(2\varphi) \begin{pmatrix} S_1^{\rm bs} \\ S_3^{\rm bs} \end{pmatrix}, \quad \begin{pmatrix} \xi_1' \\ \xi_3' \end{pmatrix} = R(2\varphi) \begin{pmatrix} S_1' \\ S_3' \end{pmatrix}, \qquad \xi_2 = S_2^{\rm bs}, \quad \xi_2' = S_2'. \tag{3.84}$$

In order to determine the Stokes parameters $S_i^{(0)}$ of the photon beam, which enters the strong laser pulse, we set $\theta = 0$ in the basis $\tilde{e}_i^\mu$ [$i = 1, 2$; see Eq. (3.83)] as $\theta \ll 1$ for all selected photons, and integrate the cross section [see Eq. (3.73)] over φ. Finally, we obtain that (see [Berestetskii et al., 1982])

$$S_1^{(0)} = \frac{F_{11} + F_{33}}{2F_0} S_1^{\rm bs}, \quad S_2^{(0)} = \frac{F_{22}}{F_0} S_2^{\rm bs}, \quad S_3^{(0)} = \frac{F_{11} + F_{33}}{2F_0} S_3^{\rm bs}. \tag{3.85}$$

Note that for $\theta = 0$ we obtain $\frac{(F_{11}+F_{33})}{2F_0} = 0$ and $\frac{F_{22}}{F_0} = -1$.

3.3.2 Pair production in a Coulomb field

One of the main experimental challenges is to analyze the final polarization state of the gamma photons. Here, we consider pair production in a screened Coulomb field of charge $Z|e|$ [Hunter et al., 2014; Bernard, 2013; Kelner et al., 1975; Olsen and Maximon, 1959].

The cross section of electron-positron photoproduction by a photon with energy $\omega \gg m$ colliding with an atom was derived by Olsen and Maximon (1959). After summing their result {see Eq. (10.3) of [Olsen and Maximon, 1959]} over the spin states of the produced electron and positron, we obtain for the cross section:

$$d\sigma_{\rm pp} = \frac{d\varphi}{2\pi} \left[\sigma_0 + \sigma_1(2|\hat{\boldsymbol{u}}\boldsymbol{e}_\gamma|^2 - 1)\right], \tag{3.86}$$

where

$$\sigma_0 = 2\frac{Z^2\alpha r_e^2}{\omega^3} \int\limits_m^{\omega-m} d\epsilon \int\limits_{m^2/\epsilon^2}^{1} d\zeta \left\{(\epsilon^2 + \epsilon'^2)(3 + 2\Gamma) + 2\epsilon\epsilon'\left[1 + 4\boldsymbol{u}^2\zeta^2\Gamma\right]\right\} \tag{3.87}$$

and

$$\sigma_1 = 2\frac{Z^2\alpha r_e^2}{\omega^3} \int\limits_m^{\omega-m} d\epsilon \int\limits_{m^2/\epsilon^2}^{1} d\zeta \, 8\epsilon\epsilon' \boldsymbol{u}^2\zeta^2\Gamma \tag{3.88}$$

Here, φ denotes the azimuth angle of the electron momentum in the transverse plane (see Fig. 3.5), $\boldsymbol{p}$ denotes the electron momentum, $\epsilon = \sqrt{m^2 + \boldsymbol{p}^2}$ and $\epsilon' = \omega - \epsilon$ are the energy of the produced electron and positron, respectively; $\boldsymbol{e}_\gamma$ denotes the polarization vector of the incoming photon; $\boldsymbol{u}$ is the component of $\boldsymbol{p}$ (scaled by m) perpendicular to $\boldsymbol{k}$, it is defined as $\boldsymbol{u} = [\boldsymbol{p} - \hat{\boldsymbol{k}}(\hat{\boldsymbol{k}}\boldsymbol{p})]/m$, where $\hat{\boldsymbol{k}} = \boldsymbol{k}/\omega$. In the frame, that we consider ($\boldsymbol{k} = |\boldsymbol{k}|\boldsymbol{e}_z$, $|\boldsymbol{k}| = \omega$), we have: $\boldsymbol{u} = \{\boldsymbol{u}_x, \boldsymbol{u}_y\} = |\boldsymbol{u}|\{\cos\varphi, \sin\varphi\}$, where $\hat{\boldsymbol{u}} = \boldsymbol{u}/|\boldsymbol{u}|$. Furthermore, $\zeta = 1/(1+\boldsymbol{u}^2)$ and

$$\Gamma = \ln(1/\delta) - 2 - f(Z) + \mathcal{F}(\delta/\zeta), \tag{3.89}$$

where $\delta = m\omega/(2\epsilon\epsilon')$,

$$f(Z) = (Z\alpha)^2 \sum_{n=1}^{\infty} \frac{1}{n[n^2 + (Z\alpha)^2]}. \tag{3.90}$$

The term $\mathcal{F}(\delta/\zeta)$ takes the screening into account. We employ the Thomas-Fermi model with Molière parametrization [Olsen and Maximon, 1959; Molière, 1947], i.e., the screening term is given by

$$\mathcal{F}(\delta/\zeta) = -\frac{1}{2}\sum_{i=1}^{3} \alpha_i^2 \ln(1+B_i) + \sum_{\substack{i,j=1\\ i\neq j}}^{3} \alpha_i\alpha_j \left[\frac{1+B_j}{B_i - B_j}\ln(1+B_j) + \frac{1}{2}\right] \tag{3.91}$$

with $B_i = (\beta_i\zeta/\delta)^2$, $\beta_i = (Z^{1/3}/121)b_i$ and

$$\begin{aligned} &\alpha_1 = 0.1, \quad \alpha_2 = 0.55, \quad \alpha_3 = 0.35,\\ &b_1 = 6.0, \quad b_2 = 1.2, \quad b_3 = 0.3. \end{aligned} \tag{3.92}$$

We rewrite the cross section given in Eq. (3.86) as

$$\mathrm{d}\sigma_{\mathrm{pp}} = \frac{\mathrm{d}\varphi}{2\pi}\sum_{i,j=1}^{3}[\sigma_0\delta^{ij} + \sigma_1(2\hat{u}^i\hat{u}^j - \delta^{ij})]e_\gamma^i e_\gamma^{*j}. \tag{3.93}$$

Furthermore, we introduce the density matrix ρ and the Stokes vector $S = \{S_0, \boldsymbol{S}\}$ for the incoming photons as

$$e_\gamma^i e_\gamma^{*j} \to \sum_{a,b=1,2} e_a^i e_b^j \rho_{ab}, \quad \rho = \frac{1}{2}(S_0 + \boldsymbol{S}\boldsymbol{\sigma}), \tag{3.94}$$

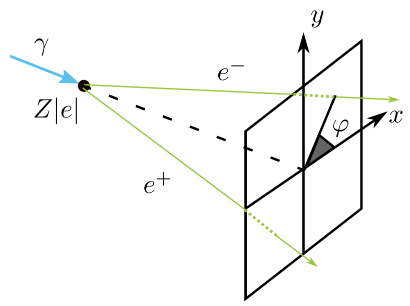

Fig. 3.5. Scheme of electron-positron pair production by a gamma photon in a Coulomb field $Z|e|$. The distribution in the momentum in the plane xy depends on the polarization of the photon.

where $\boldsymbol{e}_1$ and $\boldsymbol{e}_2$ are spatial components of Λ_1^μ and Λ_2^μ, respectively. Combining Eqs. (3.93) and (3.94) we obtain for the pair production cross section:

$$\mathrm{d}\sigma_{\mathrm{pp}} = \frac{\mathrm{d}\varphi}{2\pi} \Big\{ \sigma_0 S_0 + \sigma_1 [S_1 \sin(2\varphi) + S_3 \cos(2\varphi)] \Big\}. \tag{3.95}$$

An analogous expression was obtained by Kelner et al. (1975).

Note that the cross section given by Eqs. (3.95), (3.87), and (3.88) neglects electron-induced pair production and inelastic contributions. In the numerical calculations we assume tungsten ($Z = 74$) as conversion material, therefore both effects are subdominant (Z vs. Z^2 scaling) [Tsai, 1974]. Moreover, most of the pairs are produced near the forward direction such that we can neglect the nuclear form factors [Tsai, 1974].

Also note that the cross section σ_0 represents the unpolarized part [see Eq. (3.87)], whereas σ_1 determines the significance of polarization effects [see Eq. (3.88)].

Now we are ready to discuss, which polarization of the probe photons provides advantages for the experiment. The pair-production cross section in Eq. (3.95) is only sensitive to linear polarization (S_1 and S_3), therefore, from Eq. (3.62) we conclude that employing linearly polarized probe photons results in the effect $\sim (\delta\kappa)^2$ for $|\delta\kappa| \ll 1$. Utilizing circularly polarized probe photons, however, results in the effect which depend on $\delta\kappa$, rather than $(\delta\kappa)^2$ [see Eq. (3.62)]. Therefore, inverting the standard scheme by using circularly instead of linearly polarized probe photons is highly beneficial in the regime $|\delta\kappa| \lesssim 0.1$ (see also [Cantatore et al., 1991; Wistisen and Uggerhøj, 2013]).

3.3.3 Statistical analysis

If we take $S^{(0)} = \{1, 0, -1, 0\}$ for the incoming gamma photons, the outgoing ones have nonzero parameters S_1 and S_3, according to Eq. (3.62). The parameter S_1 is sensitive to vacuum birefringence ($\delta\kappa$), whereas S_3 depends on vacuum dichroism ($\delta\lambda$). In order to disentangle both effects, we introduce the following asymmetries:

$$\begin{aligned} R_{\mathrm{B}} &= \frac{(N_{\pi/4} + N_{5\pi/4}) - (N_{3\pi/4} + N_{7\pi/4})}{(N_{\pi/4} + N_{5\pi/4}) + (N_{3\pi/4} + N_{7\pi/4})}, \\ R_{\mathrm{D}} &= \frac{(N_0 + N_\pi) - (N_{\pi/2} + N_{3\pi/2})}{(N_0 + N_\pi) + (N_{\pi/2} + N_{3\pi/2})}, \end{aligned} \tag{3.96}$$

where N_{β_0} denotes the number of pairs detected in the azimuth angle range $\varphi \in (\beta_0 - \beta, \beta_0 + \beta)$ of the transverse plane, with β being specified below (see Fig. 3.6).

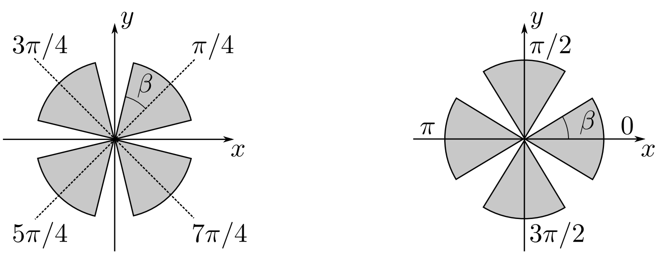

Fig. 3.6. Regions of the transverse plane (gray), which are used to define the observables R_{B} (left) and R_{D} (right) [see Eq. (3.96)].

Let us calculate the expectation values for R_B and R_D. The quantities introduced in Eq. (3.96) are asymmetries of the type

$$R = \frac{N_A - N_B}{N_A + N_B}, \tag{3.97}$$

where N_A and N_B are experimentally measured numbers of events.

We describe the experiment in the following way: with probabilities p_A and p_B a probe photon decays inside the detector such that the produced pair contributes to N_A and N_B, respectively, and the probability $p_C = 1 - p_A - p_B$ accounts for all other possibilities (the photon decays inside the strong laser pulse, passes through the detector, or the produced pair is detected out of the range corresponding to N_A and N_B). Therefore, the two random variables N_A and N_B are distributed according to a multinomial distribution [Riley et al., 2006; James, 2006]. Their expectation values are given by $\langle N_A\rangle = p_A N_\gamma$ and $\langle N_B\rangle = p_B N_\gamma$, respectively, where N_γ denotes the number of gamma photons generated via Compton backscattering [see Eq. (3.68)]. The standard deviations are given by $\Delta N_A = \sqrt{N_\gamma p_A(1-p_A)}$ and $\Delta N_B = \sqrt{N_\gamma p_B(1-p_B)}$, respectively.

Assuming that the number of events counted is large we approximate the expectation value of the asymmetry defined in Eq. (3.97) by [Riley et al., 2006; James, 2006; Ku, 1966]

$$\langle R\rangle = \frac{\langle N_A\rangle - \langle N_B\rangle}{\langle N_A\rangle + \langle N_B\rangle} \tag{3.98}$$

and the variance by [Riley et al., 2006; James, 2006; Ku, 1966]

$$\begin{aligned}(\Delta R)^2 = {}& \left(\frac{\partial R}{\partial\langle N_A\rangle}\Delta N_A\right)^2 + \left(\frac{\partial R}{\partial\langle N_B\rangle}\Delta N_B\right)^2 \\ & + 2\left(\frac{\partial R}{\partial\langle N_A\rangle}\right)\left(\frac{\partial R}{\partial\langle N_B\rangle}\right)\mathrm{Cov}[N_A, N_B],\end{aligned} \tag{3.99}$$

where

$$\frac{\partial R}{\partial\langle N_i\rangle} = \left.\frac{\partial R}{\partial N_i}\right|_{N_j = \langle N_j\rangle} \qquad (i, j = A, B) \tag{3.100}$$

and $\mathrm{Cov}[N_A, N_B] = -p_A p_B N_\gamma$. Using Eqs. (3.98) and (3.99) we find that

$$\langle R\rangle = \frac{p_A - p_B}{p_A + p_B}, \quad (\Delta R)^2 = \frac{1 - \langle R\rangle^2}{N_\gamma(p_A + p_B)}. \tag{3.101}$$

Assuming $\langle R\rangle^2 \ll 1$ we conclude that the standard deviation of the asymmetry is given by $\Delta R \approx 1/\sqrt{N_\gamma(p_A + p_B)}$. The number of required incoming gamma photons for the $n\sigma$ confidence level is now obtained from the condition $\langle R\rangle - \langle R_0\rangle = n\Delta R$, where $\langle R_0\rangle = 0$ is the expectation value of the asymmetry if vacuum birefringence/dichroism is absent. We conclude that

$$N_\gamma = \frac{n^2}{\langle R\rangle^2(p_A + p_B)}. \tag{3.102}$$

The probabilities p_A and p_B are given by $p_{A/B} = n_z l \sigma_{A/B}$, where n_z and l are the number density and the thickness of the conversion material, respectively, and

$$\sigma_{A/B} = \frac{2\beta}{\pi} S_0\sigma_0 \pm \frac{\sin(2\beta)}{\pi} S_i\sigma_1 \tag{3.103}$$

Table 3.2. Parameters for measuring vacuum birefringence at the considered facilities. Here, ϵ denotes the electron energy, $\theta_{\max}$ is the selected maximal scattering angle (chosen such that $|F_{22}/F_0| > 0.999$), σ_{bs} is the Compton scattering cross section [see Eq. (3.80)], ω is the outgoing probe photon energy [see Eq. (3.78)], σ_0 and σ_1 are pair production cross sections in tungsten ($Z = 74$) for the obtained photon energies, the ratio σ_1/σ_0 determines the sensitivity to polarization effects. For FACET-II, we take the maximal designed energy $\epsilon = 10$ GeV for the electrons (this corresponds to $\chi = 0.165$ for the generated photons). For the other facilities, we choose ϵ such that $\chi = 0.25$. The final photon energy ω differs by less than 2% from the given value in the range $0 \leqslant \theta \leqslant \theta_{\max}$.

	ϵ [GeV]	$\theta_{\max}$ [rad]	$\sigma_{\text{bs}}[r_e^2]$	ω [GeV]	$\sigma_0[r_e^2]$	$\sigma_1[r_e^2]$	σ_1/σ_0
Apollon/ELI-NP	2.5	3.0×10^{-5}	0.232	0.14	344	26.7	0.078
ELI-BL	4.5	1.6×10^{-5}	0.197	0.43	393	31.0	0.079
FACET-II	10	6.0×10^{-6}	0.113	1.9	420	32.3	0.077
LINAC-PW	8.4	7.6×10^{-6}	0.135	1.4	417	32.3	0.077

with $S_i = S_1$ and $S_i = S_3$ for R_{B} and R_{D}, respectively.

Then the expectation values of R_{B} and R_{D} [see Eq. (3.96)] are given by

$$\langle R_{\text{B}} \rangle = \frac{\sin(2\beta)}{2\beta}\frac{\sigma_1}{\sigma_0}\frac{S_1}{S_0}, \quad \langle R_{\text{D}} \rangle = \frac{\sin(2\beta)}{2\beta}\frac{\sigma_1}{\sigma_0}\frac{S_3}{S_0}. \tag{3.104}$$

And from Eq. (3.102) we define, how many gamma photons one would need in order to detect respectively vacuum birefringence and dichroism at the $n\sigma$ confidence level on average:

$$N_\gamma^{\text{B}} = \frac{\pi n^2}{4\eta\beta S_0 \langle R_{\text{B}} \rangle^2}, \quad N_\gamma^{\text{D}} = \frac{\pi n^2}{4\eta\beta S_0 \langle R_{\text{D}} \rangle^2}, \tag{3.105}$$

where $\eta = n_z l \sigma_0$ denotes the photon to pair conversion efficiency. By minimizing N_γ^{B} and N_γ^{D} with respect to β, we find the optimal angle $\beta = \beta_{\text{opt}} \approx 0.58 \approx 33°$ for both observables.

The thickness of a conversion foil should be $\lesssim 1$ milliradiation length (mRL), otherwise multiple Coulomb scattering affects the measured angle [Kelner et al., 1975; Hunter et al., 2014]. Supposing that several conversion foils alternating with silicon detectors are cascaded [Tavani et al., 2003; Atwood et al., 2009; Peitzmann, 2013], we employ $\eta = 10^{-2}$ (i.e., an effective thickness of ~ 10 mRL).

Table 3.3. Duration τ of the vacuum birefringence experiment. S_0 and S_1, $\langle R_{\text{B}} \rangle$, and N_γ^{B} follow from Eq. (3.62), Eq. (3.104) and Eq. (3.105), respectively ($S^{(0)} = \{1, 0, -1, 0\}$; 5σ confidence level, i.e., $n = 5$). Note that the pair production probability in the strong laser field is much smaller than the conversion efficiency in the detector [$(1 - S_0) \ll \eta = 10^{-2}$].

	$1 - S_0$	S_1	$\langle R_{\text{B}} \rangle$	N_γ^{B}	τ
Apollon	1.9×10^{-5}	0.06	3.4×10^{-3}	3.0×10^{8}	45 days
ELI-NP	3.1×10^{-5}	0.09	5.6×10^{-3}	1.1×10^{8}	10 days
ELI-BL	6.3×10^{-5}	0.18	1.1×10^{-2}	2.6×10^{7}	11 hours
FACET-II	6.2×10^{-9}	0.004	2.5×10^{-4}	5.4×10^{11}	2 days
LINAC-PW	3.8×10^{-6}	0.01	6.8×10^{-4}	7.4×10^{9}	2 days

3.3.4 Results

We assume that $N_e = 10^8$ monoenergetic few-GeV electrons are used in one experimental cycle for the generation of probe gamma photons via Compton backscattering. FACET-II is expected to produce high-density electron bunches, for this facility we use $N_e = 10^9$. The laser beam for Compton backscattering has $S_1^{\text{bs}} = S_3^{\text{bs}} = 0$, $S_2^{\text{bs}} = 1$. Therefore, $S_1^{(0)} = S_3^{(0)} = 0$, $S_2^{(0)} \approx -1$ for small θ_{max}. In order to obtain a highly polarized beam we choose θ_{max} such that $|F_{22}/F_0| > 0.999$ for all selected photons. For the considered facilities, the parameters and cross sections for Compton backscattering, as well as the cross sections of the pair production are shown in Table 3.2.

The estimations for the vacuum birefringence experiment are shown in Table 3.3 (we choose the 5σ confidence level).

As we see from Table 3.3, the pair production inside the laser pulse is much smaller than the conversion efficiency [$(1 - S_0) \ll \eta = 10^{-2}$], therefore it does not affect the experimental results.

We conclude, that the vacuum birefringence experiment could be performed within a few days, with the expected duration of the experiment for ELI-BL less than one day.

As the number of required gamma photons N_γ^{B} scales as $\langle R_{\text{B}} \rangle^{-2}$ [see Eq. (3.105)], the use of circularly polarized probe photons instead of linearly polarized ones reduces the measurement time by a factor ≈ 100 ($\delta\kappa \approx 0.1$, see Fig. 3.4).

Finally, we consider the case $\chi = 2.5$, which is attainable at ELI-NP by utilizing 8.4 GeV electrons for backscattering. The parameters are the following: $\theta_{\text{max}} = 7.6 \times 10^{-6}$, $\sigma_{\text{bs}} = 0.135 r_e^2$, $\omega = 1.4$ GeV. For the pair production, the ratio $\sigma_1/\sigma_0 = 0.077$.

In the regime $\chi = 2.5$ vacuum dichroism and anomalous dispersion come into play and the Euler-Heisenberg approximation breaks down completely (see Fig. 3.4). Note that the production of particles, heavier than electrons and positrons, and QCD corrections are still suppressed [Bern et al., 2001].

For $S^{(0)} = \{1, 0, -1, 0\}$, we obtain that $S = \{0.18, 0.11, -0.12, 0.09\}$ at ELI-NP (see Fig. 3.7). Correspondingly, $\langle R_{\text{B}} \rangle = 3.6 \times 10^{-2}$ and $\langle R_{\text{D}} \rangle = 3.0 \times 10^{-2}$, implying a measurement time of 3-4 days for reaching the 5σ confidence level.

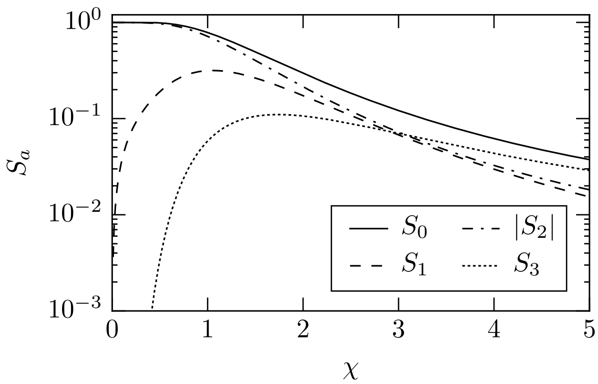

Fig. 3.7. Final Stokes parameters [see Eq. (3.62)] for gamma photons propagating through the ELI-NP 10 PW laser pulse ($S^{(0)} = \{1, 0, -1, 0\}$). The strongest effect is obtained around $\chi = 1$ (note that pair production becomes sizable for $\chi \gtrsim 1$). As we consider the tunneling regime $1/\xi \ll 1$, cusplike structures – characteristic for multiphoton pair production [Villalba-Chávez et al., 2016; Becker and Mitter, 1975] – are absent.

4

Electron-positron annihilation into two photons

Among the tree-level diagrams in an external laser field, trident process is the most studied one [Hu et al., 2010; Ilderton, 2011; King and Ruhl, 2013; Dinu and Torgrimsson, 2018b; King and Fedotov, 2018; Mackenroth and Di Piazza, 2018]. This process was also observed experimentally, at SLAC in late 90's [Burke et al., 1997].

Recently, also double Compton scattering in a general plane-wave field was evaluated by Dinu and Torgrimsson (2018a).

First results on two-particle scattering in a laser field were published by [Oleinik, 1967, 1968], who studied electron-electron and Compton scattering in a monochromatic plane-wave field, with the focus on the resonant effects. Here, by resonance, we mean that an intermediate particle goes on shell. The resonance manifests itself as a divergence due to the pole structure of the propagator. Resonance behavior of two-particle scattering has been studied in later works (see [Voroshilo et al., 2016] and references therein).

Compton scattering and electron-positron production by two photons in a circularly polarized laser field were studied by Hartin (2006).

Though the resonances seem to be an interesting feature of the processes under consideration, we expect our theory to be finite and it is important to understand how to deal with the divergencies. In our approach, we use the proper-time representation for the propagators, therefore, the resonances appear as the divergencies in the integral over the proper-time variable. We will see below, however, that for large values of the variable, the densities of the colliding wave packets have to be taken into account. Since the wave packets are assumed to have finite sizes, the integral is expected to converge. Another aspect is that if an intermediate particle propagates over sufficiently long distances inside a laser pulse, then the radiative corrections has to be taken into account (see, e.g., [Meuren and Di Piazza, 2011] for the consideration of the corrections to the electron wave function). Those corrections, in general, induce a decay of the intermediate particle, therefore, again, we should obtain a final result.

In this chapter, we consider the cross section for electron-positron annihilation into two photons in a plane-wave field of a general shape. The two leading order diagrams are shown in Fig. 4.1. The diagram in Fig. 4.1a will be referred to as direct diagram, and the diagram in Fig. 4.1b as exchange diagram.

First, we reconsider scattering formalism and find out, when it is possible to define a cross section. Then we evaluate the part of the cross section, which comes upon squaring each of the diagram, i.e., we do not evaluate the interference part. Finally, we analyze the obtained result.

4.1 Cross section

We proceed in the same way as in Chapter 2, and obtain for the matrix element:

$$S_{fi} = \int \frac{\mathcal{V}\tilde{\mathrm{d}}^3 q_2}{(2\pi)^3} \frac{\mathcal{V}\tilde{\mathrm{d}}^3 q_1}{(2\pi)^3} f_2(q_2) f_1(q_1) (2\pi)^3 \delta^{(+,\perp)}(k_2 + k_1 - q_2 - q_1) \times \int \mathrm{d}x_2^+ \mathrm{d}x_1^+ \exp\left[i\Phi_{q_2 q_1}(x_2^+, x_1^+)\right] \frac{iM(\phi_2, \phi_1, q_2, q_1)}{2\mathcal{V}\sqrt{q_2^+ q_1^+}} \prod_i \frac{1}{\sqrt{2k_i^+ \mathcal{V}}}, \tag{4.1}$$

where

$$\Phi_{q_2 q_1}(x_2^+, x_1^+) = -iq_2^- x_2^+ + i\mathcal{S}_{-q_2}(\phi_2) - iq_1^- x_1^+ - i\mathcal{S}_{q_1}(\phi_1). \tag{4.2}$$

and $M(\phi_2, \phi_1, q_2, q_1)$ is defined via

$$M(q_2, q_1) = \int \mathrm{d}x_2^+ \mathrm{d}x_1^+ \exp\left[\Phi_{q_2 q_1}(x_2^+, x_1^+)\right] M(\phi_2, \phi_1, q_2, q_1), \tag{4.3}$$

with $M(q_2, q_1)$ being the reduced matrix element. The complete expression for $M(q_2, q_1)$ is given below. For now, it is important to note that $M(\phi_2, \phi_1, q_2, q_1)$ is a slowly varying function of q_2^μ and q_1^μ.

Upon squaring S_{fi} and transforming the delta functions [see Eq. (2.13)], one obtains:

$$|S_{fi}|^2 = \int \mathrm{d}^2 x^\perp \mathrm{d}x^- \mathrm{d}x_4^+ \mathrm{d}x_3^+ \mathrm{d}x_2^+ \mathrm{d}x_1^+ f_2(\boldsymbol{x}^\perp, x^-, x_4^+) f_2^*(\boldsymbol{x}^\perp, x^-, x_1^+) \times f_1(\boldsymbol{x}^\perp, x^-, x_3^+) f_1^*(\boldsymbol{x}^\perp, x^-, x_2^+) (2\pi)^3 \delta^{(+,\perp)}(k_2 + k_1 - p_2 - p_1) \times \frac{M(\phi_4, \phi_3, p_2, p_1) M^*(\phi_1, \phi_2, p_2, p_1)}{4p_2^+ p_1^+} \prod_i \frac{1}{2k_i^+ \mathcal{V}}. \tag{4.4}$$

As the next step, we make a change of variables (recall the discussion of the probability, obtained from the matrix element written in position space, in Chapter 2):

$$x^+ = (X_2^+ + X_1^+)/2, \quad \delta^+ = X_2^+ - X_1^+, \quad \delta_2^+ = x_1^+ - x_4^+, \quad \delta_1^+ = x_3^+ - x_2^+, \tag{4.5}$$

where $X_2^+ = (x_1^+ + x_4^+)/2$ and $X_1^+ = (x_3^+ + x_2^+)/2$.

Let us look at the product of the distribution densities for the electron (for the positron we proceed analogously). We have:

$$f_1(\boldsymbol{x}^\perp, x^-, x_3^+) f_1^*(\boldsymbol{x}^\perp, x^-, x_2^+) = F_1\left(\boldsymbol{x}^\perp, x^-, x^+ - \delta^+/2 + \delta_1^+/2\right) F_1^*\left(\boldsymbol{x}^\perp, x^-, x^+ - \delta^+/2 - \delta_1^+/2\right) \times \exp\left[-ip_1^- x_3^+ - i\mathcal{S}_{p_1}(\phi_3) + ip_1^- x_2^+ + i\mathcal{S}_{p_1}(\phi_2)\right]. \tag{4.6}$$

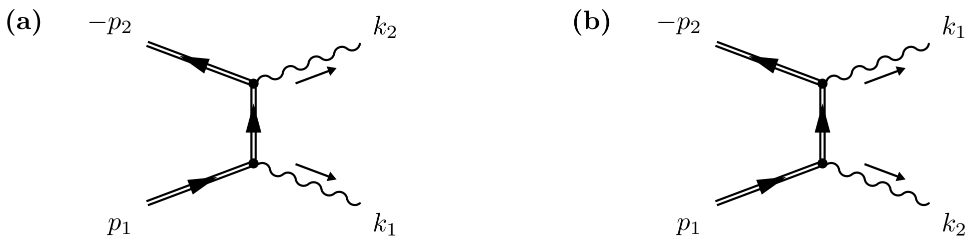

Fig. 4.1. The leading-order diagrams or electron-positron annihilation into two photons in a plane-wave field: (a) the direct diagram, and (b) the exchange diagram.

If we could neglect δ^+ and δ_1^+ in the arguments of F_1's, we would obtain the particle density $|F_1(x)|^2 = |f_1(x)|^2$, as in the vacuum case.

In the regime $\xi \gg 1$, the reasoning for neglectinig δ_1^+ is the same as in the case of the annihilation into one photon.

As for δ^+, if it is neglected in the arguments of F_1's and F_2's, then the integration is to be performed over the whole range in general. The parameter δ^+ can be understood as the (light-cone) time difference between the instants of the emissions of the two final photons. In a plane-wave field, the intermediate fermion can go on shell, therefore, δ^+ can be, in principle, infinitely large (it should be noted that for large values of δ^+ the radiative corrections may become sizable, see, e.g., [Meuren and Di Piazza, 2011]).

Neglecting δ^+ implies that we need to restrict our consideration to the process, happening locally.

If we consider the local process only, we can formally define a cross section, analogously to how it is done for scattering in vacuum. We obtain for the differential probability per unit phase unit volume:

$$\mathrm{d}\dot{w} = |f_2(x)|^2 |f_1(x)|^2 (2\pi)^3 \delta^{(+,\perp)}(k_2 + k_1 - p_2 - p_1) \frac{\mathcal{M}(x^+, p_2, p_1)}{4p_2^+ p_1^+} \prod_i \mathrm{d}\Gamma_{k_i}, \tag{4.7}$$

where

$$\begin{aligned}
\mathcal{M}(x^+, p_2, p_1) = &\int \mathrm{d}\delta^+ \mathrm{d}\delta_2^+ \mathrm{d}\delta_1^+ \\
&\times \exp\left[-ip_2^-(x_1^+ - x_4^+) + i\mathcal{S}_{-p_2}(\phi_1, \phi_4) - ip_1^-(x_3^+ - x_2^+) - i\mathcal{S}_{p_1}(\phi_3, \phi_2)\right] \\
&\times M(\phi_4, \phi_3, p_2, p_1) M^*(\phi_1, \phi_2, p_2, p_1).
\end{aligned} \tag{4.8}$$

Then the total cross section, averaged (summed) over the initial (final) polarization states, is given by

$$\sigma(x^+) = \prod_i \mathrm{d}\Gamma_{k_i} (2\pi)^3 \delta^{(+,\perp)}(k_2 + k_1 - p_2 - p_1) \frac{1}{16I(\phi)} \sum_{\text{polarization}} \mathcal{M}(x^+, p_2, p_1). \tag{4.9}$$

Due to the delta function, we perform the integrals over the momentum components of photon 2, and obtain:

$$\sigma(x^+) = \int_0^{p_2^+ + p_1^+} \frac{\mathrm{d}k_1^+}{2\pi} \int \frac{\mathrm{d}^2 k_1^\perp}{(2\pi)^2} \frac{1}{32k_2^+ k_1^+ I(\phi)} \frac{1}{4} \sum_{\text{polarization}} \mathcal{M}(x^+, p_2, p_1), \tag{4.10}$$

with $k_2^{(+,\perp)} = (p_2 + p_1 - k_1)^{(+,\perp)}$. In Eq. (4.10) the result is divided by 2, in order to account for the double counting of the final states of the two identical particles.

Analogously to how it was done in Chapter 2, we define the cross section, normalized to the flux at $x^+ \to -\infty$:

$$\sigma_0(x^+) = \int_0^{p_2^+ + p_1^+} \frac{\mathrm{d}k_1^+}{2\pi} \int \frac{\mathrm{d}^2 k_1^\perp}{(2\pi)^2} \frac{1}{32k_2^+ k_1^+ I} \frac{1}{4} \sum_{\text{polarization}} \mathcal{M}(x^+, p_2, p_1). \tag{4.11}$$

4.2 Reduced matrix element

The reduced matrix element is given by

$$M(p_2,p_1) = -e^2\overline{v}_2\left[\int\frac{\mathrm{d}p_3^-}{2\pi}\Gamma^{\mu}_{-23}(k_2)\frac{\gamma\tilde{p}_3+m}{p_3^2-m^2+i\epsilon}\Gamma^{\nu}_{31}(k_1)+\frac{\Gamma^{\mu\nu}_{-21}(k_2,-k_1)}{2p_3^+}\right]u_1\epsilon^*_{2\mu}\epsilon^*_{1\nu} + (\gamma_2\leftrightarrow\gamma_1), \tag{4.12}$$

where the lower indices indicate momentum variables (or collectively momentum and polarization variables), the lower index '–2' means that the momentum p_2^μ should be taken with a minus sign, and $(\gamma_2\leftrightarrow\gamma_1)$ denotes the exchange term (the photon quantum numbers are swapped, see Fig. 4.1b). The vertex functions are given by Eqs. (1.82) and (1.87).

The matrix element (4.12) contains 4 distinct terms. Taking the modulus squared yields 16 terms. However, only 8 of them are different after we sum over the states of the final photons. 4 of them, arising from squaring the direct diagram (see Fig. 4.1a), are considered below. We call these terms direct-direct terms.

Summing over the final photon polarizations results in the replacement

$$\epsilon_i^\mu\epsilon_i^{*\nu}\to -g^{\mu\nu},\quad i=1,2 \tag{4.13}$$

(we discard the terms with k_i^μ and k_i^ν due to the Ward identity).

Averaging over the polarization states of the initial particles results in the replacements [Berestetskii et al., 1982]

$$u_1\overline{u}_1\to\rho_1,\quad v_2\overline{v}_2\to\rho_2^{(-)}=-\rho_{-2}, \tag{4.14}$$

and taking the trace over the bispinor part of $|M(p_2,p_1)|^2$. The quantities ρ_1 and $\rho_2^{(-)}$ denote the electron and positron density matrices, respectively. In the case of the initial particles being unpolarized (which we assume below), we have:

$$\rho_1=\frac{1}{2}(\gamma p_1+m),\quad \rho_2^{(-)}=-\rho_{-2}=-\frac{1}{2}(\gamma p_{-2}+m). \tag{4.15}$$

Below, we deal with functions, that depend on four light-cone time variables. For clarity of the calculations, we simplify our notation in the following way: functions $f(\phi_a)$ of one light-cone time variable will be written as $f(a)$, functions $f(\phi_a,\phi_b)$ of two light-cone time variables will be written as $f(ab)$, etc.

Upon squaring the noninstantaneous part of the direct diagram [we call this term noninstantaneous-noninstantaneous direct-direct ('nndd') term], summing and averaging over the polarization states, we obtain:

$$\frac{1}{4}\sum_{\text{polarization}}M^{\text{nd}}M^{\text{nd}*}=e^4\int\frac{\mathrm{d}p_4^-}{2\pi}\frac{\mathrm{d}p_3^-}{2\pi}\int\mathrm{d}x_4^+\mathrm{d}x_3^+\mathrm{d}x_2^+\mathrm{d}x_1^+ \times\exp\left[i\Phi^{\text{dd}}(4321)\right]\frac{\mathcal{T}^{\text{nndd}}}{(p_4^2-m^2+i\epsilon)(p_3^2-m^2-i\epsilon)}, \tag{4.16}$$

where the phase $\Phi^{\text{dd}}(4321)$ is given by

$$\Phi^{\text{dd}}(4321)=(k_2^- -p_2^-)(x_4^+-x_1^+)+(k_1^- -p_1^-)(x_3^+-x_2^+) - p_4^-(x_4^+-x_3^+)-p_3^-(x_2^+-x_1^+)+\Phi_F^{\text{dd}}(4321) \tag{4.17}$$

with the field-dependent part $\Phi_F^{\mathrm{dd}}(4321)$ given by

$$\Phi_F^{\mathrm{dd}}(4321) = -\mathcal{S}_4(43) - \mathcal{S}_3(21) - \mathcal{S}_{-2}(14) - \mathcal{S}_1(32). \tag{4.18}$$

The field-dependent part of the phase (4.18) can be written as [Meuren et al., 2013]

$$\Phi_F^{\mathrm{dd}}(4321) = \mathcal{S}_{-23}(41) + \mathcal{S}_{31}(32), \tag{4.19}$$

where

$$\begin{aligned}
\mathcal{S}_{-23}(41) &= \int_{\phi_1}^{\phi_4} \mathrm{d}\beta \left[\frac{ep_{3\mu}p_{2\nu}\mathcal{F}^{\mu\nu}(\beta)}{m^2 p_3^+ p_2^+} - \frac{e^2(p_3^+ + p_2^+)p_{3\mu}p_{2\nu}\mathcal{F}^{2\mu\nu}(\beta)}{2m^3 p_3^{+2} p_2^{+2}}\right], \\
\mathcal{S}_{31}(32) &= \int_{\phi_2}^{\phi_3} \mathrm{d}\beta \left[\frac{ep_{1\mu}p_{3\nu}\mathcal{F}^{\mu\nu}(\beta)}{m^2 p_3^+ p_1^+} + \frac{e^2(p_1^+ - p_3^+)p_{1\mu}p_{3\nu}\mathcal{F}^{2\mu\nu}(\beta)}{2m^3 p_3^{+2} p_1^{+2}}\right].
\end{aligned} \tag{4.20}$$

The quantity $\mathcal{T}^{\mathrm{nndd}}$ (as well as the $\mathcal{T}$-preexponential factors for the other terms below) is the trace of the bispinor part, which we consider in detail in the next section.

For the product of the instantaneous and noninstantaneous parts [we call this term instantaneous-noninstantaneous direct-direct ('indd') term] we have

$$\frac{1}{4}\sum_{\text{polarization}} M^{\mathrm{id}}M^{\mathrm{nd}*} = e^4 \int \frac{\mathrm{d}p_3^-}{2\pi} \int \mathrm{d}x_3^+ \mathrm{d}x_2^+ \mathrm{d}x_1^+ \exp\left[i\Phi^{\mathrm{dd}}(3321)\right] \frac{\mathcal{T}^{\mathrm{indd}}}{p_3^2 - m^2 - i\epsilon}, \tag{4.21}$$

and, respectively, the product in the opposite order [we call this term noninstantaneous-instantaneous direct-direct ('nidd') term] is given by

$$\frac{1}{4}\sum_{\text{polarization}} M^{\mathrm{nd}}M^{\mathrm{id}*} = e^4 \int \frac{\mathrm{d}p_4^-}{2\pi} \int \mathrm{d}x_4^+ \mathrm{d}x_3^+ \mathrm{d}x_1^+ \exp\left[i\Phi^{\mathrm{dd}}(4311)\right] \frac{\mathcal{T}^{\mathrm{nidd}}}{p_4^2 - m^2 + i\epsilon}. \tag{4.22}$$

Finally, the product of the two instantaneous part [we call this term instantaneous-instantaneous direct-direct ('iidd') term] is given by

$$\frac{1}{4}\sum_{\text{polarization}} M^{\mathrm{id}}M^{\mathrm{id}*} = e^4 \int \mathrm{d}x_3^+ \mathrm{d}x_1^+ \exp\left[i\Phi^{\mathrm{dd}}(3311)\right] \mathcal{T}^{\mathrm{iidd}}. \tag{4.23}$$

The conservation relations for the asymptotic momenta are

$$p_3^{(+,\perp)} = p_4^{(+,\perp)} = (p_1 - k_1)^{(+,\perp)} = (k_2 - p_2)^{(+,\perp)}. \tag{4.24}$$

With the use of the canonical light-cone basis (1.29) and the momentum conservation laws we obtain that the phase is given by [note that, since $\Phi_F^{\mathrm{dd}}(4321)$ does not depend on the '$-$' momentum components, the full four-momentum conservation laws for the asymptotic momenta can be employed within this part of the phase]

$$\begin{aligned}
\Phi_F^{\mathrm{dd}}(4321) = -\frac{m}{p_3^+}\sum_{i=1,2}\Bigg[&-\frac{\xi_i}{p_2^+}(p_2^+ k_2^i - p_2^i k_2^+) I_i(14) - \frac{m\xi_i^2 k_2^+}{2p_2^+} J_i(14) \\
&+\frac{\xi_i}{p_1^+}(p_1^+ k_1^i - p_1^i k_1^+) I_i(32) - \frac{m\xi_i^2 k_1^+}{2p_1^+} J_i(32)\Bigg],
\end{aligned} \tag{4.25}$$

where

$$I_i(\phi,\phi') = \int\limits_{\phi'}^{\phi} \mathrm{d}\beta\,\psi_i(\beta), \quad J_i(\phi,\phi') = \int\limits_{\phi'}^{\phi} \mathrm{d}\beta\,\psi_i^2(\beta). \tag{4.26}$$

Note that the result (4.25) does not depend on the choice of the vector q^μ. If we choose $q^\mu = p_2^\mu + p_1^\mu$, then

$$\boldsymbol{p}_2^\perp + \boldsymbol{p}_1^\perp = \boldsymbol{k}_2^\perp + \boldsymbol{k}_1^\perp = 0 \tag{4.27}$$

and

$$\begin{aligned}\Phi_F^{\mathrm{dd}}(4321) = &-\frac{m}{p_3^+}\sum_i \xi_i k_1^i\,[I_i(14) + I_i(32)] \\ &+ \frac{m^2}{p_3^+}\sum_i t_i\xi_i \left[\frac{k_2^+}{p_2^+} I_i(14) + \frac{k_1^+}{p_1^+} I_i(32)\right] + \frac{m^2}{2p_3^+}\sum_i \xi_i^2 \left[\frac{k_2^+}{p_2^+} J_i(14) + \frac{k_1^+}{p_1^+} J_i(32)\right],\end{aligned} \tag{4.28}$$

where we defined $t_i = p_1^i/m = -p_2^i/m$ [see Eq. (1.127)].

In terms of the variables (4.5) the field-dependent part $\Phi_F^{\mathrm{dd}}(4321)$ can be written as

$$\begin{aligned}\Phi_F^{\mathrm{dd}}(4321) \to \Phi_F^{\mathrm{dd}} = &-\frac{m}{p_3^+}\sum_i \xi_i k_1^i \left[\delta_2^+ I_{2i} + \delta_1^+ I_{1i}\right] \\ &+ \frac{m^2}{p_3^+}\sum_i t_i\xi_i \left[\frac{k_2^+}{p_2^+}\delta_2^+ I_{2i} + \frac{k_1^+}{p_1^+}\delta_1^+ I_{1i}\right] + \frac{m^2}{2p_3^+}\sum_i \xi_i^2 \left[\frac{k_2^+}{p_2^+}\delta_2^+ J_{2i} + \frac{k_1^+}{p_1^+}\delta_1^+ J_{1i}\right],\end{aligned} \tag{4.29}$$

where

$$I_{ji} = \int\limits_{-1}^{1} \mathrm{d}\lambda\,\psi_i\left(mX_j^+ + \frac{1}{2}m\delta_j^+\lambda\right), \quad J_{ji} = \int\limits_{-1}^{1} \mathrm{d}\lambda\,\psi_i^2\left(mX_j^+ + \frac{1}{2}m\delta_j^+\lambda\right). \tag{4.30}$$

The form (4.29) is the same for all four direct-direct terms. However, for the 'nndd' term all four variables in Eq. (4.5) are independent, only three are independent for the 'indd' term (due to $x_4^+ = x_3^+$) and for the 'nidd' term (due to $x_2^+ = x_1^+$), and only two are independent for the 'iidd' term (due to $x_4^+ = x_3^+$ and $x_2^+ = x_1^+$).

We proceed by evaluating the traces for the direct-direct terms.

4.3 Evaluation of the traces for the direct-direct terms

The traces depend on four fermion momenta: initial p_1^μ and p_2^μ, and intermediate p_3^μ and p_4^μ. It is convenient to relabel the momenta in the following way:

$$p_{-2}^\mu \to p_4^\mu, \quad p_4^\mu \to p_3^\mu, \quad p_1^\mu \to p_2^\mu, \quad p_3^\mu \to p_1^\mu. \tag{4.31}$$

Then the conservation relations (4.24) change into

$$p_1^{(+,\perp)} = p_3^{(+,\perp)} = (p_2 - k_1)^{(+,\perp)} = (k_2 + p_4)^{(+,\perp)}. \tag{4.32}$$

In the final expressions, the initial labeling of the momenta will be restored.

As we will see below, the results are conveniently expressed via the following quantites:

$$\Delta_2^\mu = \Delta_2^\mu(32), \quad Z_2^\mu = Z_2^\mu(32), \quad \Delta_4^\mu = \Delta_4^\mu(14), \quad Z_4^\mu = Z_4^\mu(14), \tag{4.33}$$

where

$$\Delta_p^\mu(\phi,\phi') = \pi_p^\mu(\phi) - \pi_p^\mu(\phi'), \quad Z_p^\mu(\phi,\phi') = \left[\pi_p^\mu(\phi) + \pi_p^\mu(\phi')\right]/2. \tag{4.34}$$

Note that $\Delta_p^\mu(\phi,\phi')$ is a purely field-dependent function as it vanishes in the absence of the external field, and $Z_p^\mu(\phi,\phi') = p^\mu$ in this limit. Note also that $\Delta_p^+(\phi,\phi') = 0$ identically.

It is also beneficial to combine the scalar and the tensor terms of $K_{21}^\mu(\phi)$ in the three-point dressed vertex function [see Eq. (1.84)] as

$$S_{21}^\mu(\phi) + T_{21}^\mu(\phi)\gamma^1\gamma^2 = \frac{1}{2}\left[S_{21}^\mu(\phi)g_{ij} + T_{21}^\mu(\phi)\epsilon_{ij}\right]\gamma^i\gamma^j = \frac{1}{2}U_{21ij}^\mu(\phi)\gamma^i\gamma^j. \tag{4.35}$$

Then $K_{21}^\mu(\phi)$ is given by

$$K_{21}^\mu(\phi) = \left[\frac{1}{2}U_{21ij}^\mu(\phi)\gamma^i\gamma^j + V_{21}^{i\mu}\gamma_i\right]\gamma^+. \tag{4.36}$$

The advantage of using the U-function is that the results of contractions with it are more compact, than for S and T alone.

Also note the following relations:

1. UU commutativity:

$$U_{43im}^\varkappa(\phi)\gamma^i\gamma^m U_{21ks}^\mu(\phi')\gamma^k\gamma^s = U_{21ks}^\mu(\phi')\gamma^k\gamma^s U_{43im}^\varkappa(\phi)\gamma^i\gamma^m. \tag{4.37}$$

2. UV product:

$$\frac{1}{2}U_{43im}^\varkappa(\phi)\gamma^i\gamma^m V_{21}^{k\mu}\gamma_k = \gamma^i U_{43ik}^\varkappa(\phi)V_{21}^{k\mu}. \tag{4.38}$$

3. VU product:

$$V_{43}^{i\varkappa}\gamma_i\frac{1}{2}U_{21ks}^\mu(\phi)\gamma^k\gamma^s = V_{43}^{i\varkappa}U_{21ik}^\mu(\phi)\gamma^k. \tag{4.39}$$

4.3.1 Trace for the 'nndd' term

The quantity $\mathcal{T}^{\rm nndd}$ in Eq. (4.16) is given by [after the relabeling (4.31)]

$$\begin{aligned}\mathcal{T}_{4321}^{\rm nndd}(4321) = -\mathrm{Tr}\Big\{&\rho_4 K_{43}^\varkappa(4)(\gamma\tilde{p}_3 + m)K_{32}^\lambda(3)\\ &\times\rho_2 K_{21}^\mu(2)(\gamma\tilde{p}_1 + m)K_{14}^\nu(1)\Big\}g_{\varkappa\nu}g_{\lambda\mu},\end{aligned} \tag{4.40}$$

where the K-functions are given by Eq. (4.36).

As before, the trace is reduced to the one in the transverse space. We obtain:

$$\begin{aligned}\mathcal{T}_{4321}^{\rm nndd}(4321) = &-2p_4^+p_3^+p_2^+p_1^+\\ &\times\mathrm{Tr}\Big\{\left[\frac{1}{2}U_{43im}^\varkappa(4)\gamma^i\gamma^m + V_{43}^{i\varkappa}\gamma_i\right]\left[\frac{1}{2}U_{32jn}^\lambda(3)\gamma^j\gamma^n + V_{32}^{j\lambda}\gamma_j\right]\\ &\times\left[\frac{1}{2}U_{21ks}^\mu(2)\gamma^k\gamma^s + V_{21}^{k\mu}\gamma_k\right]\left[\frac{1}{2}U_{14lt}^\nu(1)\gamma^l\gamma^t + V_{14}^{l\nu}\gamma_l\right]\Big\}g_{\varkappa\nu}g_{\lambda\mu}.\end{aligned} \tag{4.41}$$

The evaluation of the trace is simplified, if we make the contractions with $g_{\varkappa\nu}$ and $g_{\lambda\mu}$ first. Since there are four linearly independent matrices in the transverse space, a general contraction may be written in the form

$$\begin{aligned}\left[\frac{1}{2}U^{\varkappa}_{43im}(\phi)\gamma^i\gamma^m + V^{i\varkappa}_{43}\gamma_i\right]\left[\frac{1}{2}U^{\mu}_{21ks}(\phi')\gamma^k\gamma^s + V^{k\mu}_{21}\gamma_k\right] g_{\varkappa\mu} \\ = S_{4321}(\phi,\phi') + V^i_{4321}(\phi,\phi')\gamma_i + T_{4321}(\phi,\phi')\gamma^1\gamma^2. \qquad (4.42)\end{aligned}$$

Then the trace (4.41) is readily calculated and we obtain:

$$\begin{aligned}\mathcal{T}^{\text{nndd}}_{4321}(4321) &= -8p_4^+p_3^+p_2^+p_1^+ \\ &\times \left[S_{3221}(32)S_{1443}(14) + V^i_{3221}(32)V^j_{1443}(14)g_{ij} - T_{3221}(32)T_{1443}(14)\right]. \qquad (4.43)\end{aligned}$$

The evaluation of the coefficients in Eq. (4.43) is straightforward, but requires some work. Useful identities are put into Appendix B.1.

After performing the contractions, we obtain the following form for the coefficients in Eq. (4.43) (note that $p_3^+ = p_1^+$):

$$\begin{aligned}
S_{3221}(32) &= \frac{1}{2p_2^{+2}p_1^{+2}}\left[-\frac{1}{2}(p_2^{+2}+p_1^{+2})\Delta_2^2 - 2k_1^+p_2^+k_1Z_2 + 2p_2^+p_1^+m^2\right],\\
S_{1443}(14) &= \frac{1}{2p_4^{+2}p_1^{+2}}\left[-\frac{1}{2}(p_4^{+2}+p_1^{+2})\Delta_4^2 - 2k_2^+p_4^+k_2Z_4 + 2p_4^+p_1^+m^2\right],\\
V^i_{3221}(32) &= \frac{m}{2p_2^{+2}p_1^{+2}}k_1^+p_2^+\Delta_2^i,\\
V^j_{1443}(14) &= -\frac{m}{2p_4^{+2}p_1^{+2}}k_2^+p_4^+\Delta_4^j, \qquad (4.44)\\
T_{3221}(32) &= \frac{2p_2^+ - k_1^+}{2p_2^{+2}p_1^{+2}}\epsilon_{\nu\rho\alpha\beta}k_1^\nu\eta^\rho\Delta_2^\alpha Z_2^\beta,\\
T_{1443}(14) &= -\frac{2p_4^+ + k_2^+}{2p_4^{+2}p_1^{+2}}\epsilon_{\sigma\tau\gamma\delta}k_2^\sigma\eta^\tau\Delta_4^\gamma Z_4^\delta.
\end{aligned}$$

And finally, the products are given by

$$\begin{aligned}
S_{3221}(32)S_{1443}(14) &= \frac{1}{4p_4^{+2}p_2^{+2}p_1^{+4}}\\
&\times\left[-\frac{1}{2}(p_2^{+2}+p_1^{+2})\Delta_2^2 - 2k_1^+p_2^+k_1Z_2 + 2p_2^+p_1^+m^2\right]\\
&\times\left[-\frac{1}{2}(p_4^{+2}+p_1^{+2})\Delta_4^2 - 2k_2^+p_4^+k_2Z_4 + 2p_4^+p_1^+m^2\right],\\
V^i_{3221}(32)V^j_{1443}(14)g_{ij} &= -\frac{m^2k_2^+k_1^+p_4^+p_2^+}{4p_4^{+2}p_2^{+2}p_1^{+4}}\Delta_2\Delta_4, \qquad (4.45)\\
T_{3221}(32)T_{1443}(14) &= -\frac{(2p_2^+-k_1^+)(2p_4^++k_2^+)}{4p_4^{+2}p_2^{+2}p_1^{+4}}\\
&\times\Big[\Delta_2\Delta_4\left(k_2^+k_1^+Z_2Z_4 + p_4^+p_2^+k_2k_1 - k_2^+p_2^+k_1Z_4 - k_1^+p_4^+k_2Z_2\right)\\
&+ k_2^+p_2^+k_1\Delta_4\Delta_2Z_4 + k_1^+p_4^+k_2\Delta_2Z_2\Delta_4\\
&- k_2^+k_1^+\Delta_2Z_4Z_2\Delta_4 - p_4^+p_2^+k_1\Delta_4k_2\Delta_2\Big].
\end{aligned}$$

4.3.2 Trace for the 'indd' term

The quantity $\mathcal{T}^{\text{indd}}$ is given by [again, we employ the relabeling (4.31)]

$$\mathcal{T}^{\text{indd}}_{4321}(321) = -\text{Tr}\left\{\rho_4 \frac{K^{\varkappa\lambda}_{42}(3)}{2p_3^+}\rho_2 K^{\mu}_{21}(2)(\gamma\tilde{p}_1 + m)K^{\nu}_{14}(1)\right\} g_{\varkappa\nu} g_{\lambda\mu}, \tag{4.46}$$

where $K^{\varkappa\lambda}_{42}(3)$ is given by Eq. (1.89), and $K^{\mu}_{21}(2)$ and $K^{\nu}_{14}(1)$ by Eq. (4.36). One obtains that

$$\begin{aligned}\mathcal{T}^{\text{indd}}_{4321}(321) = -\frac{1}{2}p_4^+p_2^+\text{Tr}\Big\{ & \left[S_2^\lambda - V_2^{j\lambda}(3)\gamma_j\right]\left[\frac{1}{2}U^{\mu}_{21ks}(2)\gamma^k\gamma^s + V^{k\mu}_{21}\gamma_k\right] \\ & \times \left[\frac{1}{2}U^{\nu}_{14lt}(1)\gamma^l\gamma^t + V^{l\nu}_{14}\right]\left[S_4^\varkappa + V_4^{i\varkappa}(3)\gamma_i\right]\Big\} g_{\varkappa\nu}g_{\lambda\mu}\end{aligned} \tag{4.47}$$

(we employed the fact, that $p_3^+ = p_1^+$).

With the use of the identities in Appendix B.2, we obtain for the trace:

$$\begin{aligned}\mathcal{T}^{\text{indd}}_{4321}(321) &= -\frac{1}{2}p_4^+p_2^+\text{Tr}\Big\{\left[S_{212} - V^j_{221}(32)\gamma_j\right]\left[S_{414} + V^i_{441}(31)\gamma_i\right]\Big\} \\ &= -2p_4^+p_2^+\left[S_{212}S_{414} - V^i_{221}(32)V^j_{441}(31)g_{ij}\right],\end{aligned} \tag{4.48}$$

where

$$\begin{aligned} S_{212} &= \frac{m(p_1^+ - k_1^+)}{p_2^+p_1^+}, \quad S_{414} = \frac{m(p_1^+ + k_2^+)}{p_4^+p_1^+}, \\ V^i_{221}(32) &= \frac{1}{p_2^+p_1^+}\left[-\frac{1}{2}(p_2^+ + p_1^+)\Delta_2^i + k_1^+Z_2^i - p_2^+k_1^i\right], \\ V^j_{441}(31) &= -\frac{1}{p_4^+p_1^+}\left[-\frac{1}{2}(p_4^+ + p_1^+)\Delta_4^j + k_2^+Z_4^j - p_4^+k_2^j\right].\end{aligned} \tag{4.49}$$

And the result is given by

$$\begin{aligned}\mathcal{T}^{\text{indd}}_{4321}(321) = -\frac{2}{p_1^{+2}}\Big[& m^2(p_1^+ - k_1^+)(p_1^+ + k_2^+) + \frac{1}{4}(p_2^+ + p_1^+)(p_4^+ + p_1^+)\Delta_2\Delta_4 \\ & - \frac{1}{2}k_2^+(p_2^+ + p_1^+)\Delta_2 Z_4 - \frac{1}{2}k_1^+(p_4^+ + p_1^+)Z_2\Delta_4 \\ & + \frac{1}{2}p_4^+(p_2^+ + p_1^+)k_2\Delta_2 + \frac{1}{2}p_2^+(p_4^+ + p_1^+)k_1\Delta_4 \\ & + k_2^+k_1^+Z_2Z_4 - k_2^+p_2^+k_1Z_4 - k_1^+p_4^+k_2Z_2 + p_4^+p_2^+k_2k_1\Big].\end{aligned} \tag{4.50}$$

4.3.3 Trace for the 'nidd' term

The quantity $\mathcal{T}^{\text{nidd}}$ is given by

$$\mathcal{T}^{\text{nidd}}_{4321}(431) = -\text{Tr}\left\{\rho_4 K^{\varkappa}_{43}(4)(\gamma\tilde{p}_3 + m)K^{\lambda}_{32}(3)\rho_2\frac{K^{\mu\nu}_{24}(1)}{2p_1^+}\right\} g_{\varkappa\nu}g_{\lambda\mu}. \tag{4.51}$$

The result is the same as for the 'indd' term, but with the replacements $\Delta_2^\mu \to -\Delta_2^\mu$, $\Delta_4^\mu \to -\Delta_4^\mu$:

$$\begin{aligned}\mathcal{T}^{\text{nidd}}_{4321}(431) = -\frac{2}{p_1^{+2}}\Bigg[& m^2(p_1^+ - k_1^+)(p_1^+ + k_2^+) + \frac{1}{4}(p_2^+ + p_1^+)(p_4^+ + p_1^+)\Delta_2\Delta_4 \\ &+ \frac{1}{2}k_2^+(p_2^+ + p_1^+)\Delta_2 Z_4 + \frac{1}{2}k_1^+(p_4^+ + p_1^+)Z_2\Delta_4 \\ &- \frac{1}{2}p_4^+(p_2^+ + p_1^+)k_2\Delta_2 - \frac{1}{2}p_2^+(p_4^+ + p_1^+)k_1\Delta_4 \\ &+ k_2^+k_1^+Z_2Z_4 - k_2^+p_2^+k_1Z_4 - k_1^+p_4^+k_2Z_2 + p_4^+p_2^+k_2k_1\Bigg].\end{aligned} \tag{4.52}$$

4.3.4 Trace for the 'iidd' term

The quantity $\mathcal{T}^{\text{iidd}}$ is given by

$$\mathcal{T}^{\text{iidd}}_{4321}(31) = -\text{Tr}\left\{\rho_4 \frac{K^{\varkappa\lambda}_{42}(3)}{2p_3^+}\rho_2\frac{K^{\mu\nu}_{24}(1)}{2p_1^+}\right\} g_{\varkappa\nu}g_{\lambda\mu}. \tag{4.53}$$

The evaluation of the trace is straightforward and leads to

$$\mathcal{T}^{\text{iidd}}_{4321}(31) = -\frac{2p_4^+p_2^+}{p_1^{+2}}. \tag{4.54}$$

4.4 Rearrangement of the traces

In principle, Eqs. (4.43), (4.45), (4.50), (4.52), and (4.54) are the final result of the trace evaluation for the direct-direct terms. They are written in a compact and manifestly Lorentz-invariant form, which is suitable for the use also in the instant-form formulation (one needs to take into account the fact, that $p^+ = k_0 p/m$). It is convenient, however, to rewrite the result. As one can notice, the traces are infrared divergent in the intermediate momentum p_1^+ [e.g., it is obvious for (4.54)], and therefore require a regularization. Instead of regularizing the traces, we will use momentum relations (see Section 1.9) in order to rearrange the traces in such a way that the infrared divergences cancel each other. Another aim is to exclude the dependence of the preexponential factor on the transverse momentum component $\boldsymbol{k}_1^\perp$, such that the integration in this component [see Eq. (4.11)] can be done straightforwardly. As we will see, both goals can be achieved at the same time.

The following energy-momentum conservation relations are valid for the 'nndd' term [wee are still working with the relabeled momenta, see Eq. (4.31)]

$$\begin{aligned}\pi_4^\mu(4) + k_2^\mu - \pi_3^\mu(4) &\sim 0,\\ \pi_3^\mu(3) + k_1^\mu - \pi_2^\mu(3) &\sim 0,\\ \pi_2^\mu(2) - k_1^\mu - \pi_1^\mu(2) &\sim 0,\\ \pi_1^\mu(1) - k_2^\mu - \pi_4^\mu(1) &\sim 0.\end{aligned} \tag{4.55}$$

For the other terms the conservation relations are obtained from Eq. (4.55), with $x_4^+ = x_3^+$ (for the 'indd' term), or $x_2^+ = x_1^+$ (for the 'nidd' term), or both $x_4^+ = x_3^+$ and $x_2^+ = x_1^+$ (for the 'iidd' term).

4.4.1 The 'nndd' term

We use the relations (1.122) in order to extract terms proportional to $(p_3^2 - m^2)$ and $(p_1^2 - m^2)$ and later include them into the corresponding instantaneous terms. For the $S_{3221}(32)S_{1443}(14)$ product we use the relations

$$k_1 Z_2 \sim -\frac{1}{4}(p_3^2 - m^2) - \frac{1}{4}(p_1^2 - m^2), \quad k_2 Z_4 \sim \frac{1}{4}(p_3^2 - m^2) + \frac{1}{4}(p_1^2 - m^2). \tag{4.56}$$

Then we obtain:

$$\begin{aligned}
&S_{3221}(32)S_{1443}(14) \\
&= \frac{1}{4p_4^{+2}p_2^{+2}p_1^{+4}}\left[-\frac{1}{2}(p_2^{+2}+p_1^{+2})\Delta_2^2 + 2p_2^+p_1^+m^2\right]\left[-\frac{1}{2}(p_4^{+2}+p_1^{+2})\Delta_4^2 + 2p_4^+p_1^+m^2\right] \\
&+ \frac{(p_3^2 - m^2) + (p_1^2 - m^2)}{8p_4^{+2}p_2^{+2}p_1^{+4}}\Bigg\{k_1^+p_2^+\left[-\frac{1}{2}(p_4^{+2}+p_1^{+2})\Delta_4^2 + 2p_4^+p_1^+m^2 - k_2^+p_4^+k_2Z_4\right] \\
&\qquad - k_2^+p_4^+\left[-\frac{1}{2}(p_2^{+2}+p_1^{+2})\Delta_2^2 + 2p_2^+p_1^+m^2 - k_1^+p_2^+k_1Z_2\right]\Bigg\}.
\end{aligned} \tag{4.57}$$

For the 'nndd' term we consider only the first line of the righthand side of Eq. (4.57). Note that the term is the product of two expressions with each of them being in fact the same, as for electron-positron annihilation into one photon [see Eq. (2.53)].

As the next step, we notice that the final expression for the 'nndd' term does not depend on the '–' momentum components (they cancel each other). Therefore, we replace all the scalar four-products with the scalar products in the transverse space: $ab \to -\boldsymbol{a}^\perp \boldsymbol{b}^\perp$.

In order to simplify the result even further, we use the canonical light-cone Lorentz basis with $q^\mu = p_4^\mu + p_2^\mu$ [see Eq. (4.27)], which implies that $\boldsymbol{p}_4^\perp + \boldsymbol{p}_2^\perp = \boldsymbol{k}_2^\perp + \boldsymbol{k}_1^\perp = 0$.

We use Eq. (4.56) in order to eliminate the dependence on $\boldsymbol{k}_1^{\perp 2}$. It can be shown that

$$Z_p^- = \frac{1}{2p^+}\left(m^2 + \boldsymbol{Z}_p^{\perp 2} + \frac{1}{4}\boldsymbol{\Delta}_p^{\perp 2}\right). \tag{4.58}$$

Then one obtains:

$$\begin{aligned}
\boldsymbol{k}_1^{\perp 2} &= \frac{1}{4}\left(\frac{k_2^+}{p_4^+} - \frac{k_1^+}{p_2^+}\right)\left[\left(p_3^2 - m^2\right) + \left(p_1^2 - m^2\right)\right] - \frac{k_2^+}{p_4^+}\boldsymbol{k}_1^\perp \boldsymbol{Z}_4^\perp + \frac{k_1^+}{p_2^+}\boldsymbol{k}_1^\perp \boldsymbol{Z}_2^\perp \\
&- \frac{k_2^{+2}}{2p_4^{+2}}\left(m^2 + \boldsymbol{Z}_4^{\perp 2} + \frac{1}{4}\boldsymbol{\Delta}_4^{\perp 2}\right) - \frac{k_1^{+2}}{2p_2^{+2}}\left(m^2 + \boldsymbol{Z}_2^{\perp 2} + \frac{1}{4}\boldsymbol{\Delta}_2^{\perp 2}\right).
\end{aligned} \tag{4.59}$$

In order to eliminate the terms, depending on $\boldsymbol{k}_1^\perp$ in the first power, we employ the following relations:

$$k_2\Delta_4 \sim k_1\Delta_2 \sim \frac{1}{2}(p_1^2 - m^2) - \frac{1}{2}(p_3^2 - m^2), \quad \Delta_p^- = \frac{1}{p^+}\boldsymbol{Z}_p^\perp \boldsymbol{\Delta}_p^\perp. \tag{4.60}$$

Then we obtain (the contributions to the instantaneous terms are excluded):

$$
\begin{aligned}
S_{3221}(32)S_{1443}(14) &= \frac{1}{4p_4^{+2}p_2^{+2}p_1^{+4}}\left[\frac{1}{2}(p_2^{+2}+p_1^{+2})\boldsymbol{\Delta}_2^{\perp 2}+2p_2^+p_1^+m^2\right] \\
&\qquad\qquad\times\left[\frac{1}{2}(p_4^{+2}+p_1^{+2})\boldsymbol{\Delta}_4^{\perp 2}+2p_4^+p_1^+m^2\right], \\
V^i_{3221}(32)V^j_{1443}(14)g_{ij} &= \frac{m^2k_2^+k_1^+p_4^+p_2^+}{4p_4^{+2}p_2^{+2}p_1^{+4}}\boldsymbol{\Delta}_2^\perp\boldsymbol{\Delta}_4^\perp, \\
T_{3221}(32)T_{1443}(14) &= -\frac{(2p_2^+-k_1^+)(2p_4^++k_2^+)}{4p_4^{+2}p_2^{+2}p_1^{+4}}\Bigg\{\boldsymbol{\Delta}_2^\perp\boldsymbol{\Delta}_4^\perp \\
\times\Bigg[k_2^+k_1^+\boldsymbol{Z}_2^\perp\boldsymbol{Z}_4^\perp &+\frac{k_2^{+2}p_2^+}{2p_4^+}\left(m^2+\boldsymbol{Z}_4^{\perp 2}+\frac{1}{4}\boldsymbol{\Delta}_4^{\perp 2}\right)+\frac{k_1^{+2}p_4^+}{2p_2^+}\left(m^2+\boldsymbol{Z}_2^{\perp 2}+\frac{1}{4}\boldsymbol{\Delta}_2^{\perp 2}\right)\Bigg] \\
&\qquad -\frac{k_2^{+2}p_2^+}{p_4^+}\boldsymbol{Z}_4^\perp\boldsymbol{\Delta}_4^\perp\boldsymbol{\Delta}_2^\perp\boldsymbol{Z}_4^\perp-\frac{k_1^{+2}p_4^+}{p_2^+}\boldsymbol{Z}_2^\perp\boldsymbol{\Delta}_2^\perp\boldsymbol{Z}_2^\perp\boldsymbol{\Delta}_4^\perp \\
&\qquad -k_2^+k_1^+\boldsymbol{\Delta}_2^\perp\boldsymbol{Z}_4^\perp\boldsymbol{Z}_2^\perp\boldsymbol{\Delta}_4^\perp-k_2^+k_1^+\boldsymbol{Z}_2^\perp\boldsymbol{\Delta}_2^\perp\boldsymbol{Z}_4^\perp\boldsymbol{\Delta}_4^\perp\Bigg\}.
\end{aligned}
\tag{4.61}
$$

The contributions, which are to be included into the corresponding instantaneous terms:

$$
\Delta\mathcal{T}^{\mathrm{indd}}=\Delta\mathcal{T}_{SS}+\Delta\mathcal{T}_{TT,1}+\Delta\mathcal{T}_{TT,2},\quad \Delta\mathcal{T}^{\mathrm{nidd}}=\Delta\mathcal{T}_{SS}-\Delta\mathcal{T}_{TT,1}+\Delta\mathcal{T}_{TT,2}, \tag{4.62}
$$

where

$$
\begin{aligned}
\Delta\mathcal{T}_{SS} &= -\frac{2}{p_1^{+2}}\Bigg[\frac{k_1^+}{4p_4^+}\left(p_4^{+2}+p_1^{+2}\right)\boldsymbol{\Delta}_4^{\perp 2}-\frac{k_2^+}{4p_2^+}\left(p_2^{+2}+p_1^{+2}\right)\boldsymbol{\Delta}_2^{\perp 2} \\
&\qquad\qquad +k_1^+p_1^+m^2-k_2^+p_1^+m^2-\frac{1}{2}k_2^+k_1^+k_2Z_4+\frac{1}{2}k_2^+k_1^+k_1Z_2\Bigg], \\
\Delta\mathcal{T}_{TT,1} &= -\frac{2}{p_1^{+2}}(2p_2^+-k_1^+)(2p_4^++k_2^+) \\
&\quad\times\Bigg[\frac{1}{4}\boldsymbol{k}_1^\perp\boldsymbol{\Delta}_4^\perp-\frac{1}{4}\boldsymbol{k}_1^\perp\boldsymbol{\Delta}_2^\perp-\frac{k_2^+}{4p_4^+}\boldsymbol{Z}_4^\perp\boldsymbol{\Delta}_4^\perp-\frac{k_1^+}{4p_2^+}\boldsymbol{Z}_2^\perp\boldsymbol{\Delta}_2^\perp \\
&\qquad\qquad -\frac{k_2^+}{2p_4^+}\boldsymbol{\Delta}_2^\perp\boldsymbol{Z}_4^\perp-\frac{k_1^+}{2p_2^+}\boldsymbol{Z}_2^\perp\boldsymbol{\Delta}_4^\perp\Bigg], \\
\Delta\mathcal{T}_{TT,2} &= -\frac{2}{p_1^{+2}}(2p_2^+-k_1^+)(2p_4^++k_2^+)\left[-\frac{1}{4}\left(\frac{k_2^+}{p_4^+}-\frac{k_1^+}{p_2^+}\right)\boldsymbol{\Delta}_2^\perp\boldsymbol{\Delta}_4^\perp\right].
\end{aligned}
\tag{4.63}
$$

Note that $\Delta\mathcal{T}^{\mathrm{indd}}$ and $\Delta\mathcal{T}^{\mathrm{nidd}}$ differ by the change $\boldsymbol{\Delta}_4^\perp\to-\boldsymbol{\Delta}_4^\perp$, $\boldsymbol{\Delta}_2^\perp\to-\boldsymbol{\Delta}_2^\perp$, which, in essense, is the same change that we need to make in order to convert $\mathcal{T}^{\mathrm{indd}}$ into $\mathcal{T}^{\mathrm{nidd}}$, and vice versa.

4.4.2 The ‘indd’ term

As with the ‘nndd’ term, we notice, that the result (4.50) does not depend on the ‘−’ momentum components. Therefore, we can replace all the four-scalar products with the corresponding scalar products over the transverse components.

The obtained expression should be combined with the contributions (4.63) from the ‘nndd’ term [see Eqs. (4.62) and (4.63)]. We use the momentum relations (1.122), which imply that

$$\begin{aligned} k_2 Z_4 &= \frac{1}{2}(p_1^2 - m^2) - \frac{k_1^+}{2p_2^+}\boldsymbol{Z}_2^\perp \boldsymbol{\Delta}_2^\perp + \frac{1}{2}\boldsymbol{k}_1^\perp \boldsymbol{\Delta}_2^\perp, \\ k_1 Z_2 &= -\frac{1}{2}(p_1^2 - m^2) + \frac{k_2^+}{2p_4^+}\boldsymbol{Z}_4^\perp \boldsymbol{\Delta}_4^\perp + \frac{1}{2}\boldsymbol{k}_1^\perp \boldsymbol{\Delta}_4^\perp. \end{aligned} \tag{4.64}$$

On the other hand, the products $k_2 Z_4$ and $k_1 Z_2$ can be written as

$$\begin{aligned} k_2 Z_4 &= \frac{p_4^+ \boldsymbol{k}_1^{\perp 2}}{2k_2^+} + k_2^+ Z_4^- + \boldsymbol{k}_1^\perp \boldsymbol{Z}_4^\perp, \\ k_1 Z_2 &= \frac{p_2^+ \boldsymbol{k}_1^{\perp 2}}{2k_1^+} + k_1^+ Z_2^- - \boldsymbol{k}_1^\perp \boldsymbol{Z}_2^\perp, \end{aligned} \tag{4.65}$$

which allows us to eliminate the terms, quadratic in $\boldsymbol{k}_1^\perp$.

Combining the terms $\mathcal{T}_{4321}^{\text{indd}}(321)$ and $\Delta\mathcal{T}^{\text{indd}}$, one obtains (note, that all the terms, linear in $\boldsymbol{k}_1^\perp$, cancel each other):

$$\begin{aligned} \mathcal{T}_{4321}^{\text{indd}}(321) = &-\frac{1}{p_1^{+2} p_4^+ p_2^+}\Bigg\{ \left[2p_4^+ p_2^+ (p_1^{+2} - k_2^+ k_1^+) - k_2^{+2} p_2^{+2} - k_1^{+2} p_4^{+2}\right] m^2 \\ &- \left[k_2^+ p_2^+ \boldsymbol{Z}_2^\perp + k_1^+ p_4^+ \boldsymbol{Z}_4^\perp + \frac{1}{2}p_1^+(p_2^+ + p_1^+)\boldsymbol{\Delta}_2^\perp + \frac{1}{2}p_1^+(p_4^+ + p_1^+)\boldsymbol{\Delta}_4^\perp\right]^2 \\ &+ \left[\frac{1}{2}k_1^+(p_4^+ + p_1^+)\boldsymbol{\Delta}_4^\perp - \frac{1}{2}k_2^+(p_2^+ + p_1^+)\boldsymbol{\Delta}_2^\perp\right]^2 \\ &+ 4p_1^{+2} p_4^+ p_2^+ \left(\boldsymbol{\Delta}_4^{\perp 2} + \boldsymbol{\Delta}_2^{\perp 2}\right)\Bigg\} + (p_3^2 - m^2)\Delta\mathcal{T}^{\text{iidd}}, \end{aligned} \tag{4.66}$$

where

$$\Delta\mathcal{T}^{\text{iidd}} = \frac{1}{p_1^{+2}}(k_2^+ k_1^+ - k_2^+ p_2^+ + k_1^+ p_4^+) \tag{4.67}$$

is a contribution to the ‘iidd’ term.

4.4.3 The ‘nidd’ term

We can use the results, obtained for the ‘indd’ term. One finds that

$$\begin{aligned}\mathcal{T}^{\text{nidd}}_{4321}(431) = -\frac{1}{p_1^{+2}p_4^+p_2^+}\Big\{ &\left[2p_4^+p_2^+(p_1^{+2}-k_2^+k_1^+) - k_2^{+2}p_2^{+2} - k_1^{+2}p_4^{+2}\right]m^2 \\ &- \left[k_2^+p_2^+\boldsymbol{Z}_2^\perp + k_1^+p_4^+\boldsymbol{Z}_4^\perp - \frac{1}{2}p_1^+(p_2^+ + p_1^+)\boldsymbol{\Delta}_2^\perp - \frac{1}{2}p_1^+(p_4^+ + p_1^+)\boldsymbol{\Delta}_4^\perp\right]^2 \\ &+ \left[\frac{1}{2}k_1^+(p_4^+ + p_1^+)\boldsymbol{\Delta}_4^\perp - \frac{1}{2}k_2^+(p_2^+ + p_1^+)\boldsymbol{\Delta}_2^\perp\right]^2 \\ &+ 4p_1^{+2}p_4^+p_2^+\left(\boldsymbol{\Delta}_4^{\perp 2} + \boldsymbol{\Delta}_2^{\perp 2}\right)\Big\} + (p_1^2 - m^2)\Delta\mathcal{T}^{\text{iidd}},\end{aligned} \tag{4.68}$$

where $\mathcal{T}^{\text{iidd}}$ is given by Eq. (4.67).

4.4.4 The ‘iidd’ term

Upon adding the contributions from the ‘nidd’ and ‘indd’ terms [see Eq. (4.67)] to the expression (4.54), we come to a very simple result:

$$\mathcal{T}^{\text{iidd}}_{4321}(31) + 2\Delta\mathcal{T}^{\text{iidd}} = -2. \tag{4.69}$$

4.4.5 The final result for the traces

Let us restore the initial labeling of the momenta and collect together all the expressions, that we have obtained. We have:

$$\mathcal{T}^{\text{nndd}} \to \frac{2m^8}{p_2^+p_1^+p_3^{+2}}\widetilde{\mathcal{T}}^{\text{nndd}}, \tag{4.70}$$

$$\begin{aligned}\widetilde{\mathcal{T}}^{\text{nndd}} = &\frac{1}{m^8}\left[\frac{1}{2}(p_1^{+2}+p_3^{+2})\boldsymbol{\Delta}_1^{\perp 2} + 2p_1^+p_3^+m^2\right]\left[\frac{1}{2}(p_2^{+2}+p_3^{+2})\boldsymbol{\Delta}_{-2}^{\perp 2} - 2p_2^+p_3^+m^2\right] \\ &- \frac{k_2^+k_1^+p_2^+p_1^+}{m^6}\boldsymbol{\Delta}_1^\perp\boldsymbol{\Delta}_{-2}^\perp + \frac{(2p_1^+ - k_1^+)(k_2^+ - 2p_2^+)}{m^8}\Big\{\boldsymbol{\Delta}_1^\perp\boldsymbol{\Delta}_{-2}^\perp \\ \times &\left[k_2^+k_1^+\boldsymbol{Z}_1^\perp\boldsymbol{Z}_{-2}^\perp - \frac{k_2^{+2}p_1^+}{2p_2^+}\left(m^2 + \boldsymbol{Z}_{-2}^{\perp 2} + \frac{1}{4}\boldsymbol{\Delta}_{-2}^{\perp 2}\right) - \frac{k_1^{+2}p_2^+}{2p_1^+}\left(m^2 + \boldsymbol{Z}_1^{\perp 2} + \frac{1}{4}\boldsymbol{\Delta}_1^{\perp 2}\right)\right] \\ &+ \frac{k_2^{+2}p_1^+}{p_2^+}\boldsymbol{Z}_{-2}^\perp\boldsymbol{\Delta}_{-2}^\perp\boldsymbol{\Delta}_1^\perp\boldsymbol{Z}_{-2}^\perp + \frac{k_1^{+2}p_2^+}{p_1^+}\boldsymbol{Z}_1^\perp\boldsymbol{\Delta}_1^\perp\boldsymbol{Z}_1^\perp\boldsymbol{\Delta}_{-2}^\perp \\ &- k_2^+k_1^+\boldsymbol{\Delta}_1^\perp\boldsymbol{Z}_{-2}^\perp\boldsymbol{Z}_1^\perp\boldsymbol{\Delta}_{-2}^\perp - k_2^+k_1^+\boldsymbol{Z}_1^\perp\boldsymbol{\Delta}_1^\perp\boldsymbol{Z}_{-2}^\perp\boldsymbol{\Delta}_{-2}^\perp\Big\};\end{aligned} \tag{4.71}$$

$$\mathcal{T}^{\text{indd}} \to \frac{m^6}{p_2^+p_1^+p_3^{+2}}\widetilde{\mathcal{T}}^{\text{indd}}, \tag{4.72}$$

$$\widetilde{\mathcal{T}}^{\text{indd}} = \frac{1}{m^6}\bigg\{ \Big[-2p_2^+p_1^+(p_3^{+2} - k_2^+k_1^+) - k_2^{+2}p_1^{+2} - k_1^{+2}p_2^{+2}\Big]\, m^2$$
$$- \Big[k_2^+p_1^+\boldsymbol{Z}_1^\perp - k_1^+p_2^+\boldsymbol{Z}_{-2}^\perp + \frac{1}{2}p_3^+(p_1^+ + p_3^+)\boldsymbol{\Delta}_1^\perp - \frac{1}{2}p_3^+(p_2^+ - p_3^+)\boldsymbol{\Delta}_{-2}^\perp\Big]^2$$
$$+ \Big[\frac{1}{2}k_1^+(p_2^+ - p_3^+)\boldsymbol{\Delta}_{-2}^\perp + \frac{1}{2}k_2^+(p_1^+ + p_3^+)\boldsymbol{\Delta}_1^\perp\Big]^2 - 4p_3^{+2}p_2^+p_1^+\left(\boldsymbol{\Delta}_{-2}^{\perp 2} + \boldsymbol{\Delta}_1^{\perp 2}\right)\bigg\}; \quad (4.73)$$

$$\mathcal{T}^{\text{nidd}} \to \frac{m^6}{p_2^+p_1^+p_3^{+2}}\widetilde{\mathcal{T}}^{\text{nidd}}, \quad \widetilde{\mathcal{T}}^{\text{nidd}} = \widetilde{\mathcal{T}}^{\text{indd}}\big|_{\boldsymbol{\Delta}_1^\perp \to -\boldsymbol{\Delta}_1^\perp, \boldsymbol{\Delta}_{-2}^\perp \to -\boldsymbol{\Delta}_{-2}^\perp}; \quad (4.74)$$

$$\mathcal{T}^{\text{iidd}} \to -2. \quad (4.75)$$

Here, p_3^+ is defined by Eq. (4.24).

The check of the finiteness of the obtained expressions will be done in Section 4.7, after the evaluation of the integrals.

4.5 Evaluation of the integrals for the direct-direct terms

4.5.1 Integrals for the 'nndd' term

For the propagator denominators in Eq. (4.16) we use the proper-time representation:

$$\frac{1}{p_4^2 - m^2 + i\epsilon} = -i\int_0^\infty \mathrm{d}s\, \mathrm{e}^{i(p_4^2 - m^2 + i\epsilon)s}, \quad \frac{1}{p_3^2 - m^2 - i\epsilon} = i\int_0^\infty \mathrm{d}t\, \mathrm{e}^{-i(p_3^2 - m^2 - i\epsilon)t}. \quad (4.76)$$

We do not write the terms with $i\epsilon$ in the following, but keep them in mind.

With the help of the representation (4.76) we evaluate the integrals in p_3^- and p_4^- [see Eqs. (4.16) and (4.17)]:

$$\int \frac{\mathrm{d}p_4^-}{2\pi}\frac{\mathrm{d}p_3^-}{2\pi} \to \delta[2p_4^+s - (x_4^+ - x_3^+)]\,\delta[2p_3^+t + (x_2^+ - x_1^+)], \quad (4.77)$$

In place of s and t in Eq. (4.76) we introduce variables τ and v:

$$\tau = s + t, \quad v = \frac{s - t}{s + t}, \qquad \int_0^\infty \mathrm{d}s\,\mathrm{d}t \to \int_{-1}^1 \mathrm{d}v \int_0^\infty \mathrm{d}\tau\, \frac{\tau}{2}. \quad (4.78)$$

In terms of the new variables the delta functions in Eq. (4.77) can be written as

$$\delta[2p_4^+s - (x_4^+ - x_3^+)]\,\delta[2p_3^+t + (x_2^+ - x_1^+)] = \delta(\delta^+ - p_3^+\tau)\,\delta(\delta_2^+ + \delta_1^+ + 2p_3^+v\tau). \quad (4.79)$$

Due to the change (4.5) we obtain the following integrals in the light-cone time variables:

$$\int \mathrm{d}x_4^+\mathrm{d}x_3^+\mathrm{d}x_2^+\mathrm{d}x_1^+ \to \int \mathrm{d}x^+\mathrm{d}\delta^+\mathrm{d}\delta_1^+\mathrm{d}\delta_2^+. \quad (4.80)$$

We use the delta functions in Eq. (4.79) to do the integrals in δ^+ and δ_2^+, so

$$\delta^+ = p_3^+\tau, \quad \delta_2^+ = 2p_3^+v\tau - \delta_1^+. \quad (4.81)$$

After all the steps the phase (4.17) is given by [see also Eq. (4.29)]

$$\Phi^{\mathrm{dd}}(4321) \to \Phi^{\mathrm{dd}} = \frac{\boldsymbol{k}_1^{\perp 2}}{2p_3^+}\left(\frac{p_2^+}{k_2^+}\delta_2^+ + \frac{p_1^+}{k_1^+}\delta_1^+\right) - \frac{\boldsymbol{k}_1^{\perp}\boldsymbol{p}_1^{\perp}}{p_3^+}\left(\delta_2^+ + \delta_1^+\right) + \frac{\boldsymbol{p}_1^{\perp 2}+m^2}{2p_3^+}\left(\frac{k_2^+}{p_2^+}\delta_2^+ + \frac{k_1^+}{p_1^+}\delta_1^+\right) + \Phi_F^{\mathrm{dd}}, \tag{4.82}$$

In place of δ_1^+ we define variable ρ as

$$\rho = \frac{m^2 p_2^+}{k_2^+ p_3^+}\delta_2^+ + \frac{m^2 p_1^+}{k_1^+ p_3^+}\delta_1^+, \quad \int \mathrm{d}\delta_1^+ \to \frac{k_2^+ k_1^+}{m^2(p_2^+ + p_1^+)}\int \mathrm{d}\rho, \tag{4.83}$$

such that

$$\delta_1^+ = \frac{p_3^+ k_1^+}{2m^2 p_1^+}(1+u)\rho, \quad \delta_2^+ = \frac{p_3^+ k_2^+}{2m^2 p_2^+}(1-u)\rho, \tag{4.84}$$

where the parameter u is given by

$$u = \left[4v\frac{m^2\tau}{\rho} + \left(\frac{k_2^+}{p_2^+} + \frac{k_1^+}{p_1^+}\right)\right] \Big/ \left(\frac{k_2^+}{p_2^+} - \frac{k_1^+}{p_1^+}\right). \tag{4.85}$$

The dependence on ρ is only via δ_1^+ and δ_2^+, and the dependence on v is only via u. We notice that, upon changing the sign of ρ and the simultaneous change $v \to -v$, the parameter u does not change, but both δ_1^+ and δ_2^+ change their signs. It can be also seen that the phase in Eq. (4.82) is odd with respect to the simultaneous swap of the signs of δ_1^+ and δ_2^+. As for the preexponential factor in Eqs. (4.70) and (4.71), it is even in ρ. Then the integral in ρ can be written as

$$\int \mathrm{d}\rho \to 2\mathrm{Re}\int_0^\infty \mathrm{d}\rho, \tag{4.86}$$

with Re denoting the real part of the expression to the right.

We rescale τ:

$$\frac{m^2\tau}{\rho} \to \tau, \tag{4.87}$$

so that u does not depend on ρ [see Eq. (4.85)]:

$$u = \left[4v\tau + \left(\frac{k_2^+}{p_2^+} + \frac{k_1^+}{p_1^+}\right)\right] \Big/ \left(\frac{k_2^+}{p_2^+} - \frac{k_1^+}{p_1^+}\right). \tag{4.88}$$

Then the reduced matrix element modulus squared for the ‘nndd’ term [see Eq. (4.16)] is given by

$$\frac{1}{4}\sum_{\text{polarization}} M^{\mathrm{nd}} M^{\mathrm{nd}*} = \frac{e^4 k_2^+ k_1^+}{m^6(p_2^+ + p_1^+)}\mathrm{Re}\int \mathrm{d}x^+ \int_{-1}^{1}\mathrm{d}v \int_0^\infty \mathrm{d}\rho \int_0^\infty \mathrm{d}\tau\, \tau\rho^2 \times \exp\left(i\Phi^{\mathrm{dd}}\right)\mathcal{T}^{\mathrm{nndd}}, \tag{4.89}$$

where

$$\Phi^{\mathrm{dd}} = \frac{\rho}{2m^2}(\boldsymbol{k}_1^{\perp 2} + 2\boldsymbol{k}_1^{\perp}\boldsymbol{R}^{\perp}) + \frac{\rho(1+t_1^2+t_2^2)}{4}\left[\frac{k_2^{+2}}{p_2^{+2}}(1-u) + \frac{k_1^{+2}}{p_1^{+2}}(1+u)\right]$$
$$+ \frac{\rho}{2}\sum_i t_i\xi_i\left[\frac{k_2^{+2}}{p_2^{+2}}(1-u)I_{2i} + \frac{k_1^{+2}}{p_1^{+2}}(1+u)I_{1i}\right]$$
$$+ \frac{\rho}{4}\sum_i \xi_i^2\left[\frac{k_2^{+2}}{p_2^{+2}}(1-u)J_{2i} + \frac{k_1^{+2}}{p_1^{+2}}(1+u)J_{1i}\right], \tag{4.90}$$

with

$$R^i = 2mt_i v\tau - \frac{1}{2}m\xi_i\left[\frac{k_2^+}{p_2^+}(1-u)I_{2i} + \frac{k_1^+}{p_1^+}(1+u)I_{1i}\right]. \tag{4.91}$$

4.5.2 Integrals for the 'indd' and 'nidd' term

Among the variables (4.5), we choose x^+, δ^+, and δ_1^+ as the independent ones, then

$$\int \mathrm{d}x_3^+\mathrm{d}x_2^+\mathrm{d}x_1^+ \to \int \mathrm{d}x^+\mathrm{d}\delta^+\mathrm{d}\delta_1^+, \tag{4.92}$$

and

$$\delta_2^+ = 2\delta^+ - \delta_1^+. \tag{4.93}$$

For the propagator in Eq. (4.21) we use the proper-time representation as in Eq. (4.76), therefore:

$$\int \frac{\mathrm{d}p_3^-}{2\pi}\frac{\mathrm{e}^{-ip_3^-(x_2^+-x_1^+)}}{p_3^2-m^2-i\epsilon} = i\int_0^\infty \mathrm{d}t\,\mathrm{e}^{i(\boldsymbol{p}_3^{\perp 2}+m^2+i\epsilon)}\delta(x_2^+-x_1^++2p_3^+t)$$
$$= i\int_0^\infty \mathrm{d}t\,\mathrm{e}^{i(\boldsymbol{p}_3^{\perp 2}+m^2+i\epsilon)}\frac{1}{2}\delta(\delta^+-p_3^+t). \tag{4.94}$$

Again, we suppress the terms with $i\epsilon$ in the following.

After the evaluation of the integral in δ^+ with the use of the delta function in Eq. (4.94), we come to the following relations

$$\delta^+ = p_3^+t, \quad \delta_2^+ = 2p_3^+t - \delta_1^+, \tag{4.95}$$

which are similar to the ones in Eq. (4.81), apart from the absense of the parameter v.

The parameter ρ is introduced according to Eq. (4.83), and the parameter τ is defined as [compare with Eq. (4.87)]

$$\tau = \frac{m^2t}{|\rho|}. \tag{4.96}$$

We split the integral in ρ into two:

$$\int \mathrm{d}\rho = \int_0^\infty \mathrm{d}\rho + \int_{-\infty}^0 \mathrm{d}\rho, \tag{4.97}$$

and make the change $\rho \to -\rho$ in the second integral. It turns out that after this the phase in the first integral is the same as for the 'nndd' term, but with $v = -1$, and the phase in the second integral is also the same as for the 'nndd' term, but with $v = 1$, and an overall minus sign. We denote them as $\Phi^{\rm dd}_{-1}$ and $-\Phi^{\rm dd}_{1}$, respectively.

Finally, we obtain for the 'indd' term:

$$\begin{aligned}\frac{1}{4}\sum_{\rm polarization} M^{\rm id}M^{\rm nd*} =& \frac{ie^4k_2^+k_1^+}{2m^4(p_2^+ + p_1^+)}\int {\rm d}x^+ \int_0^\infty {\rm d}\rho \int_0^\infty {\rm d}\tau\, \rho \\ &\times \left[\exp\left(i\Phi^{\rm dd}_{-1}\right)\mathcal{T}^{\rm indd}\big|_\rho + \exp\left(-i\Phi^{\rm dd}_{1}\right)\mathcal{T}^{\rm indd}\big|_{-\rho}\right], \end{aligned} \tag{4.98}$$

where $\mathcal{T}^{\rm indd}$ in the first term is evaluated at ρ and in the second term at $-\rho$.

For the 'nidd' term [see Eq. (4.22)] the steps are analogous, and they lead to the following result:

$$\begin{aligned}\frac{1}{4}\sum_{\rm polarization} M^{\rm nd}M^{\rm id*} =& \frac{ie^4k_2^+k_1^+}{2m^4(p_2^+ + p_1^+)}\int {\rm d}x^+ \int_0^\infty {\rm d}\rho \int_0^\infty {\rm d}\tau\, \rho \\ &\times \left[\exp\left(i\Phi^{\rm dd}_{1}\right)\mathcal{T}^{\rm nidd}\big|_\rho + \exp\left(-i\Phi^{\rm dd}_{-1}\right)\mathcal{T}^{\rm nidd}\big|_{-\rho}\right]. \end{aligned} \tag{4.99}$$

4.5.3 Integrals for the 'iidd' term

The 'iidd' term [see Eq. (4.23)] contains only two integrals over the light-cone time. We employ the change given by Eq. (4.5), which in this case is reduced to

$$x^+ = (x_3^+ + x_1^+)/2, \quad \delta^+ = x_3^+ - x_1^+. \tag{4.100}$$

Then the 'iidd' term is written as

$$\frac{1}{4}\sum_{\rm polarization} M^{\rm id}M^{\rm id*} = e^4 \int {\rm d}x^+{\rm d}\delta^+ \exp\left[i\Phi^{\rm iidd}\right]\mathcal{T}^{\rm iidd}, \tag{4.101}$$

where

$$\Phi^{\rm iidd} = \frac{\boldsymbol{k}_1^{\perp 2}(p_2^+ + p_1^+)}{2k_2^+k_1^+}\delta^+ - \frac{m^2(p_2^+ + p_1^+)}{2p_2^+p_1^+}\delta^+ + \Phi^{\rm iidd}_F \tag{4.102}$$

with

$$\Phi^{\rm iidd}_F = -\frac{m^2(p_2^+ + p_1^+)}{2p_2^+p_1^+}\delta^+\sum_i\left[(t_i + \xi_i I_i)^2 + \xi_i^2(J_i - I_i^2)\right], \tag{4.103}$$

$$I_i = \int_{-1}^{1}{\rm d}\lambda\,\psi_i\left(mx^+ + \frac{1}{2}m\delta^+\lambda\right), \quad J_i = \int_{-1}^{1}{\rm d}\lambda\,\psi_i^2\left(mx^+ + \frac{1}{2}m\delta^+\lambda\right). \tag{4.104}$$

4.6 Direct-direct contribution to the cross section

Each of the four direct-direct terms contributes to the cross section (4.11). We combine the contributions from the 'nidd' and 'indd' terms together, such that the total direct-direct contribution to the cross section is written as the sum of three terms:

$$\sigma_0^{\rm dd}(x^+) = \sigma_0^{\rm nndd}(x^+) + \sigma_0^{\rm [in]dd}(x^+) + \sigma_0^{\rm iidd}(x^+), \tag{4.105}$$

where $\sigma_0^{\rm [in]dd}(x^+) = \sigma_0^{\rm indd}(x^+) + \sigma_0^{\rm nidd}(x^+)$.

4.6.1 The 'nndd' term

The intergrals in $\boldsymbol{k}_1^\perp$ [see Eqs. (4.10) and (4.90)] are the Fresnel integrals and are evaluated analytically:

$$\int \frac{\mathrm{d}^2 k_1^\perp}{(2\pi)^2} \exp\left[i\frac{\rho}{2m^2}(\boldsymbol{k}_1^{\perp 2} + 2\boldsymbol{k}_1^\perp \boldsymbol{R}^\perp)\right] = \frac{im^2}{2\pi\rho}\exp\left[-i\frac{\rho \boldsymbol{R}^{\perp 2}}{2m^2}\right]. \tag{4.106}$$

where $\boldsymbol{R}^\perp$ is given by Eq. (4.91).

Rearranging the terms, we obtain the following expression for the phase (4.90) after the integration:

$$\begin{aligned}\Phi^{\mathrm{dd}} &= \frac{m\rho}{4}\left[\frac{k_2^{+2}}{p_2^{+2}}(1+u) + \frac{k_1^{+2}}{p_1^{+2}}(1-u)\right] \\ &+ \frac{m\rho}{8}(1-u^2)\sum_i \left[\frac{k_2^+}{p_2^+}\left(t_i + \xi_i I_{2i}\right) - \frac{k_1^+}{p_1^+}\left(t_i + \xi_i I_{1i}\right)\right]^2 \\ &+ \frac{m\rho}{4}\sum_i \xi_i^2 \left[\frac{k_2^{+2}}{p_2^{+2}}(1+u)\left(J_{2i} - I_{2i}^2\right) + \frac{k_1^{+2}}{p_1^{+2}}(1-u)\left(J_{1i} - I_{1i}^2\right)\right].\end{aligned} \tag{4.107}$$

And the contribution to the cross section is given by

$$\begin{aligned}\sigma_0^{\mathrm{nndd}}(x^+) = \mathrm{Im} \int\limits_0^{p_2^+ + p_1^+} \mathrm{d}k_1^+ \left(-\frac{r_e^2 m^6}{4I p_2^+ p_1^+ p_3^{+2}(p_2^+ + p_1^+)}\right) \\ \times \int\limits_{-1}^{1} \mathrm{d}v \int\limits_0^\infty \mathrm{d}\rho \int\limits_0^\infty \mathrm{d}\tau\, \tau\rho \exp\left[i\Phi^{\mathrm{dd}}\right] \widetilde{\mathcal{T}}^{\mathrm{nndd}},\end{aligned} \tag{4.108}$$

where Im denotes the imaginary part and $\widetilde{\mathcal{T}}^{\mathrm{nndd}}$ is given by Eq. (4.71).

4.6.2 The 'indd' and 'nidd' terms

As can be seen from Eqs. (4.98) and (4.99), we need to sum four terms. We notice that upon changing $\rho \to -\rho$ the quantities Z_1^μ and Z_{-2}^μ do not change, but Δ_1^μ and Δ_{-2}^μ change their sign, therefore:

$$\mathcal{T}^{\mathrm{indd}}\big|_{-\rho} = \mathcal{T}^{\mathrm{nidd}}\big|_{\rho}, \quad \mathcal{T}^{\mathrm{nidd}}\big|_{-\rho} = \mathcal{T}^{\mathrm{indd}}\big|_{\rho}. \tag{4.109}$$

The integration in $\boldsymbol{k}_1^\perp$ is performed in the same way as for the 'nndd' term [see Eq. (4.106)], and we obtain:

$$\begin{aligned}\sigma_0^{[\mathrm{in}]\mathrm{dd}}(x^+) = \mathrm{Re} \int\limits_0^{p_2^+ + p_1^+} \mathrm{d}k_1^+ \left(-\frac{r_e^2 m^6}{4I p_2^+ p_1^+ p_3^{+2}(p_2^+ + p_1^+)}\right) \int\limits_0^\infty \mathrm{d}\rho \int\limits_0^\infty \mathrm{d}\tau \\ \times \left[\exp\left(i\Phi_{-1}^{\mathrm{dd}}\right)\widetilde{\mathcal{T}}^{\mathrm{indd}}\big|_\rho + \exp\left(i\Phi_{1}^{\mathrm{dd}}\right)\widetilde{\mathcal{T}}^{\mathrm{nidd}}\big|_\rho\right],\end{aligned} \tag{4.110}$$

where $\widetilde{\mathcal{T}}^{\mathrm{indd}}$ and $\widetilde{\mathcal{T}}^{\mathrm{nidd}}$ are given by Eqs. (4.73) and (4.74), respectively.

4.6.3 The 'iidd'

For the 'iidd' term, the integral in $\boldsymbol{k}_1^\perp$ can be exchanged with the integral in ρ, after we shift the integration in ρ off the real axis [Dinu, 2013], then one obtains the following result:

$$\sigma_0^{\text{iidd}}(x^+) = \int_0^{p_2^+ + p_1^+} \mathrm{d}k_1^+ \left(-\frac{r_e^2 m^2}{2I(p_2^+ + p_1^+)} \right) \left[\int_0^\infty \frac{\mathrm{d}\rho}{\rho} \left(\sin \Phi^{\text{iidd}} - \sin \Phi_0^{\text{iidd}} \right) + \pi \right], \tag{4.111}$$

where

$$\Phi^{\text{iidd}} = \rho + \rho \sum_i (t_i + \xi_i I_i)^2 + \rho \sum_i \xi_i^2 (J_i - I_i^2), \tag{4.112}$$

$$\Phi_0^{\text{iidd}} = \rho + \rho \sum_i [t_i + \xi_i \psi_i(\phi)]^2. \tag{4.113}$$

4.7 Discussion of the result

The steps, that we have performed in order to obtain the cross section, are inspired by the analogous calculations for electron-positron annihilation into one photon and the polarization operator in a plane-wave field, that we have done in Chapters 2 and 3. The result, of course, bears some similarities with the ones, obtained before [compare, e.g., the phases (2.59), (4.107), and (4.112)], though is more complicated.

Let us check that the result is finite as $|p_3^+| \to 0$. For the 'iidd' contribution this statement is obvious since the contribution does not depend on p_3^+ [see Eqs. (4.111), (4.112), and (4.113)].

Let us consider the other contributions. From Eq. (4.24) it follows that $k_1^+ \to p_1^+$ and $k_2^+ \to p_2^+$ as $|p_3^+| \to 0$, therefore, $\delta_2^+ \to -\delta_1^+$ [see Eq. (4.84)]. Also note that $\delta^+ \to 0$ as $|p_3^+| \to 0$ [see Eqs. (4.81) and (4.95)]. It is easy to find the asymptotics in the case of vanishing ρ and τ. One obtains that

$$Z_1^i \approx Z_{-2}^i \approx p_1^i - eA^i(\phi), \quad \Delta_1^i \approx \Delta_{-2}^i \approx 0, \tag{4.114}$$

where $\phi = mx^+$ [see Eq. (4.5)].

Then, to leading order in p_3^+, we obtain for the 'nndd' term [see Eq. (4.71)]:

$$\widetilde{\mathcal{T}}^{\text{nndd}} \approx -\frac{4p_2^+ p_1^+ p_3^{+2}}{m^4}, \tag{4.115}$$

For the 'indd' term, the leading order is given by [see Eq. (4.73)]

$$\widetilde{\mathcal{T}}^{\text{indd}} \approx -\frac{2p_2^+ p_1^+ p_3^{+2}}{m^4} - \frac{(p_2^+ + p_1^+)^2 p_3^{+2}}{m^6} (m^2 + \boldsymbol{Z}_1^{\perp 2}), \tag{4.116}$$

and the same expression is obtained for the 'nidd' term. Note that the asymptotics are the same for the vacuum case, with the replacement $Z_1^i \to p_1^i$. In the case of general ρ and τ, the expressions are less trivial, but the scaling $\propto p_3^{+2}$ for the leading terms does not change. Also note that the phases remain finite as $|p_3^+| \to 0$. Therefore, we conclude, that the direct-direct contribution to the cross section is finite in the limit $|p_3^+| \to 0$.

Another question is the finiteness of the result with respect to the integration in τ and ρ. The integrals in τ and ρ are related to the initial integrals in the light-cone time variables (4.5) [see Eqs. (4.83), (4.81), and (4.95)], therefore, we require that they converge in a sufficiently small region, such that we can neglect the change of the wave-packet distribution densities. As might be expected, this is not satisfied, in particular with respect to the integral in τ, even in the constant-crossed field limit. The integral in τ does not converge for the 'nndd' term [see Eq. (4.108)] as $v \to 0$.

One of the solutions to this problem is the use of the full expression (4.4). Another solution is to single out the two-step contribution, i.e., the part which corresponds to the combination of the two diagrams (nonlinear Compton scattering and annihilation into one photon), summed over the states of the intermediate fermion. A naive assumption, which needs to be verified, is that the 'nndd' term is in fact the two-step contribution. An investigation of a proper way of excluding the two-step contribution is a subject for a future work.

Summary and outlook

The front-form formulation of quantum field theory has several advantages with respect to the instant-form one, and it allows to tackle some problems which seem to be very complicated in the instant-form approach. For QED in an intense plane-wave background, the front-form approach appears to be the most natural way of formulating the theory.

With the lightfront formulation, the coordinate system accounts for the conservation laws in a plane-wave field. Moreover, the lightfront treatment of the bispinor part allows for a significant simplification of the structure of the interaction vertices. In fact, we have seen that the theory becomes somewhat similar to vacuum QED, the change is the replacement of vacuum four-momenta with their dressed counterparts. Results for probabilities of scattering processes can be conveniently expressed via scalar products of photon and dressed fermion momenta, analogous to the Mandelstam variables in vacuum QED. The developed techniques allow to see QED in a plane-wave field from a different perspective, and could be very useful for studing higher-order processes.

Vacuum polarization effects have been a subject of many theoretical and experimental endeavors. With upcoming laser technologies, it seems possible to finally detect vacuum birefringence and also, though with greater challenges, study vacuum dichroism. We have discussed the physical background and evaluated the main stages of a high-energy vacuum birefringence/dichroism experiment, based on Compton scattering for the generation of probe gamma photons and pair production in a screened Coulomb field for the detection of the probe photon polarization change after the propagation through an intense laser pulse. Our estimations have shown that for high-power laser systems, the verification of the QED prediction at the 5σ significance level is possible on a timescale of a few days. As we have seen, an improvement of about two orders of magnitude for the required statistics in the vacuum birefringence experiment is achieved, if circularly polarized gamma photons are used to probe the vacuum. Two variations of the setup have been considered, one employs two high-power lasers and relies on laser-wakefield acceleration for the production of a high-energy electron beam, the other employs a conventional electron accelerator and a high-power laser. We have assessed different sets of the parameters and both aforementioned options turn out to be viable for the vacuum birefringence experiment. Of course, a more detailed numerical evaluation, taking into account effects like focusing of the high-power laser pulse and possible noise, would be necessary if a high-energy vacuum birefringence/dichroism experiment were to be performed. Such experiment would allow to test QED in the nonperturbative regime and possibly improve our understanding of the foundations of the model, that we use for the electromagnetic interaction.

Two-particle scattering processes inside a laser field are qualitatively different from the ones in vacuum. First of all, the former are in fact three-body collision processes, in comparison with the latter being two body ones. In the lightfront formulation, the field tensor for a laser field, approximated as a plane wave, is a function only of the time variable. Therefore, a relative advance or delayed arrival of the laser pulse at the two-particle collision point can be included simply as the corresponding shift in the argument. A more complex feature of collisions inside a laser field is the fact that particles become unstable. Photons decay via nonlinear Breit-Wheeler process and electrons "decay" via nonlinear Compton scattering. If the laser pulse is sufficiently long, then in general, a possible decay should be taken into account, also for the intermediate particles. One more peculiarity is the fact that an intermediate particle in, e.g., a tree-level process can become real. Therefore, a tree-level matrix element in a laser field includes two contributions: a two-step process with the intermediate particle being real and a one-step process with the intermediate particle being virtual. The former contribution, in principle, should be possible to reconstruct as the sum of the corresponding lower-order diagrams, the latter needs to be evaluated directly.

Finally, as we have seen, in general, the evolution of colliding wave packets can not be factorized out in expressions for probabilities, in contrast to the vacuum case. This feature is related to the conservation of only three asymptotic momentum components in a plane-wave field and seems to be the most troublesome one, since it forbids the definition of a cross section in a way, analogous to the one for quantum field theory in vacuum. For first-order processes, however, we have managed to construct a cross section for the case of the highly nonlinear regime ($\xi \gg 1$). For second-order processes, the idea, which is expected to be checked in a subsequent work, is that a cross section is also possible to define for one-step contributions in highly nonlinear regime, but one needs to exclude explicitly the two-step contribution for a considered process. It is important to note that in the present work the cross section has been introduced in a physically transparent way, it reduces to the usual vacuum one in the absence of the field, and therefore, the definition allows for a consistent separation of the vacuum and external-field parts. Moreover, the defined cross section for one-step processes is, in principle, suitable for the inclusion into laser-plasma interaction simulation tools, e.g., particle-in-cell routines. Hopefully, in the future, the current work will be finished to produce a complete picture of two-particle scattering in a laser field.

We have considered two examples of scattering in a plane-wave field: electron-positron annihilation into one and two photons, respectively. For the annihilation into one photon, the final photon four-momentum is completely defined by the initial electron and positron four-momenta. Consequently, a nonnegligible probability is obtained for a very limited set of the initial four-momenta. This fact renders the annihilation into one photon insignificant for laser-plasma interactions. For the annihilation into two photons, on the contrary, the phase space of the final states is much larger and this process, despite being a second-order one, may become sizable at a sufficiently high plasma density. In this work, an important step of the analytical evalution of the direct-direct contribution to the annihilation into two photons has been made. In the future, it is planned to complete the calculation and to assess the significance of this process for laser-plasma interactions.

Appendices

A Derivation of the lightfront Hamiltonian

Here we show some details of the derivation of the lightfront Hamiltonian, presented in Section 1.4. We start with Eq. (1.52), which we reproduce here:

$$T^{+-} = \overline{\Psi}[\gamma^+ i\partial_+ - (\gamma i\partial - m)]\Psi - \hat{F}^{+\sigma}\partial_+\hat{A}_\sigma + \frac{1}{4}\hat{F}_{\mu\nu}\hat{F}^{\mu\nu} - J^\sigma(A_\sigma + \hat{A}_\sigma). \tag{A.1}$$

Let us consider the gauge-field part first:

$$\begin{aligned} H_{\mathrm{G}} &= \int \mathrm{d}^2x^\perp \mathrm{d}x^- \Big(- \hat{F}^{+\sigma}\partial_+\hat{A}_\sigma + \frac{1}{4}\hat{F}_{\mu\nu}\hat{F}^{\mu\nu}\Big) \\ &= \int \mathrm{d}^2x^\perp \mathrm{d}x^- \Big[- \frac{1}{2}(\partial_-\hat{A}^-)^2 - (\partial_k\hat{A}^-)(\partial_-\mathcal{A}^k) + \frac{1}{2}(\partial_1\mathcal{A}_2 - \partial_2\mathcal{A}_1)^2\Big]. \end{aligned} \tag{A.2}$$

After writing $\hat{A}^-$ as $\hat{A}^- = \mathcal{A}^- + \alpha^-$, performing a couple of integration by parts and using the constraint relation, one obtains:

$$H_{\mathrm{G}} = \frac{1}{2}\int \mathrm{d}^2x^\perp \mathrm{d}x^- \Big[(\partial_-\mathcal{A}^-)^2 + \frac{1}{2}(\partial_1\mathcal{A}_2 - \partial_2\mathcal{A}_1)^2 - J^+\frac{1}{(i\partial_-)^2}J^+\Big]. \tag{A.3}$$

The fermionic part is given by

$$\begin{aligned} H_{\mathrm{F}} &= \int \mathrm{d}^2x^\perp \mathrm{d}x^- \overline{\Psi}[\gamma^+ i\partial_+ - (\gamma i\partial - m)]\Psi \\ &= \int \mathrm{d}^2x^\perp \mathrm{d}x^- \overline{\Psi}\{ - \gamma^- i\partial_- + [-\gamma^k(i\partial_k - eA_k - e\hat{A}_k) + m]\}\Psi. \end{aligned} \tag{A.4}$$

Again, with the use of some integration by parts and the constraint relation, it can be shown that

$$\int \mathrm{d}^2x^\perp \mathrm{d}x^- \overline{\Psi}[-\gamma^k(i\partial_k - eA_k - e\hat{A}_k) + m]\}\Psi = 2\int \mathrm{d}^2x^\perp \mathrm{d}x^- \overline{\Psi}\gamma^- i\partial_-\Psi, \tag{A.5}$$

therefore

$$\begin{aligned} H_{\mathrm{F}} &= \int \mathrm{d}^2x^\perp \mathrm{d}x^- \overline{\Psi}\gamma^- i\partial_-\Psi \\ &= \int \mathrm{d}^2x^\perp \mathrm{d}x^- (\overline{\psi}\gamma^- i\partial_-\psi + \overline{\chi}\gamma^- i\partial_-\chi + e\overline{\psi}\gamma^k\psi\mathcal{A}_k). \end{aligned} \tag{A.6}$$

Finally, after combining the gauge-field, fermionic and interacting parts together, we obtain the final expression (1.53) for the lightfront Hamiltonian.

B Contraction identities for the dressed vertices

B.1 Three-point dressed vertex contraction identities

General relations for all momenta being different are given by:

1. UU contraction:

$$\frac{1}{2}U^{\varkappa}_{43im}(2)\gamma^i\gamma^m\frac{1}{2}U^{\mu}_{21ks}(1)\gamma^k\gamma^s g_{\varkappa\mu} = \left[S^{\varkappa}_{43}(2)S^{\mu}_{21}(1) - T^{\varkappa}_{43}(2)T^{\mu}_{21}(1)\right] g_{\varkappa\mu} + \left[S^{\varkappa}_{43}(2)T^{\mu}_{21}(1) + T^{\varkappa}_{43}(2)S^{\mu}_{21}(1)\right] g_{\varkappa\mu}\gamma^1\gamma^2, \tag{B.1}$$

where

$$\begin{aligned}\left[S^{\varkappa}_{43}(2)S^{\mu}_{21}(1) - T^{\varkappa}_{43}(2)T^{\mu}_{21}(1)\right] g_{\varkappa\mu} =& \frac{1}{2p_4^+p_3^+p_2^+p_1^+} \\ &\times \Big[p_4^+p_1^+\pi_3(2)\pi_2(1) + p_3^+p_2^+\pi_4(2)\pi_1(1) \\ &- p_4^+p_3^+\pi_2(1)\pi_1(1) - p_2^+p_1^+\pi_4(2)\pi_3(2) \\ &+ p_4^+p_3^+m^2 + p_2^+p_1^+m^2\Big], \\ \left[S^{\varkappa}_{43}(2)T^{\mu}_{21}(1) + T^{\varkappa}_{43}(2)S^{\mu}_{21}(1)\right] g_{\varkappa\mu} =& -\frac{1}{2p_4^+p_3^+p_2^+p_1^+}\epsilon_{ij} \\ &\times \Big[p_4^+p_1^+\pi_3^i(2)\pi_2^j(1) - p_3^+p_2^+\pi_4^i(2)\pi_1^j(1) \\ &+ p_4^+p_3^+\pi_2^i(1)\pi_1^j(1) + p_2^+p_1^+\pi_4^i(2)\pi_3^j(2)\Big].\end{aligned} \tag{B.2}$$

2. VV contraction:

$$V^{i\varkappa}_{43}\gamma_i V^{k\mu}_{21}\gamma_k g_{\varkappa\mu} = \frac{m^2}{2p_4^+p_3^+p_2^+p_1^+}(p_4^+ - p_3^+)(p_2^+ - p_1^+). \tag{B.3}$$

3. UV contraction:

$$\frac{1}{2}U^{\varkappa}_{43im}(2)\gamma^i\gamma^m V^{k\mu}_{21}\gamma_k g_{\varkappa\mu} = \frac{m}{2p_4^+p_3^+p_2^+p_1^+}\left[(p_2^+ - p_1^+)p_3^+\pi_4^k(2) - p_4^+p_3^+(p_2^k - p_1^k)\right]\gamma_k. \tag{B.4}$$

4. VU contraction:

$$V^{i\varkappa}_{43}\gamma_i\frac{1}{2}U^{\mu}_{21ks}(1)\gamma^k\gamma^s g_{\varkappa\mu} = \frac{m}{2p_4^+p_3^+p_2^+p_1^+}\left[(p_4^+ - p_3^+)p_2^+\pi_1^i(1) - p_2^+p_1^+(p_4^i - p_3^i)\right]\gamma_i. \tag{B.5}$$

Then:

$$\left[\frac{1}{2}U^{\varkappa}_{43im}(2)\gamma^i\gamma^m + V^{i\varkappa}_{43}\gamma_i\right]\left[\frac{1}{2}U^{\mu}_{21ks}(1)\gamma^k\gamma^s + V^{k\mu}_{21}\gamma_k\right] g_{\varkappa\mu} = S_{4321}(21) + V^i_{4321}(21)\gamma_i + T_{4321}(21)\gamma^1\gamma^2, \tag{B.6}$$

where

$$
\begin{aligned}
S_{4321}(21) &= \left[S_{43}^{\varkappa}(2)S_{21}^{\mu}(1) - T_{43}^{\varkappa}(2)T_{21}^{\mu}(1)\right] g_{\varkappa\mu} + V_{43}^{i\varkappa}\gamma_i V_{21}^{k\mu}\gamma_k g_{\varkappa\mu} \\
&= \frac{1}{2p_4^+p_3^+p_2^+p_1^+}\Big[p_4^+p_1^+\pi_3(2)\pi_2(1) + p_3^+p_2^+\pi_4(2)\pi_1(1) \\
&\qquad - p_4^+p_3^+\pi_2(1)\pi_1(1) - p_2^+p_1^+\pi_4(2)\pi_3(2) \\
&\qquad + p_4^+p_3^+m^2 + p_2^+p_1^+m^2 + p_4^+p_2^+m^2 + p_3^+p_1^+m^2 \\
&\qquad - p_3^+p_2^+m^2 - p_4^+p_1^+m^2\Big], \\
V_{4321}^{i}(21)\gamma_i &= \left[\frac{1}{2}U_{43im}^{\varkappa}(2)\gamma^i\gamma^m V_{21}^{k\mu}\gamma_k + V_{43}^{i\varkappa}\gamma_i\frac{1}{2}U_{21ks}^{\mu}(1)\gamma^k\gamma^s\right] g_{\varkappa\mu} \\
&= \frac{m}{2p_4^+p_3^+p_2^+p_1^+}\Big[(p_2^+ - p_1^+)p_3^+\pi_4^i(2) + (p_4^+ - p_3^+)p_2^+\pi_1^i(1) \\
&\qquad - p_4^+p_3^+(p_2^i - p_1^i) - p_2^+p_1^+(p_4^i - p_3^i)\Big]\gamma_i, \\
T_{4321}(21)\gamma^1\gamma^2 &= \left[S_{43}^{\varkappa}(2)T_{21}^{\mu}(1) + T_{43}^{\varkappa}(2)S_{21}^{\mu}(1)\right] g_{\varkappa\mu}\gamma^1\gamma^2 \\
&= -\frac{1}{2p_4^+p_3^+p_2^+p_1^+}\epsilon_{ij}\Big[p_4^+p_3^+\pi_2^i(1)\pi_1^j(1) + p_2^+p_1^+\pi_4^i(2)\pi_3^j(2) \\
&\qquad + p_4^+p_1^+\pi_3^i(2)\pi_2^j(1) - p_3^+p_2^+\pi_4^i(2)\pi_1^j(1)\Big]\gamma^1\gamma^2.
\end{aligned}
\tag{B.7}
$$

B.2 Mixed three-point and seagull dressed vertex contraction identities

General relations for all momenta being different are given by:

$$
\begin{aligned}
& S_3^{\lambda}S_{21}^{\mu}(1)g_{\lambda\mu} = \frac{m}{p_3^+}, \\
& S_3^{\lambda}V_{21}^{k\mu}g_{\lambda\mu} = S_3^{\lambda}T_{21}^{\mu}(1)g_{\lambda\mu} = 0, \\
& V_3^{j\lambda}(2)S_{21}^{\mu}(1)g_{\lambda\mu} = \frac{1}{2p_3^+p_2^+p_1^+}\left\{p_3^+\left[p_2^+\pi_1^j(1) + p_1^+\pi_2^j(1)\right] - 2p_2^+p_1^+\pi_3^j(2)\right\}, \\
& V_3^{j\lambda}(2)V_{21}^{k\mu}g_{\lambda\mu} = \frac{m}{2p_2^+p_1^+}(p_2^+ - p_1^+)g^{jk}, \\
& V_3^{j\lambda}(2)T_{21}^{\mu}(1)g_{\lambda\mu} = \frac{1}{2p_2^+p_1^+}\epsilon^{jk}\left[p_2^+\pi_{1k}(1) - p_1^+\pi_{2k}(1)\right], \\
& S_3^{\lambda}\frac{1}{2}U_{21ks}^{\mu}(1)\gamma^k\gamma^s g_{\lambda\mu} = \frac{m}{p_3^+}, \\
& V_3^{j\lambda}(2)\gamma_j\frac{1}{2}U_{21ks}^{\mu}(1)\gamma^k\gamma^s g_{\lambda\mu} = \frac{1}{2}U_{12ks}^{\mu}(1)\gamma^k\gamma^s V_3^{j\lambda}(2)\gamma_j g_{\lambda\mu} \\
& \qquad = \frac{1}{p_3^+p_1^+}\left[p_3^+\pi_1^j(1) - p_1^+\pi_3^j(2)\right]\gamma_j.
\end{aligned}
\tag{B.8}
$$

Then:

$$
\begin{aligned}
&\left[S_3^{\lambda} + V_3^{j\lambda}(2)\gamma_j\right]\left[\frac{1}{2}U^{\mu}_{21ks}(1)\gamma^k\gamma^s + V_{21}^{k\mu}\gamma_k\right]g_{\lambda\mu} = S_{321} + V_{321}^{j}(21)\gamma_j, \\
&S_{321} = \left[S_3^{\lambda}\frac{1}{2}U^{\mu}_{21ks}(1)\gamma^k\gamma^s + V_3^{j\lambda}(2)\gamma_j V_{21}^{k\mu}\gamma_k\right]g_{\lambda\mu} = \frac{m}{p_3^+} + \frac{m}{p_2^+p_1^+}(p_2^+ - p_1^+), \\
&V_{321}^{j}(21)\gamma_j = V_3^{j\lambda}(2)\gamma_j\frac{1}{2}U^{\mu}_{21ks}(1)\gamma^k\gamma^s g_{\lambda\mu} = \frac{1}{p_3^+p_1^+}\left[p_3^+\pi_1^j(1) - p_1^+\pi_3^j(2)\right]\gamma_j.
\end{aligned}
\tag{B.9}
$$

Bibliography

[Abel et al., 2008] S. A. Abel, J. Jaeckel, V. V. Khoze, and A. Ringwald. Illuminating the hidden sector of string theory by shining light through a magnetic field. *Phys. Lett. B* **666**, 66 (2008).

[Akhiezer and Berestetskii, 1969] A. I. Akhiezer and V. B. Berestetskii. *Quantum electrodynamics* (in Russian). Nauka, Moscow, 3d edition (1969).

[Atwood et al., 2009] W. B. Atwood, A. A. Abdo, M. Ackermann, et al. The Large Area Telescope on the Fermi Gamma-ray Space Telescope Mission. *Astrophys. J.* **697**, 1071 (2009).

[Baier and Breitenlohner, 1967] R. Baier and P. Breitenlohner. Photon propagation in external fields. *Acta. Phys. Austr.* **25**, 212 (1967).

[Baier et al., 1989] V. Baier, V. Katkov, and V. Strakhovenko. Quantum radiation theory in inhomogeneous external fields. *Nucl. Phys. B* **328**, 387 (1989).

[Baier et al., 1976] V. N. Baier, A. I. Milstein, and V. M. Strakhovenko. Interaction between a photon and an intense electromagnetic wave. *Sov. Phys. JETP* **42**, 961 (1976).

[Barone et al., 2002] V. Barone, A. Drago, and P. G. Ratcliffe. Transverse polarisation of quarks in hadrons. *Phys. Rep.* **359**, 1 (2002).

[Becker and Mitter, 1975] W. Becker and H. Mitter. Vacuum polarization in laser fields. *J. Phys. A* **8**, 1638 (1975).

[Berestetskii et al., 1982] V. B. Berestetskii, E. M. Lifshitz, and L. P. Pitaevskii. *Quantum electrodynamics*. Pergamon Press, Oxford, England, 2nd edition (1982).

[Bergou and Varró, 1980] J. Bergou and S. Varró. Wavefunctions of a free electron in an external field and their application in intense field interactions. II. Relativistic treatment. *J. Phys. A: Math. Gen.* **13**, 2823 (1980).

[Bergou and Varró, 1981] J. Bergou and S. Varró. Nonlinear scattering processes in the presence of a quantised radiation field. II. Relativistic treatment. *J. Phys. A: Math. Gen.* **14**, 2281 (1981).

[Bern et al., 2001] Z. Bern, A. De Freitas, A. Ghinculov, et al. QCD and QED corrections to light-by-light scattering. *J. High Energy Phys.* **2001**(11), 031 (2001).

[Bernard, 2013] D. Bernard. Polarimetry of cosmic gamma-ray sources above e^+e^- pair creation threshold. *Nucl. Instrum. Methods Phys. Res., Sect. A* **729**, 765 (2013).

[Berson, 1969] I. Berson. Electron in the quantized field of a monochromatic electromagnetic wave. *Sov. Phys. JETP* **29**, 871 (1969).

[Bialynicka-Birula and Bialynicki-Birula, 1970] Z. Bialynicka-Birula and I. Bialynicki-Birula. Nonlinear effects in quantum electrodynamics. photon propagation and photon splitting in an external field. *Phys. Rev. D* **2**, 2341 (1970).

[Bjorken et al., 1971] J. D. Bjorken, J. B. Kogut, and D. E. Soper. Quantum Electrodynamics at Infinite Momentum: Scattering from an External Field. *Phys. Rev. D* **3**, 1382 (1971).

[Blum, 2012] K. Blum. *Density matrix theory and applications*. Springer, Berlin, 3rd edition (2012).

[Boca and Florescu, 2010] M. Boca and V. Florescu. The completeness of Volkov spinors. *Rom. Journ. Phys.* **55**, 511 (2010).

[Born and Wolf, 1999] M. Born and E. Wolf. *Principles of optics: electromagnetic theory of propagation, interference and diffraction of light*. Cambridge University Press, Cambridge, 7th edition (1999).

[Brodsky, 2002] S. Brodsky. Physics at the light-front. *Nucl. Phys. B Proc. Suppl.* **108**, 327 (2002).

[Brodsky et al., 1998] S. J. Brodsky, H.-C. Pauli, and S. S. Pinsky. Quantum chromodynamics and other field theories on the light cone. *Phys. Rep.* **301**, 299 (1998).

[Brodsky et al., 2015] S. J. Brodsky, G. F. de Téramond, H. G. Dosch, and J. Erlich. Light-front holographic QCD and emerging confinement. *Phys. Rep.* **584**, 1 (2015).

[Brown and Kibble, 1964] L. S. Brown and T. W. B. Kibble. Interaction of Intense Laser Beams with Electrons. *Phys. Rev.* **133**, A705 (1964).

[Burke et al., 1997] D. L. Burke, R. C. Field, G. Horton-Smith, et al. Positron Production in Multiphoton Light-by-Light Scattering. *Phys. Rev. Lett.* **79**, 1626 (1997).

[Cabibbo, 1963] N. Cabibbo. Unitary Symmetry and Leptonic Decays. *Phys. Rev. Lett.* **10**, 531 (1963).

[Cadène et al., 2014] A. Cadène, P. Berceau, M. Fouché, et al. Vacuum magnetic linear birefringence using pulsed fields: status of the BMV experiment. *Eur. Phys. J. D* **68**, 16 (2014).

[Cameron et al., 1993] R. Cameron, G. Cantatore, A. C. Melissinos, et al. Search for nearly massless, weakly coupled particles by optical techniques. *Phys. Rev. D* **47**, 3707 (1993).

[Cantatore et al., 1991] G. Cantatore, F. Della Valle, E. Milotti, et al. Proposed measurement of the vacuum birefringence induced by a magnetic field on high energy photons. *Phys. Lett. B* **265**, 418 (1991).

[Capparelli et al., 2017] L. M. Capparelli, A. Damiano, L. Maiani, and A. D. Polosa. A note on polarized light from magnetars. *Eur. Phys. J. C* **77**, 754 (2017).

[Chen et al., 2007] S.-J. Chen, H.-H. Mei, and W.-T. Ni. Q&A experiment to search for vacuum dichroism, pseudoscalar–photon interaction and millicharged fermions. *Mod. Phys. Lett. A* **22**, 2815 (2007).

[Danson et al., 2015] C. Danson, D. Hillier, N. Hopps, and D. Neely. Petawatt class lasers worldwide. *High Power Laser Sci. Eng.* **3**, e3 (2015).

[Della Valle et al., 2016] F. Della Valle, A. Ejlli, U. Gastaldi, et al. The PVLAS experiment: measuring vacuum magnetic birefringence and dichroism with a birefringent Fabry–Perot cavity. *Eur. Phys. J. C* **76**, 24 (2016).

[Di Piazza, 2014] A. Di Piazza. Ultrarelativistic Electron States in a General Background Electromagnetic Field. *Phys. Rev. Lett.* **113**, 040402 (2014).

[Di Piazza, 2015] A. Di Piazza. Analytical tools for investigating strong-field QED processes in tightly focused laser fields. *Phys. Rev. A* **91**, 042118 (2015).

[Di Piazza, 2016] A. Di Piazza. Nonlinear Breit-Wheeler Pair Production in a Tightly Focused Laser Beam. *Phys. Rev. Lett.* **117**, 213201 (2016).

[Di Piazza, 2018] A. Di Piazza. Completeness and orthonormality of the Volkov states and the Volkov propagator in configuration space. *Phys. Rev. D* **97**, 056028 (2018).

[Di Piazza et al., 2006] A. Di Piazza, K. Z. Hatsagortsyan, and C. H. Keitel. Light Diffraction by a Strong Standing Electromagnetic Wave. *Phys. Rev. Lett.* **97**, 083603 (2006).

[Di Piazza et al., 2012] A. Di Piazza, C. Müller, K. Z. Hatsagortsyan, and C. H. Keitel. Extremely high-intensity laser interactions with fundamental quantum systems. *Rev. Mod. Phys.* **84**, 1177 (2012).

[Di Piazza et al., 2018] A. Di Piazza, M. Tamburini, S. Meuren, and C. H. Keitel. Implementing nonlinear Compton scattering beyond the local-constant-field approximation. *Phys. Rev. A* **98**, 012134 (2018).

[Dinu, 2013] V. Dinu. Exact final-state integrals for strong-field QED. *Phys. Rev. A* **87**, 052101 (2013).

[Dinu and Torgrimsson, 2018a] V. Dinu and G. Torgrimsson. Single, double and higher-order nonlinear Compton scattering. *arXiv*:1811.00451 (2018).

[Dinu and Torgrimsson, 2018b] V. Dinu and G. Torgrimsson. Trident pair production in plane waves: Coherence, exchange, and spacetime inhomogeneity. *Phys. Rev. D* **97**, 036021 (2018).

[Dinu et al., 2014] V. Dinu, T. Heinzl, A. Ilderton, et al. Vacuum refractive indices and helicity flip in strong-field QED. *Phys. Rev. D* **89**, 125003 (2014).

[Dinu et al., 2016] V. Dinu, C. Harvey, A. Ilderton, et al. Quantum Radiation Reaction: From Interference to Incoherence. *Phys. Rev. Lett.* **116**(4) (2016).

[Dirac, 1949] P. A. M. Dirac. Forms of Relativistic Dynamics. *Rev. Mod. Phys.* **21**, 392 (1949).

[Dittrich and Gies, 2000] W. Dittrich and H. Gies. *Probing the Quantum Vacuum.* Springer, Berlin, Heidelberg (2000).

[Dunne, 2012] G. V. Dunne. The Heisenberg-Euler effective action: 75 years on. *Int. J. Mod. Phys. A* **27**, 1260004 (2012).

[ELI-Beamlines] ELI-Beamlines lasers. `https://www.eli-beams.eu/en/facility/lasers/`.

[ELI-NP] Extreme Light Infrastructure – Nuclear Physics. `http://www.eli-np.ro`.

[EuroXFEL] European XFEL facility. `https://www.xfel.eu`.

[FACET-II] FACET-II project. `https://portal.slac.stanford.edu/sites/ard_public/facet/Pages/FACET-II.aspx`.

[Fedotov, 2017] A. Fedotov. Conjecture of perturbative QED breakdown at $\alpha\chi^{2/3} \gtrsim 1$. *Journal of Physics: Conf. Series* **826**, 012027 (2017).

[Fillion-Gourdeau et al., 2015] F. Fillion-Gourdeau, C. Lefebvre, and S. MacLean. Scheme for the detection of mixing processes in vacuum. *Phys. Rev. A* **91**, 031801 (2015).

[Fradkin et al., 1991] E. S. Fradkin, D. M. Gitman, and S. M. Shvartsman. *Quantum electrodynamics with unstable vacuum.* Springer, Berlin (1991).

[Fry, 2017] A. Fry. Laser upgrade options: >100TW, transport and quality improvement. Presentation at FACET-II Science Workshop (2017).

[Fukuda et al., 2003] M. Fukuda, T. Aoki, K. Dobashi, et al. Polarimetry of Short-Pulse Gamma Rays Produced through Inverse Compton Scattering of Circularly Polarized Laser Beams. *Phys. Rev. Lett.* **91**, 164801 (2003).

[Furry, 1951] W. H. Furry. On Bound States and Scattering in Positron Theory. *Phys. Rev.* **81**, 115 (1951).

[Gies et al., 2006] H. Gies, J. Jaeckel, and A. Ringwald. Polarized Light Propagating in a Magnetic Field as a Probe for Millicharged Fermions. *Phys. Rev. Lett.* **97**, 140402 (2006).

[Gies et al., 2015] H. Gies, F. Karbstein, and N. Seegert. Quantum reflection of photons off spatio-temporal electromagnetic field inhomogeneities. *New J. Phys.* **17**, 043060 (2015).

[Ginzburg et al., 1984] I. F. Ginzburg, G. L. Kotkin, S. L. Panfil, et al. Colliding γe and $\gamma\gamma$ beams based on single-pass e^+e^- accelerators II. Polarization effects, monochromatization improvement. *Nucl. Instr. Meth. Phys. Res.* **219**, 5 (1984).

[Goldberger and Watson, 1964] M. L. Goldberger and K. M. Watson. *Collision theory.* John Wiley & Sons, New York (1964).

[Gonoskov et al., 2015] A. Gonoskov, S. Bastrakov, E. Efimenko, et al. Extended particle-in-cell schemes for physics in ultrastrong laser fields: Review and developments. *Phys. Rev. E* **92**, 023305 (2015).

[Halzen and Martin, 1984] F. Halzen and A. D. Martin. *Quarks and leptons: an introductory course in modern particle physics*. Wiley, New York (1984).

[Hartin, 2016] A. Hartin. Fierz relations for Volkov spinors and the simplification of Furry picture traces. *Phys. Rev. D* **94**, 073002 (2016).

[Hartin, 2006] A. F. Hartin. *Second Order QED Processes in an Intense Electromagnetic Field*. Ph.D. thesis (2006).

[Heinzl and Ilderton, 2009] T. Heinzl and A. Ilderton. Exploring high-intensity QED at ELI. *Eur. Phys. J. D* **55**, 359 (2009).

[Heinzl et al., 2006] T. Heinzl, B. Liesfeld, K. Amthor, et al. On the observation of vacuum birefringence. *Opt. Commun.* **267**, 318 (2006).

[Heisenberg and Euler, 1936] W. Heisenberg and H. Euler. Folgerungen aus der Diracschen Theorie des Positrons. *Z. Phys.* **98**, 714 (1936).

[Heitler, 1954] W. Heitler. *The Quantum Theory of Radiation*. Oxford University Press, Oxford, England, 3rd edition (1954).

[Homma et al., 2011] K. Homma, D. Habs, and T. Tajima. Probing vacuum birefringence by phase-contrast Fourier imaging under fields of high-intensity lasers. *Appl. Phys. B* **104**, 769 (2011).

[Hu and Huang, 2014] H. Hu and J. Huang. Modified light-cone condition via vacuum polarization in a time-dependent field. *Phys. Rev. A* **90**, 062111 (2014).

[Hu et al., 2010] H. Hu, C. Müller, and C. H. Keitel. Complete QED Theory of Multiphoton Trident Pair Production in Strong Laser Fields. *Phys. Rev. Lett.* **105**, 080401 (2010).

[Hunter et al., 2014] S. D. Hunter, P. F. Bloser, G. O. Depaola, et al. A pair production telescope for medium-energy gamma-ray polarimetry. *Astropart. Phys.* **59**, 18 (2014).

[Ilderton, 2011] A. Ilderton. Trident Pair Production in Strong Laser Pulses. *Phys. Rev. Lett.* **106**, 020404 (2011).

[Ilderton and Marklund, 2016] A. Ilderton and M. Marklund. Prospects for studying vacuum polarisation using dipole and synchrotron radiation. *J. Plasma Phys.* **82**, 655820201 (2016).

[Ilderton and Torgrimsson, 2013] A. Ilderton and G. Torgrimsson. Radiation reaction from QED: Lightfront perturbation theory in a plane wave background. *Phys. Rev. D* **88**, 025021 (2013).

[Ilderton et al., 2011] A. Ilderton, P. Johansson, and M. Marklund. Pair annihilation in laser pulses: Optical versus x-ray free-electron laser regimes. *Phys. Rev. A* **84**, 032119 (2011).

[Itzykson and Zuber, 1980] C. Itzykson and J. B. Zuber. *Quantum field theory*. McGraw-Hill International Book Co, New York (1980).

[Jaeckel and Ringwald, 2010] J. Jaeckel and A. Ringwald. The Low-Energy Frontier of Particle Physics. *Annu. Rev. Nucl. Part. Sci.* **60**(1), 405 (2010).

[Jaeckel and Spannowsky, 2016] J. Jaeckel and M. Spannowsky. Probing MeV to 90 GeV axion-like particles with LEP and LHC. *Phys. Lett. B* **753**, 482 (2016).

[James, 2006] F. James. *Statistical Methods in Experimental Physics*. World Scientific, 2 edition (2006).

[Jeong and Lee, 2014] T. M. Jeong and J. Lee. Femtosecond petawatt laser. *Ann. Phys.* **526**, 157 (2014).

[Karbstein and Shaisultanov, 2015] F. Karbstein and R. Shaisultanov. Photon propagation in slowly varying inhomogeneous electromagnetic fields. *Phys. Rev. D* **91**, 085027 (2015).

[Karbstein and Sundqvist, 2016] F. Karbstein and C. Sundqvist. Probing vacuum birefringence using x-ray free electron and optical high-intensity lasers. *Phys. Rev. D* **94**, 013004 (2016).

[Kelner et al., 1975] S. R. Kelner, Y. D. Kotov, and V. M. Logunov. Methods of measuring linear polarization of gamma quanta. *Sov. J. Nucl. Phys.* **21**, 313 (1975).

[Kim et al., 2017] H. T. Kim, V. B. Pathak, K. Hong Pae, et al. Stable multi-GeV electron accelerator driven by waveform-controlled PW laser pulses. *Sci. Rep.* **7**, 10203 (2017).

[King and Elkina, 2016] B. King and N. Elkina. Vacuum birefringence in high-energy laser-electron collisions. *Phys. Rev. A* **94**, 062102 (2016).

[King and Fedotov, 2018] B. King and A. Fedotov. Effect of interference on the trident process in a constant crossed field. *Phys. Rev. D* **98**, 016005 (2018).

[King and Keitel, 2012] B. King and C. H. Keitel. Photon-photon scattering in collisions of intense laser pulses. *New J. Phys.* **14**, 103002 (2012).

[King and Ruhl, 2013] B. King and H. Ruhl. Trident pair production in a constant crossed field. *Phys. Rev. D* **88**, 013005 (2013).

[King et al., 2010] B. King, A. Di Piazza, and C. H. Keitel. A matterless double slit. *Nat. Photonics* **4**(2), 92 (2010).

[Klein and Nigam, 1964] J. J. Klein and B. P. Nigam. Birefringence of the Vacuum. *Phys. Rev.* **135**, B1279 (1964).

[Kobayashi and Maskawa, 1973] M. Kobayashi and T. Maskawa. CP-Violation in the Renormalizable Theory of Weak Interaction. *Progr. Theor. Phys.* **49**, 652 (1973).

[Kogut and Soper, 1970] J. B. Kogut and D. E. Soper. Quantum Electrodynamics in the Infinite-Momentum Frame. *Phys. Rev. D* **1**, 2901 (1970).

[Kryuchkyan and Hatsagortsyan, 2011] G. Y. Kryuchkyan and K. Z. Hatsagortsyan. Bragg Scattering of Light in Vacuum Structured by Strong Periodic Fields. *Phys. Rev. Lett.* **107**, 053604 (2011).

[Ku, 1966] H. Ku. Notes on the use of propagation of error formulas. *J. Res. Nat. Bur. Stand.* **70C**(4), 263 (1966).

[Landau and Lifshitz, 1987] L. D. Landau and E. M. Lifshitz. *The Classical Theory of Fields*. Butterworth-Heinemann, Oxford, England, 4th edition (1987).

[Latal et al., 2001] H. Latal, W. Schweiger, R. Beig, et al. (editors). *Methods of Quantization*, volume 572 of *Lecture Notes in Physics*. Springer, Berlin, Heidelberg (2001).

[Le Garrec et al., 2014] B. Le Garrec, S. Sebban, D. Margarone, et al. ELI-beamlines: extreme light infrastructure science and technology with ultra-intense lasers. *Proc. SPIE* **8962**, 89620I (2014).

[Leemans et al., 2014] W. P. Leemans, A. J. Gonsalves, H.-S. Mao, et al. Multi-GeV Electron Beams from Capillary-Discharge-Guided Subpetawatt Laser Pulses in the Self-Trapping Regime. *Phys. Rev. Lett.* **113**, 245002 (2014).

[Leibbrandt, 1984] G. Leibbrandt. Light-cone gauge in Yang-Mills theory. *Phys. Rev. D* **29**, 1699 (1984).

[Lepage and Brodsky, 1980] G. P. Lepage and S. J. Brodsky. Exclusive processes in perturbative quantum chromodynamics. *Phys. Rev. D* **22**, 2157 (1980).

[Lundström et al., 2006] E. Lundström, G. Brodin, J. Lundin, et al. Using High-Power Lasers for Detection of Elastic Photon-Photon Scattering. *Phys. Rev. Lett.* **96**, 083602 (2006).

[Mackenroth and Di Piazza, 2011] F. Mackenroth and A. Di Piazza. Nonlinear Compton scattering in ultrashort laser pulses. *Phys. Rev. A* **83**, 032106 (2011).

[Mackenroth and Di Piazza, 2018] F. Mackenroth and A. Di Piazza. Nonlinear trident pair production in an arbitrary plane wave: A focus on the properties of the transition amplitude. *Phys. Rev. D* **98**, 116002 (2018).

[Mandelstam, 1983] S. Mandelstam. Light-cone superspace and the ultraviolet finiteness of the N=4 model. *Nucl. Phys. B* **213**, 149 (1983).

[Mantovani et al., 2016] L. Mantovani, B. Pasquini, X. Xiong, and A. Bacchetta. Revisiting the equivalence of light-front and covariant QED in the light-cone gauge. *Phys. Rev. D* **94**, 116005 (2016).

[Mertig et al., 1991] R. Mertig, M. Böhm, and A. Denner. Feyn Calc - Computer-algebraic calculation of Feynman amplitudes. *Computer Physics Communications* **64**, 345 (1991).

[Metsaev et al., 2001] R. R. Metsaev, C. B. Thorn, and A. A. Tseytlin. Light-cone superstring in space–time. *Nucl. Phys. B* **596**, 151 (2001).

[Meuren, 2015] S. Meuren. *Nonlinear quantum electrodynamic and electroweak processes in strong laser fields*. Ph.D. thesis (2015).

[Meuren and Di Piazza, 2011] S. Meuren and A. Di Piazza. Quantum Electron Self-Interaction in a Strong Laser Field. *Phys. Rev. Lett.* **107**, 260401 (2011).

[Meuren et al., 2013] S. Meuren, C. H. Keitel, and A. Di Piazza. Polarization operator for plane-wave background fields. *Phys. Rev. D* **88**, 013007 (2013).

[Meuren et al., 2015] S. Meuren, K. Z. Hatsagortsyan, C. H. Keitel, and A. Di Piazza. Polarization-operator approach to pair creation in short laser pulses. *Phys. Rev. D* **91**, 013009 (2015).

[Meuren et al., 2016] S. Meuren, C. H. Keitel, and A. Di Piazza. Semiclassical picture for electron-positron photoproduction in strong laser fields. *Phys. Rev. D* **93**, 085028 (2016).

[Mignani et al., 2017] R. P. Mignani, V. Testa, D. González Caniulef, et al. Evidence for vacuum birefringence from the first optical-polarimetry measurement of the isolated neutron star RX J1856.5–3754. *Mon. Not. R. Astron. Soc.* **465**, 492 (2017).

[Mitter, 1975] H. Mitter. Quantum electrodynamics in laser fields. *Acta Phys. Austriaca, Suppl.* **XIV**, 397 (1975).

[Mohammadi et al., 2014] R. Mohammadi, I. Motie, and S.-S. Xue. Circular polarization from linearly-polarized-laser-beam collisions. *Phys. Rev. A* **89**, 062111 (2014).

[Molière, 1947] V. G. Molière. Theorie der Streuung schneller geladener Teilchen I. Einzelstreuung am abgeschirmten Coulomb-Feld. *Z. Naturforsch.* **2a**, 133 (1947).

[Monden and Kodama, 2012] Y. Monden and R. Kodama. Interaction of two counterpropagating laser beams with vacuum. *Phys. Rev. A* **86**, 033810 (2012).

[Muramatsu et al., 2014] N. Muramatsu, Y. Kon, S. Daté, et al. (on behalf of the LEPS Collaboration). Development of high intensity laser-electron photon beams up to 2.9 GeV at the SPring-8 LEPS beamline. *Nucl. Instrum. Meth. A* **737**, 184 (2014).

[Mustaki et al., 1991] D. Mustaki, S. Pinsky, J. Shigemitsu, and K. Wilson. Perturbative renormalization of null-plane QED. *Phys. Rev. D* **43**, 3411 (1991).

[Nakamiya and Homma, 2017] Y. Nakamiya and K. Homma. Probing vacuum birefringence under a high-intensity laser field with gamma-ray polarimetry at the GeV scale. *Phys. Rev. D* **96**, 053002 (2017).

[Negoita et al., 2016] F. Negoita, M. Roth, P. G. Thirolf, et al. Laser driven nuclear physics at ELI-NP. *Rom. Rep. Phys.* **68**(Supplement), S37 (2016).

[Neville and Rohrlich, 1971] R. A. Neville and F. Rohrlich. Quantum Electrodynamics on Null Planes and Applications to Lasers. *Phys. Rev. D* **3**, 1692 (1971).

[Nikishov and Ritus, 1964a] A. I. Nikishov and V. I. Ritus. Quantum Processes in the Field of a Plane Electromagnetic Wave and in a Constant Field. *Sov. Phys. JETP* **19**, 1191 (1964).

[Nikishov and Ritus, 1964b] A. I. Nikishov and V. I. Ritus. Quantum Processes in the Field of a Plane Electromagnetic Wave and in a Constant Field. I. *Sov. Phys. JETP* **19**, 529 (1964).

[Okun, 1984] L. B. Okun. *Leptons and Quarks*. North-Holland, Amsterdam (1984).

[Oleinik, 1967] V. P. Oleinik. Resonance effects in the field of an intense laser beam. *Sov. Phys. JETP* **25**, 697 (1967).

[Oleinik, 1968] V. P. Oleinik. Resonance effects in the field of an intense laser ray. II. *Sov. Phys. JETP* **26**, 1132 (1968).

[Olsen and Maximon, 1959] H. Olsen and L. C. Maximon. Photon and Electron Polarization in High-Energy Bremsstrahlung and Pair Production with Screening. *Phys. Rev.* **114**, 887 (1959).

[Olver et al., 2010] F. W. J. Olver, D. W. Lozier, R. F. Boisvert, and C. W. Clark (editors). *NIST handbook of mathematical functions*. Cambridge University Press, New York (2010).

[Papadopoulos et al., 2016] D. Papadopoulos, J. Zou, C. Le Blanc, et al. The Apollon 10 PW laser: experimental and theoretical investigation of the temporal characteristics. *High Power Laser Sci. Eng.* **4**, e34 (2016).

[Peitzmann, 2013] T. Peitzmann (for the ALICE FoCal Collaboration). Prototype studies for a forward EM calorimeter in ALICE. *arXiv*:1308.2585 (2013).

[Peskin and Schroeder, 1995] M. E. Peskin and D. V. Schroeder. *An introduction to quantum field theory*. Addison-Wesley Pub. Co, Reading, Massachusetts (1995).

[Piskarskas et al., 1986] A. Piskarskas, A. Stabinis, and A. Yankauskas. Phase phenomena in parametric amplifiers and generators of ultrashort light pulses. *Sov. Phys. Usp.* **29**, 869 (1986).

[Riley et al., 2006] K. F. Riley, M. P. Hobson, and S. J. Bence. *Mathematical Methods for Physics and Engineering*. Cambridge University Press, Cambridge, 3rd edition (2006).

[Ritus, 1985] V. I. Ritus. Quantum effects of the interaction of elementary particles with an intense electromagnetic field. *J. Sov. Laser Res.* **6**, 497 (1985).

[Rus et al., 2013] B. Rus, P. Bakule, D. Kramer, et al. ELI-Beamlines laser systems: status and design options. *Proc. SPIE* **8780**, 87801T (2013).

[Schlenvoigt et al., 2016] H.-P. Schlenvoigt, T. Heinzl, U. Schramm, et al. Detecting vacuum birefringence with x-ray free electron lasers and high-power optical lasers: a feasibility study. *Phys. Scripta* **91**, 023010 (2016).

[Schwinger, 1951] J. Schwinger. On Gauge Invariance and Vacuum Polarization. *Phys. Rev.* **82**, 664 (1951).

[Seipt and Kämpfer, 2012] D. Seipt and B. Kämpfer. Two-photon Compton process in pulsed intense laser fields. *Phys. Rev. D* **85**, 101701 (2012).

[Shakeri et al., 2017] S. Shakeri, S. Z. Kalantari, and S.-S. Xue. Polarization of a probe laser beam due to nonlinear QED effects. *Phys. Rev. A* **95**, 012108 (2017).

[Skoromnik et al., 2013] O. D. Skoromnik, I. D. Feranchuk, and C. H. Keitel. Collapse-and-revival dynamics of strongly laser-driven electrons. *Phys. Rev. A* **87**, 052107 (2013).

[SNO, 2001] SNO (collaboration). Measurement of the Rate of $\nu_e + d \to p + p + e^-$ Interactions Produced by ^{8}B Solar Neutrinos at the Sudbury Neutrino Observatory. *Phys. Rev. Lett.* **87**, 071301 (2001).

[SNO, 2002] SNO (collaboration). Direct Evidence for Neutrino Flavor Transformation from Neutral-Current Interactions in the Sudbury Neutrino Observatory. *Phys. Rev. Lett.* **89**, 011301 (2002).

[Srivastava and Brodsky, 2002] P. P. Srivastava and S. J. Brodsky. Light-front formulation of the standard model. *Phys. Rev. D* **66** (2002).

[Strickland and Mourou, 1985] D. Strickland and G. Mourou. Compression of amplified chirped optical pulses. *Opt. Commun.* **55**, 447 (1985).

[Sung et al., 2017] J. H. Sung, H. W. Lee, J. Y. Yoo, et al. 4.2 PW, 20 fs Ti:sapphire laser at 0.1 Hz. *Opt. Lett.* **42**, 2058 (2017).

[Super-Kamiokande, 1998] Super-Kamiokande (collaboration). Evidence for Oscillation of Atmospheric Neutrinos. *Phys. Rev. Lett.* **81**(8), 1562 (1998).

[Takahashi, 1957] Y. Takahashi. On the Generalized Ward Identity. *Nuovo Cimento* **6**, 371 (1957).

[Tavani et al., 2003] M. Tavani, G. Barbiellini, A. Argan, et al. The AGILE instrument. *Proc. SPIE* **4851**, 1151 (2003).

[Tennant, 2016] D. M. Tennant. Four wave mixing as a probe of the vacuum. *Phys. Rev. D* **93**, 125032 (2016).

[Thorn, 1979] C. B. Thorn. Asymptotic freedom in the infinite-momentum frame. *Phys. Rev. D* **20**, 1934 (1979).

[Toll, 1952] J. S. Toll. *The dispersion relation for light and its application to problems involving electron pairs.* Ph.D. thesis (1952).

[Tommasini et al., 2008] D. Tommasini, A. Ferrando, H. Michinel, and M. Seco. Detecting photon-photon scattering in vacuum at exawatt lasers. *Phys. Rev. A* **77**, 042101 (2008).

[Tommasini et al., 2009] D. Tommasini, A. Ferrando, H. Michinel, and M. Seco. Precision tests of QED and non-standard models by searching photon-photon scattering in vacuum with high power lasers. *J. High Energ. Phys.* **2009**, 043 (2009).

[Tsai, 1974] Y.-S. Tsai. Pair production and bremsstrahlung of charged leptons. *Rev. Mod. Phys.* **46**, 815 (1974).

[Turcu et al., 2016] I. C. E. Turcu, F. Negoita, D. A. Jaroszynski, et al. High Field Physics and QED Experiments at ELI-NP. *Rom. Rep. Phys.* **68**(Supplement), S145 (2016).

[Turolla et al., 2017] R. Turolla, S. Zane, R. Taverna, et al. A comment on 'A note on polarized light from Magnetars: QED effects and axion-like particles' by L.M. Capparelli, L. Maiani and A.D. Polosa. *arXiv*:1706.02505 (2017).

[Villalba-Chávez and Di Piazza, 2013] S. Villalba-Chávez and A. Di Piazza. Axion-induced birefringence effects in laser driven nonlinear vacuum interaction. *J. High Energ. Phys.* **2013**, 136 (2013).

[Villalba-Chávez et al., 2016] S. Villalba-Chávez, S. Meuren, and C. Müller. Minicharged particles search by strong laser pulse-induced vacuum polarization effects. *Phys. Lett. B* **763**, 445 (2016).

[Volkov, 1935] D. M. Volkov. Über eine Klasse von Lösungen der Diracschen Gleichung. *Z. Phys.* **94**, 250 (1935).

[Voroshilo et al., 2016] A. I. Voroshilo, S. P. Roshchupkin, and V. N. Nedoreshta. Resonant two-photon annihilation of an electron-positron pair in a pulsed electromagnetic wave. *Phys. Rev. A* **94**, 032128 (2016).

[Vulkan] Vulkan Laser. `https://www.clf.stfc.ac.uk/Pages/Vulcan-laser.aspx`.

[Wang et al., 2013] X. Wang, R. Zgadzaj, N. Fazel, et al. Quasi-monoenergetic laser-plasma acceleration of electrons to 2 GeV. *Nat. Commun.* **4**, 1988 (2013).

[Ward, 1950] J. C. Ward. An Identity in Quantum Electrodynamics. *Phys. Rev.* **78**, 182 (1950).

[Weisskopf, 1936] V. Weisskopf. Über die Elektrodynamik des Vakuums auf Grund des Quanten-Theorie des Elektrons. *Mat. Fys. Medd.* **14**, 1 (1936).

[Weller et al., 2009] H. R. Weller, M. W. Ahmed, H. Gao, et al. Research opportunities at the upgraded HIγS facility. *Prog. Part. Nucl. Phys.* **62**, 257 (2009).

[Wilson et al., 1994] K. G. Wilson, T. S. Walhout, A. Harindranath, et al. Nonperturbative QCD: A weak-coupling treatment on the light front. *Phys. Rev. D* **49**, 6720 (1994).

[Wistisen and Uggerhøj, 2013] T. N. Wistisen and U. I. Uggerhøj. Vacuum birefringence by Compton backscattering through a strong field. *Phys. Rev. D* **88**, 053009 (2013).

[Yabashi et al., 2015] M. Yabashi, H. Tanaka, and T. Ishikawa. Overview of the SACLA facility. *J. Synchrotron Radiat.* **22**(3), 477 (2015).

[Yakaboylu, 2015] E. Yakaboylu. Volkov wave function: its orthonormality and completeness. *arXiv*:1505.02801v2 (2015).

[Zakowicz, 2005] S. Zakowicz. Square-integrable wave packets from the Volkov solutions. *J. Math. Phys.* **46**, 032304 (2005).

[Zavattini et al., 2016] G. Zavattini, F. Della Valle, A. Ejlli, and G. Ruoso. A polarisation modulation scheme for measuring vacuum magnetic birefringence with static fields. *Eur. Phys. J. C* **76**, 294 (2016).